Supercritical Fluids for Fischer Tropsch Synthesis and Related Reactions

by

Joseph Edgar Durham II

A dissertation submitted to the Graduate Faculty of
Auburn University
in partial fulfillment of the
requirements for the Degree of
Doctor of Philosophy

Auburn, Alabama
May 9, 2011

Keywords: Fischer Tropsch, Supercritical, Aldehyde, Mechanism, Reactor Design

Approved by

Christopher Roberts, Chair, Professor of Chemical Engineering
Mario Eden, Associate Professor of Chemical Engineering
Ram Gupta, Professor of Chemical Engineering
Sushil Adhikari, Assistant Professor of Biosystems Engineering

Abstract

Fischer Tropsch Synthesis (FTS) is a process for the hydrogenation of carbon monoxide. FTS can be used to synthesize hydrocarbon and oxygenated hydrocarbon fuels and chemicals from any carbonaceous feedstock. The process dates back to Germany between WW1 and WW2 and has been continuously utilized industrially in South Africa for over 50 years. Industrially, FTS is operated in two modes: High Temperature (HTFT: 300^{o}C – 350^{o}C) for the production of light olefins and gasoline and Low Temperature (LTFT: 210^{o}C – 250^{o}C) for the production of diesel and wax. The experimental work in this dissertation will focus exclusively on LTFT.

Supercritical fluids offer a number of interesting properties that can be useful in FTS. Supercritical fluids are miscible with gasses and can be excellent solvents for liquids and solids, with the Fischer Tropsch reaction requiring both the transport of the gaseous reactants to the active sites and the transport of the liquid products away from the active sites. Supercritical fluids, having liquid-like densities, have high thermal mass, giving them an enhanced capacity for supplying and dissipating heat. The Fischer Tropsch reaction is highly exothermic, requiring rapid heat removal.

FTS utilizing a supercritical medium (SC-FTS) has been shown to provide a number of catalytic performance advantages (such as improved selectivity and activity maintenance) and is believed to offer a number of process advantages as well. Of particular interest in this work is the opportunity that supercritical fluids offer in terms of studying reaction fundamentals by suppressing thermal gradients and stabilizing primary products.

The objective of this work is to (1) identify and demonstrate the benefits of SC-FTS operation, (2) use the supercritical reaction media to probe the fundamentals of the FTS reaction, and (3) identify a SC-FTS reactor design to improve the economics of industrial SC-FTS utilization.

In the second chapter (the first experimental chapter) of this dissertation, efforts to close the material balance for SC-FTS on a cobalt catalyst will be discussed. In the third chapter, work in which a supercritical environment was used to successfully reactivate a cobalt catalyst partially deactivated by traditional fixed-bed FTS operation will be discussed. The fourth chapter will focus on work done on an iron-based catalyst in which SC-FTS operation gave a high selectivity to heavy liquid methyl-ketones and aldehydes, with the aldehydes being shown to be one of the primary products for FTS. Secondary reactions appeared to convert these aldehydes to the corresponding olefin. Appreciable amounts of aldehydes and methyl-ketones were not seen in traditional FTS operation (fixed-bed and slurry-phase) using the same catalysts at comparable conditions. The fifth chapter will focus on the use of a novel reactor design principle for SC-FTS.

Acknowledgments

I would like to thank my parents (Grover and Carol Durham), my brother (Hugh Durham), and my cat (Bubbles). I would also like to take this opportunity to thank April and Hailee Graham, Alan and Tanya Schaeffer, Gillian Sharer, and Debbie Starr.

Brian Schweiker and Mike Hornsby provided frequent assistance without which none of this work would have been possible. I would also like to thank former members of Dr. Roberts' research group: Dr. Daniel Obrzut, Dr. Phillip Bell, Dr. Nimir Elbashir, and Kendall Hurst as well as current members Deborah Bacik, Steven Saunders, Sihe Zhang, and Rui Xu, Rajeshwar Chinnawar, and Jennifer Boice. I hope that I have provided as much help as I have received.

Finally, I would like to thank Dr. Christopher Roberts. This dissertation is the product of much time and effort, and the journey included some very dark times. Through it all, he has exceeded even the wildest over-estimate of his professional obligation to me and for that I am grateful beyond words.

Table of Contents

List of Tables

List of Figures

Chapter 1

Supercritical Fluids for Fischer Tropsch Synthesis and Related Reactions

1.1 General Review

1.1.1 Introduction and History

Fischer Tropsch Synthesis (FTS) is a catalytic process for the production of hydrocarbons (syncrude) from carbon monoxide and hydrogen (syngas), allowing for the synthesis of fuels and chemicals from non-petroleum sources including coal (CTL), natural gas (GTL), and biomass (BTL). Collectively, these can be referred to as XTL. A brief history of FTS is as follows:

- 1902 (Sabatier and Senderens): Synthesized methane from CO/CO_2 and H_2 at $T = 200^oC – 300^oC$ and atmospheric pressure on cobalt or nickel catalysts. [1]
- 1913 (BASF): Synthesis of paraffins, olefins, and oxygenates on alkali activated Co-Os catalysts at $T > 300^oC$ and $P > 100$ bar. This is the origin of methanol synthesis. [1]
- 1922 (Fischer and Tropsch): Synthesized Synthol (aliphatic oxygenates) from CO and H_2 at $T = 400^oC$ and $P = 150$ bar on alkalized iron chips. The product could be converted to Synthine (a mixture of hydrocarbons) by heating at high pressure. [1,2]
- 1923 (Fischer and Tropsch): Discovered that greater hydrocarbon productivity and heavy hydrocarbon selectivity could be realized at lower pressure ($P = 7$ bar). [2]
- 1936: First commercial scale FT plant operational (Braunkohle-Benzin). [2]
- 1938: Germany has an FT Capacity of approximately 8,000 BPD. [2]

- 1943: Worldwide FT production reaches approximately 12,000 BPD (9 German, 1 French, 4 Japanese, and 1 Manchurian facility). [1]
- 1950: 5,000 BPD Brownsville, TX natural gas FT facility opens. [3]
- 1955: Sasol 1, utilizing coal, built (3,000 BPD). [1]
- 1980: Sasol 2, utilizing coal, begins production (25,000 BPD). [1]
- 1982: Sasol 3, utilizing coal, begins production (25,000 BPD). [1,2]
- 1992: Sasol Mossgas plant (South Africa), utilizing natural gas, begins production (12,500 BPD). [4]
- 1993: Shell Bintulu plant (Malaysia), utilizing natural gas, begins production (12,500 BPD). [2,4]
- 2005: Sasol Oryx plant (Qatar), utilizing natural gas, progressing to completion (34,000 BPD & CapEx $1 billion). [2,5]
- 2006: Sasol-Chevron plant (Nigeria), utilizing natural gas, progressing to completion (20,000 BOD & CapEx $500 million – expansion to 100,000 BOD eyed). [2,6]
- 2006: Sasol in discussions with China to build two CTL FT plants (80,000 BPD & CapEx over $5 billion each – needs over $40 / BBL to be economically viable). [7]

Fischer Tropsch Synthesis is an important step in thermo-chemical conversion of carbonaceous feedstocks to fuels and chemicals. The steps in this process are shown in Figure 1.1 below.

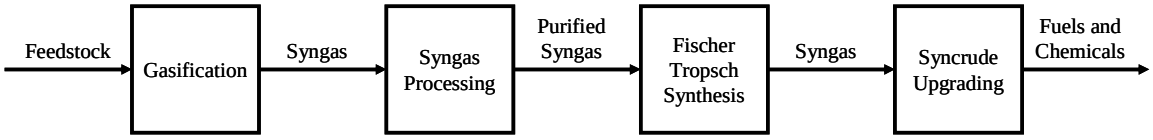

Figure 1.1 Schematic of the steps in thermo-chemical conversion of carbonaceous feedstocks using Fischer Tropsch Synthesis for CO hydrogenation.

1.1.2 Gasification

The syngas needed for FTS can be made from any carbonaceous material [8]. The sulfur level in the syngas needs to be very low (10 ppb), much lower than can be achieved by iron oxide sorbents or molecular sieves [9]. Zinc oxide, an effective sorbent, absorbs H_2S at its surface which then diffuses into the bulk. Zinc Oxide can also convert COS to H_2S [9]. CoMo and NiMo can convert most sulfur compounds to H_2S (and most halogenates to HX) [9].

Other syngas purity issues are nitrogenates (comparable to sulfur), tar and BTX - Benzene, toluene, and xylene - (below dew point), and particulates (no spec found) [10]. Other issues for an XTL plant are power generation (whether or not it sells power to the grid, it must be electrically self-sufficient) [9] and that hydrogen generation must be sufficient for both FTS and product upgrading.

Natural gas can be gasified by partial oxidation ($CH_4 + ½O_2 \rightarrow CO + 2H_2$), steam reforming ($CH_4 + H_2O \rightarrow CO + 3H_2$), or dry reforming ($CH_4 + CO_2 \rightarrow 2CO + 2H_2$). Industrially, on a small scale, steam reforming is best (due to not needing an oxygen plant) while, for large projects, partial oxidation is best (due to the economies of scale for an oxygen plant, though CO_2 removal is then required) [12].

Using cheap, stranded gas, a GTL plant would cost approximately $20 / BBL, with 50% of the cost as capital, 25% for operations, and 25% for the gas [12]. Another estimate puts the

breakdown as 64% capital, 21% operations, and 15% gas [8]. The capital cost distribution has been estimated to be 23% oxygen plant, 28% reforming, 24% FTS system, 13% product enhancement, 12% power recovery [8]. An energy efficiency of 65% and a carbon efficiency of 75% is normal for GTL [8].

Coal, because it has a far lower H/C ratio, behaves differently than natural gas [12]. This results in a higher CO_2 selectivity from gasification, leading to a lower energy and carbon efficiency [11,12]. Consequently, the capital cost for CTL is twice that for GTL [11]. The higher sulfur levels often seen in coal versus natural gas may necessitate a renewable sorbent rather than a sacrificial one [12]. Additionally, the variety of ash levels in different coals leads to differences in ideal gasifier design [12].

Biomass ("young coal") is similar to coal, gasifying at a slightly lower temperature, though it includes problems of high tar selectivity, aggressive ash formation, and challenges of size reduction for fibrous materials [13].

Approximately 75% of the capital cost in biomass to liquids through FTS is in biomass preparation (drying and size reduction), gasification, and syngas purification. Drying is an energy intensive process, but it can use plant waste heat. Dryer biomass leads to more energy efficient gasification, but leaner syngas. Drying costs increase markedly at below 10% moisture [10].

Another estimate of capital cost for BTL put the breakdown at 21% Biomass treatment, 18% Gasifier, 15% Oxygen plant, 18% Syngas cleaning, 1% WGS reaction (Water Gas Shift $CO + H_2O \leftrightarrow CO_2 + H_2$), 6% FT Reactor, 7% Gas Turbine, 11% heat recovery / steam generation, 4% other [14]. Biomass derived FT diesel has been estimated to cost 14 € / GJ (approximately $3.40 / gallon) to produce. With economies of scale and learning, it is asserted that the cost

could come down to 9 € / GJ

($1.90 / gallon) [14].

1.1.3 Fischer Tropsch Reactors

There are two modes of Fischer Tropsch operation: Low Temperature Fischer Tropsch (LTFT) and High Temperature Fischer Tropsch (HTFT) [4].

Iron is the only viable HTFT catalyst [15], with a common form being fused magnetite with K_2O and structural promoters (Al_2O_3 or MgO) [4]. The HTFT reactor is a two phase system (solid catalyst and bulk gas phase). If liquid accumulates outside of the catalyst particles, severe operational problems result [16]. Consequently, the propagation probability (indicative of the reactions tendency to produce heavy products: to be discussed in more detail later) is kept low (0.7) [17], resulting in a process geared towards light alkenes and gasoline [16].

The Brownsville, TX plant was an HTFT facility. The initial Sasol design for HTFT utilized a circulating fluidized bed. The current Sasol HTFT design (SAS) utilizes a fixed fluidized bed with tubing for cooling by steam generation. This design is smaller, cheaper, and better utilizes the catalyst [16].

The SAS catalyst size is typically 5-100μm. The SAS reactor may be operated between 20 and 40 bar and is run at approximately 340^{o}C [15]. High pressure impedes coking [19] while high temperature (especially over 350^{o}C) [16] promotes it. Between 1995 and 1999, eight SAS reactors were installed at Secunda. Four had a diameter (D) of 8m and a capacity of 11,000 BPD (capacity / D^2 = 172). The other 4 had a diameter of 10.7m and a capacity of 20,000 BPD (capacity / D^2 = 175) [16].

Table 1.1 A typical product distribution for HTFT (from Reference 15)

Methane	7%
C2-C4 olefins	24%
C2-C4 paraffins	6%
Gasoline	36%
Middle distilliates	12%
Heavy cut and waxes	9%
Oxygenates in water	6%

Table 1.2 HTFT Product Breakdown by type (from Reference 21)

Type	**C5-C10 Cut**	**C11-C14 Cut**
Paraffins	13%	15%
Olefins	70%	60%
Aromatics	5%	15%
Oxygenates	12%	10%

Both iron and cobalt are utilized for LTFT (ruthenium is highly active with excellent selectivity, but it is very rare and expensive) [19]. LTFT is carried out in two reactor types: fixed bed and slurry bed [16]. LTFT is used to generate wax and middle distillates. The wax has high value and can be sold [20] or cracked back into diesel [4].

The original Sasol LTFT design utilized iron in a fixed-bed reactor while the current Sasol design utilizes iron in a slurry-phase reactor. The Shell SMDS design utilizes cobalt in a fixed-bed reactor. The Sasol fixed-bed reactor (ARGE, several of which are still in operation)

has a diameter of 3m, holding 2050 tubes with an ID of 5 cm and a length of 12m. The reactor operates at 27 bar and 230^{o}C and originally had a capacity of 500 BPD. The catalyst is an extrudate with a diameter of 2.5mm. The reaction takes place within the tubes while steam is generated on the shell side to remove the heat of reaction [16].

In the Sasol slurry-phase reactor the syngas is bubbled through the wax media in which fine catalyst particles (40-150μm) are suspended [16]. Tubes run through the slurry in which steam is generated for heat removal. The primary operational challenge for the slurry-phase reactor is separation of the catalyst from the reaction media/produced wax [18]. In 1993, a 5m ID – 22m tall slurry-phase reactor with a capacity of 2,500 BPD was brought online [16].

There are many advantages of the slurry-phase reactor relative to fixed-bed operation. The slurry reactor gets much nearer to isothermal operation, has lower pressure drop (hydrostatic head -v- 5 bar), online catalyst removal, lower cost, and lower catalyst loading (though it should be noted that, at equal catalyst size, the slurry phase is less active [16]) [18]. It has been argued that developing a slurry reactor requires more capital and involves more economic risk [128]. Shell's SMDS process utilizes a fixed bed reactor, arguing against the advantages of slurry-bed operation.

A slurry-bed reactor was studied for HTFT, it was found that the media was continuously cracked, making this arrangement unviable [16].

Typical product distributions for LTFT on iron are as follows:

Table 1.3 LTFT product distribution using an iron-based catalyst (from Reference 21)

	Fixed-Bed Reactor		Slurry-Phase Reactor	
	C5 – C10	**C11 – C14**	**C5 – C10**	**C11 – C14**
Paraffins	53%	65%	29%	44%
Olefins	40%	28%	64%	50%
Aromatics	0%	0%	0%	0%
Oxygenates	7%	7%	7%	6%

Table 1.4 LTFT product distribution using an iron-based catalyst (from Reference 16)

	Fixed-Bed Reactor	**Slurry-Phase Reactor**
Methane	7%	5%
Gasoline	14%	15%
Hard Wax	27%	31%

Table 1.5 Wax selectivity for LTFT in fixed-bed and slurry-phase FTS (from Reference 21)

	Fixed-Bed Reactor	**Slurry-Phase Reactor**
Wax Selectivity	50% - 55%	55% - 60%

Based on the above, the slurry phase reactor gives a greater olefin selectivity, higher wax selectivity, and lower methane selectivity relative to gas-phase, fixed bed operation. Adiabatic

operation has been carried out as well, both by operating at very low single-pass conversion and by recycling liquids, but has not been industrially viable [16].

The raw FT gasoline from fixed-bed LTFT at Sasol has an RON (Research Octane Number – indicative of gasoline quality) of 35 while HTFT gasoline comes in at 88. Meanwhile, fixed-bed LTFT diesel has a cetane number (indicative of diesel quality) of 75, with HTFT coming in at 55 [51].

1.1.4 Fischer Tropsch Syncrude Refining

While energy and fuels are very high volume products, they have low value. For comparison, in 2007 WTI (West Texas Intermediate, a benchmark crude oil) had an average price of $\$.23/lb_m$ while ethylene had an average price of $\$.45/lb_m$ [22]. Detergents made from FT alcohols sell for six times the value of fuels [4]. Wax has more value as wax than as a fuel [4,23]. Consequently, an economically viable FT plant should pursue the chemical market as much as possible.

Fischer Tropsch syncrude is very different from petro-crude. Olefins are only sparingly present in petro-crude, while they are significantly present in cobalt LTFT syncrude and predominately present in iron LTFT and HTFT syncrude. The oxygenate content is very different, while syncrude lacks nitrogenates and sulfur compounds. Except for HTFT syncrude, FT syncrude is essentially free of aromatics [24].

This manifests itself in refining in several ways. Oxygenates can affect many hydroprocessing processes, including damaging catalysts. Paraffins have a harder path to coking than the compounds in petro-crude, allowing for milder refining conditions, resulting in longer catalyst life [24]. Additionally, Sasol includes an ammonia plant in their facility to make use of the nitrogen stream from the oxygen plant [25].

Some HTFT products are valuable enough to justify extraction: ethene, propene, 1-octene, and 1-decene. Other products can be reacted to form valuable chemicals, with some examples following. C6's and C7's can be aromatized to benzene and toluene. Benzene can then undergo alkylation with propene to form cumene (a valuable chemical and octane booster). C12 through C15 1-olefins can be hydroformylated to detergent alcohols (a high-value product) [20].

For fuels, what little wax is made in HTFT can be cracked back to diesel. The isomerization that occurs enhances cold-flow. While cetane is lost, raw FT diesel is well above the minimum specification. For gasoline, a great deal of isomerization is needed to achieve the necessary octane value. Light olefins can be oligomerized into the diesel and gasoline fractions. In theory, this would lead to highly branched compounds, but when it is done on a ZSM-5 catalyst, the structure of the catalyst inhibits branching [20].

The primary chemical product made by LTFT is wax. Color (whiteness) is a primary determinant of wax value (along with congealing point, penetrability, and carbon number distribution). Hydrogenation of the wax improves the color [18].

For fuels, oligomerization can be done, but using a cobalt catalyst [25] and/or a fixed bed reactor[20] make it less useful due to their lowering the olefin selectivity. Primarily, it is hydrocracking with associated isomerization that is done to increase the diesel selectivity by shifting carbon from the wax range back to diesel and improve the cold-flow properties by inducing branching. Due to stability concerns, the final product may need to be hydroprocessed to saturate olefins [20].

FT diesel has a number of advantages over petro-diesel. The first, obviously, is that it can be derived from sources besides petroleum. Beyond that, it is cleaner burning [26], it may

enhance motor oil durability [27], it has lower sulfur level even than Ultra Low Sulfur Diesel (5 ppm [28] versus 15 ppm [29]), and lower aromatic content (1% [28] versus 25% [30]).

There are problems with FT diesel, however. Due to the near-total lack of branched compounds in raw FT diesel, the cold-flow properties are problematic [20]. Due to the near-absence of aromatics, the density is below spec (The European density spec is 800-845 g / L). The raw FT diesel density is 776 (LTFT on cobalt), 770 (LTFT on iron), and 796 (HTFT) [129]. Mass density can be remedied by the addition of biodiesel, but this does not improve energy density, which can only be enhanced by the addition of aromatics [20]. The final problem is also seen with ULSD: lubricity. It has been thought that sulfur and/or aromatics were the source of lubricity, but this is undercut by biodiesel being an excellent lubricity additive [31]. It has been shown that minor components with oxygen and nitrogen promote lubricity [32]; Sasol now enhances their diesel fuel with a lubricity additive [33].

1.2 Fischer Tropsch Synthesis

1.2.1 FTS Mechanism and Kinetics

The specifics of the FT reaction mechanism remain uncertain [35]. However, it can be said that the FTS reaction is a polymerization reaction where the monomer is generated in situ from the reactants. The reaction occurs in three steps: (1) generation of the monomer / initiator / terminator, (2) chain propagation, and (3) chain termination. Even within these constraints, several plausible mechanisms have been proposed [34].

Because the FTS reaction is a polymerization process, it can be understood via the following diagram:

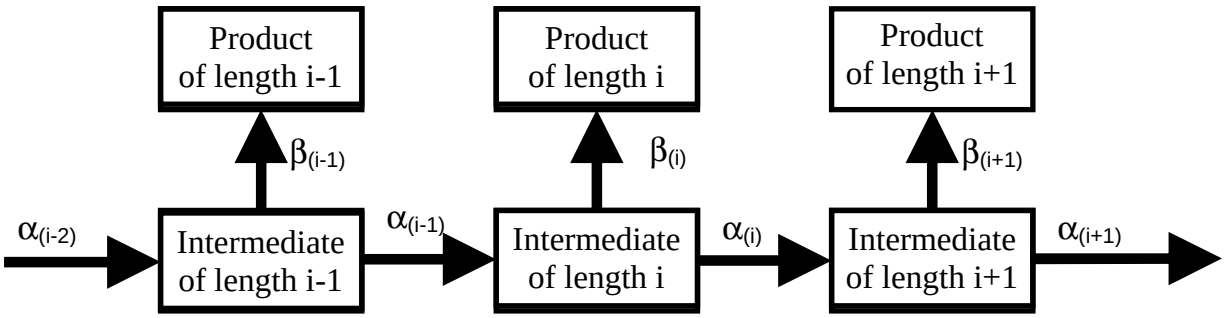

Figure 1.2 Diagram of polymerization by monomer addition

Implicit in the above model is that propagation is only by the addition of a single monomer, never by the addition of a dimer, oligomer, or polymer. The propagation probability (α_i) is the probability that a chain containing i carbons will grow larger (eventually terminating as a product with a carbon number from i+1 to ∞. The termination probability (β_i) is the probability that a chain containing i carbons will terminate to a product with i carbons. $\alpha_i + \beta_i$ must equal 1.

An additional assumption may be made, that α_i and β_i are independent of carbon number. Beginning with these assumptions and then working through the math gives:

$$\ln(n_i) = i * \ln(\alpha) + C \qquad \text{(Equation 1.1)}$$

This is the Anderson-Shulz-Flory (ASF) kinetic model. A product distribution that is consistent with this model (linear when ln (n_i) is plotted against i) is an ASF product distribution [34].

This model, which is often used to analyze FTS product distributions, creates a limit on the selectivity of the reaction to any particular product fraction, as is shown in the following plot.

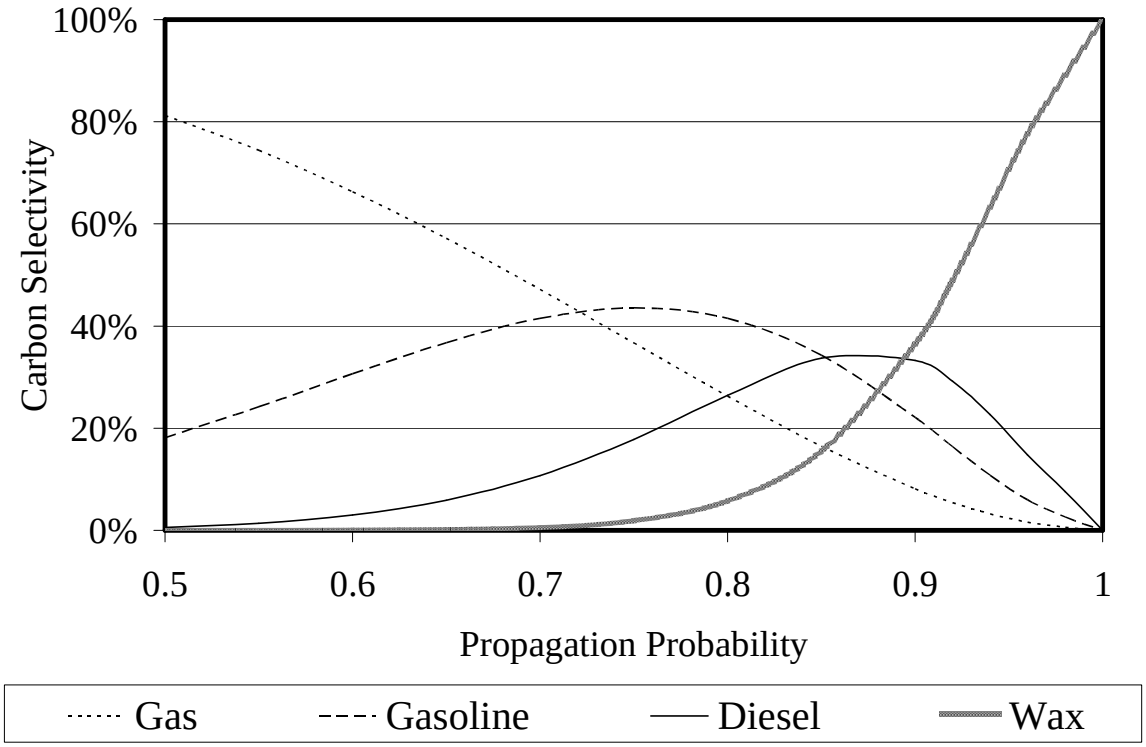

Figure 1.3 Product fraction selectivity (carbon basis) versus propagation probability

This demonstrates the importance of controlling the propagation probability in utilizing the Fischer Tropsch products.

A review of proposed mechanisms for the FTS reaction is as follows, with all reaction steps occurring on catalytic sites.

Alkyl Mechanism [34]:

1a) CO chemisorbs dissociatively

1b) C hydrogenates to CH, CH_2, CH_3

2a) The chain initiator is CH_3

2b) The chain propagator is CH_2

3a) Chain termination to alkane comes by α-hydrogenation

3b) Chain termination to alkene comes by β-dehydrogenation

Alkenyl Mechanism (Maitlis) [34]:

1a) CO chemisorbs dissociatively

1b) C hydrogenates to CH, CH_2

1c) CH and CH_2 react to form $CHCH_2$

2a) The chain initiator is $CHCH_2$

2b) The chain propagator is CH_2

2c) The olefin in the intermediate then shifts from the 2 position to the position

3a) Chain termination to alkene comes by α-hydrogenation

Enol Mechanism (Storch) [34]:

1a) CO chemisorbs non-dissociatively

1b) CO hydrogenates to CH(OH) and CH_2(OH)

2a) The chain initiator is CH(OH)

2b) The chain propagator is CH(OH) and CH_2(OH)

2c) Chain propagation is by dehydration synthesis and hydrogenation to CR(OH)

3a) Chain termination to aldehyde is by desorption

3b) Chain termination to alcohol, alkene, and alkane is by hydrogenation

CO-Insertion Mechanism (Sternberg) [34]:

1a) CO chemisorbs non-dissociatively

1b) CO hydrogenates to CH_2(OH)

1c) CH_2(OH) hydrogenates and eliminates water, producing CH_3

2a) The chain initiator is CH_3

2b) The chain propagator is CO

2c) Chain propagation forms RC=O

2d) RC=O hydrogenates to CHR(OH)

2e) CHRC(OH) hydrogenates and eliminates water, producing CH_2R

3a) CH_2CH_2R terminates to alkane by α-hydrogenation

3b) CH_2CH_2R terminates to alkene by β-dehydrogenation

3c) CHR(OH) terminates to aldehyde by dehydrogenation

3d) CHR(OH) terminates to alcohol by hydrogenation

Low Temperature Fischer Tropsch produces two classes of products: hydrocarbons and oxygenates. The predominant hydrocarbon products are n-paraffins, n-olefins (mostly terminal), and branched paraffins and olefins. Minor hydrocarbon products include aromatics and dienes. The predominant oxygenates are aldehydes (mostly linear), alcohols (mostly terminal and linear), ketones (with the carbonyl group mainly on the β-carbon), carboxylic acids (mostly linear), and esters (mostly linear). Minor oxygenate products include acetals, ethers, furans, and phenols. [34]

The Fischer Tropsch reaction is a complex combination of primary and secondary reactions with primary and secondary products. The primary product selectivity is the one seen when conversion extrapolates to zero [34]. The main primary products have generally been observed to be n-alkanes, 1-olefins, and perhaps 2-olefins[34,36,37]. Our own work to be presented in Chapter 4 should lead to some changes in this view. A proposed Fischer Tropsch mechanism should be able to account for the formation of all of the different primary products.

The first two mechanisms (alkyl and alkenyl) begin with the dissociation of CO into C and O with the oxygen making no contribution to the mechanism beyond that. As such, if these are the propagation mechanism of the reaction, oxygenate formation requires a separate step. Reactions with OH groups have been proposed to account for this, though experimental evidence

is wanting) [34,40]. CO Insertion as an alternative termination pathway for the formation of oxygenates has considerable support [34]. The enol and CO insertion mechanisms are oxygenate mechanisms and so do not require a separate step for the formation of oxygenates.

Aside from the issue with oxygenate formation, the two primary weaknesses of the alkyl mechanism are the high energy barrier for CO dissociation [47,48,131,132] and sp3-sp3 coupling [35,49]. In spite of these problems, the alkyl (aka carbide) mechanism has been asserted as the main propagation mechanism for all FT catalysts [34,40] or just for cobalt [42].

The alkenyl mechanism solves the sp3 problem of the alkyl mechanism, but adds a new problem: failing to account for the primary formation of paraffins [34,35]. The mechanism is not without its defenders, but nor is it without its detractors (one of whom concluded "*Therefore, the contribution of the mechanism proposed by Maitlis et al. does, in our opinion, not contribute to the chain growth mechanism in the Fischer–Tropsch synthesis*" [50]).

Various possible forms of non-oxygenate mechanisms were studied by Liu and Hu (2002) [35] by simulating the activation energy for various C-C couplings on Ru. The following results were generated:

Table 1.6 Simulated energy barriers for various C-C couplings (from Reference 35)

Species	Ru Step (eV)	Ru 0001 (eV)
C + C	1.05	1.51
C + CH	0.43	1.01
C + CH_2	0.56	1.08
CH + CH	0.95	0.87
CH + CH_2	1.20	0.97
CH_2 + CH_2	0.59	1.23
CH_2 + CH_3	1.40	1.80

With the exception of CH_2-CH_2 (Maitlis) coupling, coupling is only energetically preferred between very hydrogen-deficient species (C-CH, C-CH_2, CH-CH) [35]. Brady and

Pettit (1981) studied the addition of CH_2N_2 (which decomposes to give CH_2 group to the Fischer Tropsch reaction), saw enhancement in heavy product formation, and concluded that the reaction propagates by CH_2 insertion on cobalt [133]. Additionally, Barneveld and Ponec (1984) ran the FT reaction without CO, replacing it with various CH_xCl_{4-x} and found that an FT-like distribution could be realized. The product distribution became more FT-like the more hydrogen atoms were replaced with chlorine atoms[45].

However, it has been pointed out that a reaction requires both low activation energy and high surface coverage [131]. Activation energy simulation addresses the first but not the second while the addition of a potential reactant can radically alter the surface coverage.

The enol and CO insertion mechanisms are both oxygenate mechanisms in which the carbon-oxygen bond is not broken prior to insertion into a growing chain. The key difference between the two is that, in the enol mechanism, both the initiator and the propagator (monomer) are oxygenate species. Propagation is by dehydration synthesis. In CO Insertion, the initiator is a non-oxygenate group and the propagator is CO (possibly partially hydrogenated). The intermediate that results from the propagation reaction is then hydrogenated to produce the homologated initiator. Burton Davis observed that terminal alcohols produce predominantly straight-chain hydrocarbons while non-terminal alcohols produce predominantly branched hydrocarbons [81], concluding that the carbon-oxygen bond in the initiator species was not broken prior to propagation (supporting the enol mechanism). His work has made a strong argument that, on an iron catalyst, CO_2 can act as an initiator without being first converted to CO while, to act as a propagator, CO_2 must first be converted to CO [81], leading him to conclude that the initiation species is a CO_2-like species. Others, however [134] have argued that the energetic pathway for CO insertion is the most reasonable. Several variations of CO insertion

have been proposed, with RCH + CO being asserted to be especially low [131]. In Chapter 6 (Future Work), a number of observations will be aggregated, indicating a variation of CO Insertion unlike those normally proposed.

The participation of 1-olefins in the FTS process is well established, being able to undergo hydrogenation (to an alkane of the same carbon number), hydoformylation (to an alcohol of one greater carbon number), hydrogenolysis (to an alkane of one lower carbon number), isomerization (to an internal olefin of the same length), and incorporation (to heavier hydrocarbons).

The primary reaction undergone by co-fed olefins has been consistently been demonstrated to be hydrogenation [38,39,36], though Iglesia convincingly argues from the changes in selectivity with conversion / space velocity that in situ alkenes behave differently than added ones, including far less saturation and far more propagation [36]. This supports the contention [140] that the product olefinicity is partly thermodynamically driven. Some degree of hydroformylation of added olefins has also been demonstrated to occur [39,46]. Under typical FT conditions, hydrogenolysis of olefins is not significant [40]. Isomerization to internal olefins occurs, with the observation that no hydrogen exchange (shown with hydrogen – deuterium exchange) occurring in alkanes, but hydrogen exchange occurring at the 1, 2, and 3 positions for 1-olefins [41]. For incorporation, it has been demonstrated that alkenes reincorporate as chain initiators, not propagators [42].

Davis demonstrated that, on iron, alcohols are much more reactive than alkenes. Using C14 labeling, it was demonstrated that, for light hydrocarbons, the number of alcohol-origin carbons per product molecule is constant (indicating that alcohols act as initiators rather than propagators). In mid-range hydrocarbons, the number of alcohol-origin carbons per product

molecule drops to less than 1 [43]. This could be interpreted as a dual-mechanism process, but Davis interpreted it as reactor holdup [44]. Alcohols are nearly inert on cobalt catalysts under FT conditions [44]. Burt Davis' group has also shown that, in attempting to incorporate C_2D_5OH on an iron-based catalyst, no D_5 heavier products were formed [145]. This was interpreted as being due to rapid H-D exchange (there were D_0, D_1, D_2, D_3, and D_4 heavier products formed. An alternate interpretation for this observation will be given in Chapter 6 (Future Work).

Acetylenes incorporate in another interesting way on cobalt: through dimerization. Though that this occurs both before and after the catalyst has been deactivated with thiophene, so it may be that this (hydroformylation shows the same behavior) is not part of the FT process [46].

Their may be more than one active mechanism in the Fischer Tropsch process. Gaube and Klein (2008) [135] concluded that both the carbide (CH_2 insertion) and CO insertion mechanisms were present on iron and cobalt. These two mechanisms operating in parallel were used to explain the classic 2-alpha product distribution (carbide at low carbon number (low alpha) and CO insertion at high carbon number (high alpha)). It is proposed that CO insertion is more dominant for cobalt than iron. It is also argued that alkali addition increases the high carbon number propagation probability (attributed to CO Insertion) but not the low carbon number alpha value (attributed to CH_2 insertion). Other explanations given for 2-alpha behavior are (for iron) the presence of both alkalized and non-alkalized iron (though this explanation is weakened by the same behavior being present with cobalt) [136], chain-length dependent secondary reactions [137], and by an inherent multiplicity in the propagation probability [138]. Another observation of interest is that the selectivity of branched products decreases markedly with carbon number [34]. The connection between decreased probability to termination as a

branched product and decreased overall termination probability with increasing carbon number is intriguing.

The Fischer Tropsch reaction is generally seen as being kinetically controlled (as opposed to being thermodynamically controlled), as simulations have shown that thermodynamics prefers methanation to heavy product formation [17]. Diane Hildebrandt's group, however, has done work demonstrating possible thermodynamic contributions to the overall product distribution [139] and the olefinicity at each carbon number [140].

The work in chapter 4 makes a strong argument for an oxygenate mechanism for iron-based Fischer Tropsch. At the time, we argued for the standard version of CO Insertion, but have since come to believe that a modification of this theory better predicts the observations made in that chapter and work published by other groups (as will be discussed in Chapter 6. Additionally, I am skeptical that the mechanism for cobalt and iron would vary in anything but minor ways. The difference in product types that can be attributed to a different mechanism can also be attributed to cobalt's greater tendency towards catalyzing secondary reactions.

A number of kinetic equations have been proposed for FTS. Mark Dry has endorsed the following [4]:

Iron $$r = \frac{mP_{H_2}P_{CO}}{P_{CO} + aP_{H_2O}}$$

Cobalt $$r = \frac{mP_{H_2}P_{CO}}{(1 + bP_{CO})^2}$$

Figure 1.4 Proposed kinetic equations for FTS (Reference 4)

The numerator of both is the same. The denominator of both includes CO, consistent with carbon monoxide's general status as a (reversible) catalyst poison. Both kinetic equations also support hydrogenation as rate-limiting steps. The kinetic equations indicate that water inhibits iron but not cobalt. For iron at low conversion ($P_{water} \approx 0$), the FTS rate is independent of CO partial pressure. On cobalt at high CO partial pressure, the rate is proportional to P_{H_2}/P_{CO}.

1.2.2 Process Parameters and Process Performance

Increasing the reaction temperature increases the conversion and the methane selectivity while decreasing the heavy product selectivity. Skeletal isomerization increases with temperature while the alcohol selectivity decreases. The effect of temperature on olefin selectivity is less straightforward. Carbon deposition increases with temperature, but that is primarily a concern in HTFT operation [40].

Mark Dry concluded that increasing the reactor pressure has little effect on the product distribution on iron, but that wax selectivity on cobalt is markedly enhanced by increased pressure [21,51]. Increasing the total pressure has generally been said to increase the oxygenate selectivity [40,51] while decreasing the methane selectivity [40]. The olefin selectivity is not affected by pressure. The rate of coking for HTFT is proportional to $P_{CO}/P_{H_2^2}$, so with increasing pressure the rate of coking decreases [19].

Increasing the ratio of H_2 to CO in the reactor feed (the syngas ratio) decreases chain length and increases methane formation while decreasing coking. It also increases chain branching and decreases the selectivity to olefins and oxygenates [40].

Increasing space velocity decreases conversion. This increases the olefin and oxygenate selectivity while inhibiting methane formation [40]. The influence of space velocity on the carbon number distribution is debatable. Bukur found no change [40] while Iglesia [36] has

found a shift in product distribution with space velocity, which he and others have attributed to secondary reactions leading to non-ASF behavior.

1.2.3 LTFT Catalysts

1.2.3.1 Cobalt -v- Iron

The price of cobalt is three orders of magnitude higher than that of scrap iron [4]. Consequently, cobalt must have performance advantages to justify its use. Espinoza compares their activity as follows:

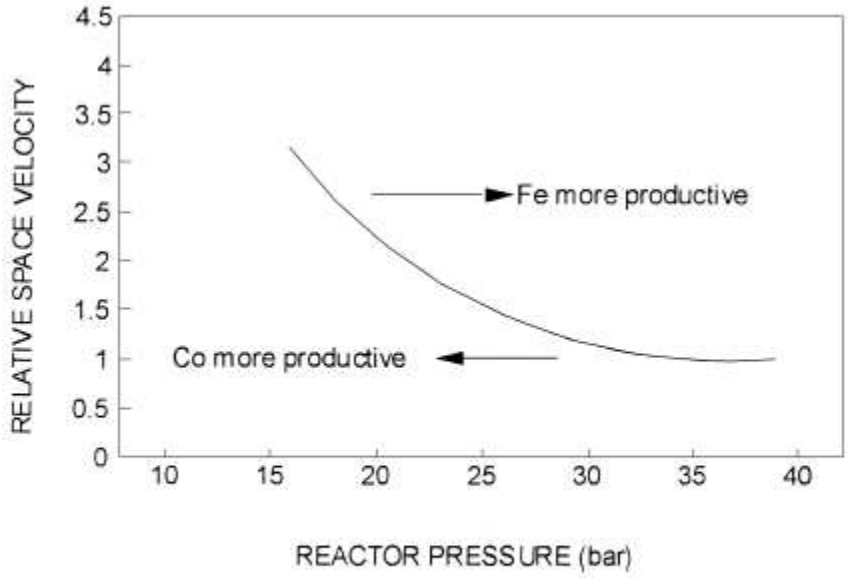

Figure 1.5 Preference curve for LTFT: iron (240^{o}C) and cobalt (220^{o}C). From Reference 18. Reproduced with permission from Elsevier through Rights Link.

A cobalt active site has a higher TOF (Turn-Over Frequency: the rate of reaction per active site) than an iron site (by a factor of 3 [54]), but an iron catalyst has a higher density of active sites, bringing the comparison closer to parity [18]. The kinetic equations above indicate the shape of the equivalence curve between iron and cobalt. At sufficiently high P_{CO}, the cobalt reaction rate is independent of pressure (assuming constant composition) while the rate on iron is

proportional to pressure. At the same time, water impedes the FT reaction on iron, so high conversion decreases the reaction rate on iron but not cobalt. As such, low space velocity (high conversion) and low pressure favor cobalt.

Cobalt is generally more resistant to deactivation (such as coking) than iron as well as offering greater attrition resistance (because of the oxide support) [2]. Iron catalysts are active for the WGS reaction (at HTFT conditions the reaction goes rapidly to equilibrium [4]), allowing for a much more broad syngas ratio (0.5 to 2.5 for iron [2] versus 2.0 [2] or 2.15 [4] for cobalt) as well as a lower usage ratio (1.7 for iron versus 2.15 for cobalt [4]). Syngas ratio is the ratio of H_2 to CO in the feed while usage ratio is the ratio of the H_2 and CO consumption rates. This, along with the somewhat lower tolerance for sulfur (100 ppb for cobalt versus 200 ppb for iron) makes cobalt particularly well suited to natural gas conversion. The primary differences in product selectivity are that iron makes more CO_2 (hence the lower usage ratio), less methane, more olefins, and has demonstrated a slightly higher maximum propagation probability (0.95 versus 0.94) [2].

1.2.3.2 Cobalt LTFT Catalysts

Because of the high cost of cobalt, it is important that the desired performance be realized using as little cobalt as possible. To that end, cobalt (metallic cobalt being the active material for FTS [2]) is usually dispersed on a high surface area support (often alumina, silica, titania, etc) at a loading of 10 to 30 g per 100g of support [4].

One of the fundamental issues in heterogenous catalysis is structural sensitivity (particle size effects). For a structure-insensitive reaction, the turnover frequency (TOF: the rate of reaction per active site) and selectivity are independent of the active material crystal size. A reaction with multiple pathways and products in which all are structure insensitive would show

no influence of the active material particle size on selectivity. Based on data using cobalt and cobalt promoted with ruthenium on a variety of supports with a cobalt dispersion from less than 1% to 10%, Iglesia concluded that the FT reaction was structure insensitive [36].

Bezemer et al [52] impregnated cobalt nanoparticles onto carbon nanotubes and discovered that there was a break at a particle size of 5 nm (approximately 27% dispersion): larger than 5nm the TOF was constant (structure insensitive) while below 5nm the TOF dropped quickly. When TOF decreased, the methane selectivity increased and the olefinicity and C5+ cut of the product dropped. They concluded that the nonclassical particle size effects were the cause. Work using homogeneous ruthenium mono-atomic and di-atomic clusters [134] demonstrated ensemble effects: the reaction requiring more than a single atom to proceed.

Bezemer also noted that EXAFS analysis showed a decrease in cobalt coordination during the reaction [52]. Shell researchers visually demonstrated the same phenomenon [53]:

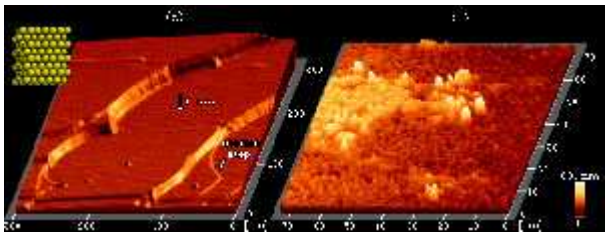

pre-reaction post-reaction

Figure 1.6 Demonstration of surface reorganization in FTS from Reference 53. Reproduced with permission from ACS through Rights Link.

Given that the particle size effects often come out of differences in the balance between different exposed facets and coordination numbers, this radical rearrangement of the catalyst surface would lessen the applicability of traditional particle size effect models to the FT reaction.

The primary function of the support is to allow for the formation of small, stable cobalt particles. The most common support is a porous oxide, frequently silica, alumina, and titania.

Enrique Iglesia [36] demonstrated little or no influence of support on TOF. He did observe some influence of support on the hydrocarbon distribution (alumina had the highest methane selectivity and steepest ASF plot with titania and silica showing very similar behavior).

Burtron Davis' group demonstrated that a silica support gives a lower dispersion than titania which gives a lower dispersion than alumina [55]. The strength of alumina's strong interaction with cobalt is high dispersion. The strength of silica's weaker interaction with cobalt is that the resulting cobalt is easier to reduce. They also showed that a higher surface area support results in a more highly dispersed, harder to reduce catalyst.

There are also non-traditional supports such as carbon / carbon nanotubes and monoliths. Oxide supports interact with cobalt to form composite oxides which are very difficult to reduce and thus are inactive. Carbon lacks these strong interactions, but pays for it by being less stable. In at least one example, carbon-supported cobalt gave entirely saturated hydrocarbons. In unpublished work in our lab, similar behavior was seen when silica was dispersed in micro-fibrous nickel and cobalt dispersed in the composite. The use of acid catalysts as FT supports will be discussed in the "Fischer Tropsch Syncrude Processing for Fuels" section.

Monolithic supports have been demonstrated to give products similar to a powder catalyst, but without the high pressure drop [62]. Adding oil circulation for heat management resulted in lower activity but improved selectivity [63].

Catalyst promoters can be split into two classes: structural promoters and electronic promoters. Structural promoters increase the number and stability of active sites without changing the behavior of the active sites. Electronic promoters change the activity (TOF) or selectivity of the active sites. [54].

The primary promoters for cobalt FT catalysts are noble metals: mainly Ru, Pt, and Re. Ruthenium has been demonstrated to promote the reduction of cobalt oxide [54,55], increasing the number of active sites. Ruthenium promotion has also generally been noted to promote C5+ selectivity [54], with Iglesia observing an increase in TOF (by a factor of 3) and C5+ selectivity (from 84.5% to 91.1%), but no change in activation energy at a Ru/Co atomic ratio of 0.0067 [56]. He concluded that ruthenium increased the active site density.

A number of studies of platinum promotion of cobalt have indicated that platinum aids in cobalt reduction and subsequently increases activity while not affecting selectivity [54]. The mechanism for Rhenium promotion is unclear, but it also appears to enhance effective dispersion (through percent reduction) without affecting selectivity [36,54].

A second class of promoters is oxides such as lanthanum oxide, zirconia, and manganese oxide. Thorium has been seen as an excellent additive for cobalt-based FTS for almost as long as there has been cobalt-based FTS [57], but was phased out due to its radioactivity [58].

Fernando Morales lists lanthanum oxide as both a structural promoter (enhancing activity and/or stability) via support stabilization and as a decorating (as opposed to alloying) electronic promoter (affecting selectivity) [54]. It has been shown to promote reduction and increase conversion, suppress methane selectivity, slightly enhance olefin selectivity, and have little or no effect on propagation probability [57]. The same study also demonstrated that simultaneous impregnation of La and Co is superior to sequential impregnation in either order.

Zirconia (ZrO_2) is described as a structural promoter via support stabilization and cobalt gluing, a decorating electronic promoter, and as a synergistic promoter (enhancing stability by promoting de-coking and H_2S absorption [54]. A study in which alumina was promoted with

zirconia prior to impregnation showed improved reducibility, enhanced activity (without affecting intrinsic activity), suppressed methane selectivity, and improved C5+ selectivity [59].

Manganese Oxide as a structural promoter through increased dispersion, a decorating electronic promoter, and a synergistic promoter (for Water-Gas-Shift) [54]. Bezemer et al [60] showed that small loadings of manganese can enhance activity and selectivity for FTS using cobalt on carbon nanofibers. Keyser et al [61] prepared a composite Co and Mn catalyst by coprecipitation and used it to very long time on stream (70 days). During early TOS, the catalyst had low activity, low methane selectivity, and moderate olefin selectivity. With increasing TOS this behavior was lost and the composite structure segregated into cobalt and manganese phases.

The most common synthesis technique for cobalt FT catalysts is incipient wetness [2] in which a precursor salt is dissolved in a precursor solution (typically water) to make a precursor solution, which is then used to fill the pore volume of the support. When the support is then dried, it has been impregnated with the precursor salt. This can then be calcined to make cobalt oxide, and finally reduced to make elemental cobalt.

Incipient wetness impregnation can utilize any salt that contains the desired metal, though two factors have a large part in determining the salt: solubility and decomposition. The higher the solubility of the salt in the precursor solution media (usually water), the higher the loading that can be achieved with a single impregnation. This makes chlorides and nitrates excellent choices. The ease of decomposing the impregnated precursor to the metal or metal oxide is the other concern; this makes chlorides impractical. Consequently, nitrates are the most common precursor salt [2].

Several studies have compared cobalt catalysts made with cobalt nitrate with those made with cobalt acetate. Girardon et al [64] showed that cobalt acetate, during calcination, led to

more cobalt silicate species than did cobalt nitrate. Consequently, the activity of a cobalt acetate-based catalyst was much lower. Additionally, they saw that cobalt acetate gave a slightly higher methane selectivity and slightly lower propagation probability. This correlation between stronger metal-support interactions and light product selectivity was noted above in Enrique Iglesia's work as well [36]. Kaoru Fujimoto's group [65] studied cobalt nitrate and acetate and found minimal influence of precursor on selectivity, but a strong influence on activity. Pure nitrate was significantly more active than pure acetate, with catalysts made from mixed precursors comparable to the nitrate. Kraum and Baerns [66] added cobalt II acetyl acetate and cobalt III acetyl acetate to the same comparison, the catalyst activity varied with precursor: acetate (26.2% conversion), AcAc3 (23.6%), nitrate (14.7%), and AcAc2 (7.6%). The propagation probability was also impacted by the precursor choice: nitrate (84%), AcAc2 (84%), acetate (74%), AcAc3 (71%). In summary, we end up back where we started: with cobalt nitrate as a good precursor salt.

Another type of precursor is cobalt carbonyls, which can use an organic solvent for impregnation, can be processed to metals without high-temperature treatment, and have been shown to give excellent catalysts [2].

Calcination is a (typically) high-temperature oxidation to convert the precursor to its metallic oxide. Reduction is a (typically) high temperature process for converting the oxide or precursor to the metal. Girardon [64] varied the calcination temperature for both a cobalt nitrate-based catalyst and a cobalt acetate-based catalyst. The cobalt nitrate-based catalyst showed an improvement in FTS activity when the calcination temperature was increased from 373K to 423K, but a decrease in activity when the calcination temperature was further increased to 673K. The activity of the acetate-based catalyst consistently dropped with increasing calcination

temperature. Duvenhage and Coville [67] studied Co-Fe composite catalysts. Increasing the reduction temperature from 250^{o}C to 300^{o}C improved the catalyst activity in each case, while the activity resulting from increasing the reduction temperature to 400^{o}C was lower than the activity after reduction at 250^{o}C or 300^{o}C. Increasing the calcination temperature through the same sequence generally hurt the resulting catalyst activity.

Increasing the catalyst loading was shown by Burtron Davis' group [55] to decrease the dispersion while increasing the reducibility. This creates a potential tradeoff controlling the effective dispersion (% dispersion x % reduction), though in that study the effective dispersion decreased with increased loading in each case. TPR analysis of these catalysts showed that the high temperature (>700K) broad bump due to hard to reduce components varied little with loading while the reducible cobalt peaks grew with increased loading. Meanwhile, Kaoru Fujimoto's group [57] showed that increasing the catalyst loading markedly increased activity per unit cobalt (this work was done on silica rather than on alumina as was used in Burtron Davis' work [55]).

A variation on the above is eggshell catalysts. Powder catalysts present reactor problems such as pressure drop while uniform pellets or spheres introduce intra-pellet diffusion. Eggshell catalysts overcome this by placing all of the active material near the pellet surface [2]. Enrique Iglesia's group [68] ran the FT reaction with a uniform sphere, an eggshall sphere, a crushed uniform sphere, and a crushed eggshell sphere catalyst. The crushed eggshell and crushed uniform pellets behave essentially identically while the uniform pellet was worse than both. The eggshell pellet's performance was much closer to the crushed pellets than the uncrushed, uniform pellet. This indicates the influence of diffusion on FTS performance, with the eggshell catalyst,

like the powder catalyst used in slurry-phase FTS, significantly decreasing diffusion length and subsequent diffusion resistance.

Two ways to make an eggshell pellet are to pre-fill the inner pore volume with a heavy hydrocarbon prior to impregnation, and to impregnate the support with a molten salt, but only allow very short contact time [68]. Another means for producing eggshell catalysts is through manipulating the drying process's parameters (including rapid drying) [69].

Other procedures for making cobalt-based FTS catalysts include wet (slurry) impregnation (which is practiced by Sasol and has been shown to give more uniform cobalt cluster size [55]), co-precipitation, deposition-precipitation, and any of the various modes of generating nanoparticles which can then be deposited on supports [2].

Two further observations have been made about cobalt-based LTFT are the response to moderate levels of water and to CO_2. Iglesia's group [36] has noted that, for cobalt on titania, water improves both the activity and selectivity (decreased methane selectivity, increased C3 olefin selectivity). He noticed the same effect on large-pore silica. Khodakov, in his review [2], notes that this is a not-uncommon observation on silica, though water has been observed to either decrease or not effect FT activity at moderate levels. According to Iglesia [36], once the water influence is 'saturated', the activity of FT cobalt active sites are independent of the support.

While iron has been regarded as an effective catalyst for hydrogenating CO_2, cobalt has not. However, it has been demonstrated that both catalyst are capable of doing so. There is a massive difference in selectivity, though, with iron giving a product distribution comparable to that seen with CO and cobalt giving mostly methane with some hydrocarbon gasses when hydrogenating CO_2 [70].

Cobalt FT catalysts deactivate for a number of reasons. Poisoning can occur by sulfur, halogens, nitrogenates, etc. as was discussed in gasification. A second mode of deactivation is oxidation. Under realistic FT conditions, bulk cobalt will not be oxidized, but cobalt spheres smaller than a 4.4 nm diameter are likely to be oxidized by water [147]. Cobalt – support composites are often amorphous, making them hard to characterize [2]. In spite of this, Chen et al identified cobalt silicate species and noted their formation as a primary mode of deactivation [71]. Sintering of the active material, leading to loss of active sites, has also been identified as a prominent source of deactivation [72]. Cobalt carbide formation has been observed as deactivation mechanism as well [141]. Finally, in a fixed-bed reactor, waxing of the catalyst may deactivate the system by increasing diffusion resistance [2]. This can be remedied by washing the catalyst with a solvent, but the benefit proves to last on the order of minutes at high-alpha operation [51].

1.2.3.3 Iron LTFT Catalysts

Iron LTFT catalysts can be categorized into two types: supported and unsupported (or self-supported). Unsupported iron catalysts can be made by either batch or continuous precipitation.

An example of a batch precipitation was given by Mark Dry [51]: a near-boiling solution of iron and copper nitrate (40 g iron and 2 g copper per liter) is poured into a hot solution of sodium carbonate over a few minutes while stirring briskly until the pH falls between 7 and 8. The precipitate is washed with hot distilled water to remove impurities. The paste is then re-slurried and impregnated with potassium silicate to give the desired silica content. Nitric acid is added to leach potassium down to the desired content. This is then washed and filtered. The

filter cake is then either pre-dried, extruded, and dried (for fixed-bed operation) [2] or re-slurried and spray-dried (for slurry bed operation) [21].

An example of a continuous precipitation procedure is given by Enrique Iglesia's group [77]: Beginning with near-boiling water (80^{o}C), a solution of iron nitrate and zinc nitrate (the catalyst in question being zinc-promoted) is added at a constant rate to water (which is being maintained at 80^{o}C and vigorously agitated) at a known rate. Ammonium carbonate is manually added to the water to maintain the pH at 7. When the desired amount of catalyst has been made, the catalysts is washed, filtered, dried, and calcined. The catalyst is then promoted via incipient wetness with copper (copper nitrate) and potassium (potassium carbonate), then dried and calcined again (at 400^{o}C)

Before the initial iron paste is dried, the pore volume of the catalyst can be enhanced by replacing the water with a low surface tension liquid like ethanol [77,51], though this does decrease the physical strength of the catalyst (which is a problem in slurry-bed applications) [51]. The catalyst activation (reduction) is usually done with hydrogen, syngas, or carbon monoxide. The advantage of syngas activation is that, in an XTL facility, it is readily present. Due to product upgrading, hydrogen will also be available in an XTL plant. Pure carbon monoxide is likely to be unavailable, however.

In terms of catalyst performance, carbon monoxide activation has generally been regarded as the best option [81]. This is especially illustrated by the following:

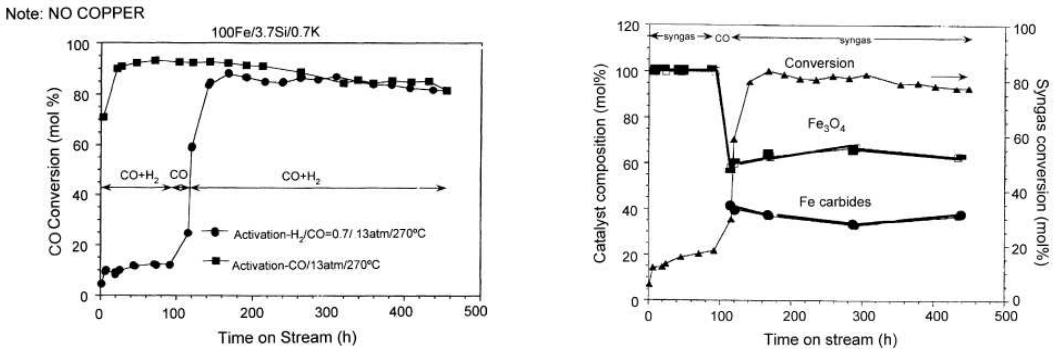

Figure 1.7 Conversion and catalyst composition –v– TOS for iron-based FTS demonstrating the superiority of CO activation to H_2 activation (from Reference 81). The catalyst used is not promoted with copper. Reproduced with permission from Elsevier through Rights Link.

Without copper, carbon monoxide activation is needed to form carbides and produce appreciable FT activity. The addition of copper improves the situation somewhat [44].

Sasol also showed that, while surface area and pore volume dropped both during reduction and FT operation, the area and volume in large pores increased noticeably [51].

Mark Dry [51] has written that catalysts made from impregnating iron on oxide supports offer inferior activity and selectivity compared with precipitated iron catalysts. The comparison is difficult because potassium partitions between the iron and silica (often regarded as the best of the traditional supports [51]), lessening the promotion effects [51]. A study by Dragomir B. Bukur showed that silica was a better support than alumina, but that the silica supported catalyst gave a more paraffinic and lighter product than the precipitated catalyst (possibly due to potassium partitioning) [82].

The following figure was taken from reference 19 (not original to that reference). It shows the changes in the composition of an HTFT catalyst with time. Similar phenomena are assumed for LTFT operation.

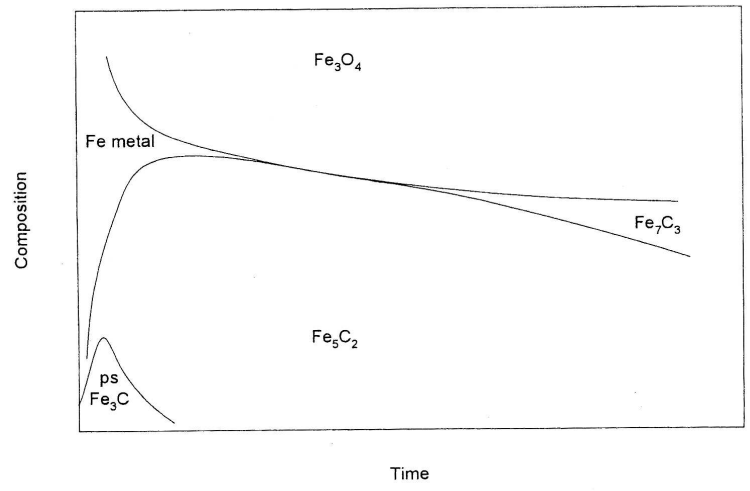

Figure 1.8 Iron HTFT catalyst: catalyst composition versus TOS from Reference 19. Reproduced with permission from Elsevier through Rights Link.

As was noted previously, the carbide phase correlates with high activity, though there doesn't appear to be a correlation between catalytic activity and carbide type [2]. Burtron Davis' group has concluded that a mature iron catalyst exists in a predominately core (iron oxide) – shell (iron carbide) form [127].

The primary classes of iron promoters are alkali promoters (which enhance basicity), reduction promoters, oxide supports, and other.

At atmospheric pressure, alkali promotion of cobalt significantly enhances wax selectivity. At the more realistic pressure of 15 bar, the advantage disappears [51]. On iron, however, increasing the K_2O content from 0% to 3% increases the hard wax selectivity (on a hydrocarbon basis) from 5% to 63% [51]. In general, the effect of promoting an iron FT catalyst with potassium is to suppress methane formation while enhancing olefin and heavy product selectivity [74].

Any of the alkali metals can be used. In theory, the promotion would increase in the order of Li < Na < K < Rb < Cs < Fr due to their basicity. Mark Dry reported [51] that, taking

potassium as a basis, the activity of iron catalysts promoted with alkali metals is: Li (40), Na (90), K (100), Rb (90). The decrease in promotion seen in going from potassium to rubidium was explained as a side-effect of high wax selectivity [51]. Burtron Davis' group [74] concluded that Rb, Cs, and Li are inhibitors while K offers the best promotion of the alkali metals. The methane selectivity (cross-plotted against conversion) was highest for the unpromoted catalyst. Lithium promotion was slightly better, sodium much better, then potassium and cesium were essentially even with rubidium slightly better still. Burtron Davis' group [75] also studied alkaline earth metals as promoters, finding that they were uniformly inferior to potassium.

Copper promotes catalyst reduction which enhances activity [76]. Enrique Iglesia's group [77] replaced copper with ruthenium and found no effect on selectivity, but an improvement in activity. This was credited to promoting nucleation of smaller domains. A similar effect was seen with palladium, though it included enhanced water-gas shift and decreased olefin content (and, while ruthenium was used in the same atomic amount, palladium use was much lower) [78]. Copper is not used with cobalt catalysts because the resulting catalyst has worse activity maintenance [51].

For iron catalysts that are primarily self-supported, support materials are still often added to improve thermal [51] and mechanical [79] stability. Silica is generally regarded as best [51]. Zinc was used as promoter by Enrique Iglesia's group [77], where it was demonstrated that zinc improved the catalyst's activity without affecting selectivity. It has also been used in our group and studied by our collaborator: Dr. Mohindar Seehra, who found that the zinc forms a composite oxide with iron. The resulting catalyst had a far smaller crystal size but comparable activity to a zinc-free catalyst. Many groups have studied manganese promotion for iron FT

catalysts [54] and have concluded that they benefit activity, selectivity (suppressing methane formation and enhancing olefin selectivity), and resistance to activity loss.

As iron FT catalysts are active for both FT and WGS, there is the question of whether the two reactions use the same site. Gerard P. van der Laan and Antonie A. C. M. Beenackers stated [83] that it is generally accepted that the FT reaction and the WGS reaction occur on different sites. Burt Davis' group concluded otherwise [84].

1.3 Supercritical Fischer Tropsch (SC-FTS)

1.3.1 Introduction

Gas Phase Fischer Tropsch suffers from a series of problems. Localized overheating ("Hot spots") leads to undesired selectivity and loss of catalyst activity [91]. The reaction's exotherm necessitates a high velocity in a high number of small tubes, resulting in a large pressure drop, poor economies of scale [16], and the potential for thermal runaway [142].

To solve these problems, Sasol developed a slurry-phase reactor. The expected advantages were realized, as noted previously. Additionally, the slurry reactor (operated with a powder catalyst compared with a fixed bed reactor operating with a pellet catalyst) requires lower catalyst loading to achieve the same production rate [16]. Several authors state that reaction rates are lower in slurry-phase operation than gas phase [86,91,94], which may be the case when a powder catalyst is used in both. The need to separate the wax media from the solid catalyst is a complication of this arrangement [16].

Supercritical Fischer Tropsch was developed to mitigate the weaknesses of gas-phase operation while allowing for fixed-bed operation.

SC-FTS has been utilized for all three FT catalyst elements: iron (6 references) [87,88,89,99,106,107], cobalt (19 references) [85-87,90-98,100-105,108], and ruthenium (2 references) [87,91]. The cobalt catalysts were on a variety of support compositions and properties. In all but one case, the iron catalyst was precipitated (in reference 106, it was a fused (HTFT) iron catalyst). In one study [95], a fluidized bed reactor was studied in addition to a fixed-bed reactor. In all other studies, supercritical FTS was studied exclusively in a fixed-bed reactor.

Kaoru Fujimoto's group proposed the following selection criteria for the SC-FTS media [87]:

1) The media critical temperature and pressure should be slightly lower than the reaction temperature and pressure
2) The media should be both inert under reaction conditions and should not poison the catalyst.
3) The media should have a high affinity for straight-chain heavy hydrocarbons.

In the literature, the following have been used as the SC media: propane (3 studies) [88,89,99], pentane (8 studies) [90,91,92,93,95,96,100,105], hexane (17 studies) [85,86,87,91,94,95,96,97,98,99,101,102,103,104,105,106,108], heptane (2 studies) [95,105], octane (2 studies) [102,106], decane (2 studies) [95,102], dodecane (1 study) [102], hexadecane (4 studies) [85,86,87,102], and CO_2(1 study) [107]. Several of the studies included mixtures of the above components as the media. The prevalence of pentane and hexane indicates that most researchers are following Fujimoto's recommendation in selecting a supercritical solvent. While LTFT (220-250^oC) operates above the critical temperature of both propane (97^oC) and CO_2 (31^oC), the reduced temperature is well above 1.0, hurting media density and decreasing non-

ideality. Similarly, studies by Davis' group [93,100] used a mixture of pentane and hexane, but added significant quantities of inert gas, modifying the phase behavior of the resulting media.

Roberts' group [98] demonstrated that the critical properties of the reactor effluent are different from the media (the critical temperature and pressure are both higher in the effluent by 10^{o}C and 10 bar).

Another important choice related to the solvent is the ratio of solvent to syngas. A common ratio in the literature between the media partial pressure and syngas partial pressure is 3.5. Roberts' group [97] varied the media to syngas molar ratio in SC-FTS. A high ratio favored selectivity (high propagation probability and low methane selectivity), but hurt activity and presents operational problems (high pressure and associated compression costs). They concluded that a ratio of 3 (3 moles hexane per mol syngas) presented an acceptable tradeoff.

1.3.2 SC-FTS Compared with Traditional FTS

The first role of the supercritical solvent (like the liquid phase in slurry-phase FTS) is the extraction of produced hydrocarbons. Fujimoto's group demonstrated this capacity in two different ways [87]. The first was to impregnate the catalyst with wax and attempt to extract the wax with the various proposed reaction mediums. Hexadecane (a liquid at reaction conditions) and hexane (a supercritical fluid at conditions) extracted nearly all the wax within 60 minutes and most by 20 minutes. Octane (at compressed gas conditions) extracted nearly all of the wax within 60 minutes, but needed 40 to 50 minutes to extract most of the wax. Nitrogen demonstrated little capacity to extract wax. The second test was in extracting any produced hydrocarbons left on the catalyst from it after an FT run. The ratio of FT products collected without extraction to total FT products (those collected without extraction + those collected during extraction) demonstrated the media's capacity to extract produced hydrocarbons. The

hexadecane media proved somewhat better than the hexane media, though the product distribution was lighter. The nitrogen media, on the other hand, proved much worse than either at extracting reaction products from the catalyst.

Davis' group [93] operated FTS under supercritical conditions immediately following GP-FTS operation. In GP-FTS operation, the wax collected was significantly less than that predicted by the overall product distribution (indicating poor wax extraction), while SC-FTS gave higher than expected wax collection (indicating that the supercritical environment extracted both the wax formed during SC-FTS and the residual wax from GP-FTS operation). Roberts' group showed that SC-FTS operation maintains activity far better than GP-FTS [97]. Work we have done that builds on the observed activity maintenance, demonstrating activity restoration by SC-FTS for a used GP-FTS cobalt catalyst is presented in Chapter 3 of this dissertation.

Another role of the supercritical solvent is in decreasing the diffusion resistance seen in a liquid reaction media (or in the wax-filled pore space seen in gas-phase operation). Bukur's group [99] showed that SC-FTS gave a conversion virtually identical to GP-FTS and much higher than slurry-phase FTS. In earlier work, Fujimoto's group [86] demonstrated that the activation energy for FTS in various mediums trended as follows: nitrogen (23 kcal / mol) > hexane (21 kcal / mol) > hexadecane (17 kcal / mol). Suppressed activation energy is indicative of diffusion resistance [143]. Fujimoto's group [90] showed that within pores SC-FTS gives a lower Thiele Modulus than GP-FTS. Consequently, the hydrogen to carbon monoxide ratio at internal active sites is lower in SC-FTS, resulting in improved selectivity (decreased methane, increased wax and olefins).

Additionally, the supercritical media is intended to assist in thermal management to prevent hotspots (The FTS reaction has an adiabatic temperature rise of almost 2000^{o}C [142]).

Some studies have measured the axial thermal temperature distribution [86,91,94] and have found less temperature variation in SC-FTS than GP-FTS. More important, though (and unmeasured), is the effect on radial temperature distribution, an important factor in fixed-bed FTS reactor design.

Conversion comparisons between SC-FTS and GP-FTS are inconclusive. SC-FTS has been observed to give a higher [88,105,106], lower [85,87], and identical [99,103] conversion. Fujimoto's group [87] studied supercritical FTS on iron, cobalt, and ruthenium and in each case found that GP-FTS (with nitrogen as the balance gas) had a higher conversion than SC-FTS (with hexane as the SC media). Given the range of mediums and process conditions, it is safest to say that conversion is comparable between GP-FTS and SC-FTS.

SC-FTS (relative to GP-FTS) has consistently been shown to suppress methane formation [85,90,93,94,97,106,108] (it had no effect in one case [99], though this was in propane, a less nonideal media). SC-FTS has also been demonstrated to suppress CO_2 formation [93,108], an observation that will be consistently reported in the chapters that follow.

A mild suppression [86,88] or no effect [94] has been seen in going from GP-FTS to SC-FTS on olefin selectivity at low carbon number while SC-FTS has consistently been observed to enhance the olefin selectivity with increasing carbon number [87,88,89,93,94,108], another observation that will be reported repeatedly in the following chapters. 2-olefin selectivities have been shown to be lower in SC-FTS [88,89]. This is in keeping with the supercritical media extracting products from catalyst pores, preventing secondary reactions (hydrogenation and double bond isomerization). This capacity to better extract and stabilize potentially reactive primary products is an important part of the work that will be presented in Chapter 4, in which an unprecedented high selectivity to diesel-length aldehydes and methyl-ketones was observed.

The literature is split on the effect of the supercritical environment on the overall product distribution (propagation probability), with some investigations reporting an enhancement of propagation probability / diesel-wax selectivity in SC-FTS [94,96,97] and others reporting no difference between SC-FTS and GP-FTS [86,93,99,108]. Some have also reported deviations from ASF behavior [92,96,97], which Fujimoto's group [92] concluded was possible at low temperature and high conversion, which was attributed to re-adsorbed olefins initiating chain growth. Davis' group [100], on the other hand, added olefins to the reaction mixture and concluded that olefin re-adsorption and propagation was not a significant influence on the chain length distribution. Iglesia's group has pointed out that the behavior of in-situ generated incorporants (determined by residence time variation) is different from that of added incorporants (whether observed by changes in the product or by tracer studies) [36], which is in keeping with Hildebrandt's assertion of the influence of thermodynamics on the FTS product spectrum [139,140].

Based on this, it is reasonable to conclude that a properly selected supercritical media will give suppressed methane and CO_2 selectivities, enhanced heavy olefin selectivity, and comparable conversion and propagation probability for SC-FTS relative to GP-FTS.

1.3.3 SC-FTS: Effect of Solvent

A number of solvents have been used in supercritical (and sub-critical) FTS. Fujimoto's group [85,86,87] found that a hexane media gave a higher conversion and activation energy (86 kJ/mol for hexane versus 71 kJ/mol for hexadecane). Hexane also gave a higher propagation probability, olefin selectivity, and maintenance of the olefin selectivity into the diesel range. Benzene as a media was shown to hamper both conversion and propagation probability while methanol proved reactive (and thus unsuitable).

Subsequent work by Fujimoto's group [95] compared pentane, hexane, heptane, and decane reaction mediums. Heptane and hexane gave some enhancement to C3-C7 selectivity and increasing solvent MW mildly decreased propagation probability. Increasing solvent MW slightly suppressed CO_2 while methane and conversion were unaffected. Heptane gave the highest olefin selectivity, followed by pentane and hexane, followed by decane.

Later work by Fujimoto's group [102] compared hexane, octane, decane, dodecane, and hexadecane mediums. It was found that, as media MW increased, conversion decreased, and that methane selectivity, CO_2 selectivity, and propagation probability were unchanged. The maintenance of the olefin selectivity into higher carbon numbers went in the order of C10 > C8 = C12 = C16 > C6. The discrepancy between these results and those in the last paragraph are difficult to explain. Both catalysts were 20% cobalt on silica, both studies were done at 45 bar and 240^{o}C, and the support pore size appears to be the same. Whether the partial pressure of the media or the volumetric flow is kept constant is unclear.

Further studies [102] were done to look at branched and cyclic solvents. Branching (trimethyl pentane versus n-octane) had minimal effect on conversion, methane and CO_2 selectivity, and propagation probability while decreasing olefin selectivity into the middle and heavy fraction. Cyclic solvents were studied by comparing decahydronapthalene (DHN) with n-decane. Conversion and methane selectivity were unaffected, carbon dioxide selectivity increased while propagation probability fell, and olefin selectivity nearly uniformly decreased with carbon number with the cyclic solvent, indicating that cyclic compounds are ill-suited to this role. As cyclic compounds are not a significant part of the FTS product spectrum, they would not be present in the media in industrial SC-FTS operation.

Another study by Fujimoto [103] compared hexane with a series of hexane-rich mixed solvents. The first two mixed solvents were 90% and 87.5% n-hexane with most of the rest close to C6. These gave behavior (conversion and selectivities) very similar to a hexane media. The third mixed solvent (75% hexane, 25% decane) gave slightly lower conversion, higher methane, and higher CO_2. The big difference in adding decane was seen in increasing the propagation probability and the olefin selectivity in the diesel and wax fractions.

Roberts' group [96] compared pentane and hexane as the reaction media, showing that pentane gave a slightly higher conversion with little impact on the carbon number distribution. Hexane gave a higher olefin selectivity. Haghtalab's group [105] used pentane, hexane, heptane, and mixtures thereof as supercritical mediums for the reaction. These solvents give comparable activity and selectivity.

Taking hexane as the baseline media, there is potential for benefits in going to a slightly heavier media (though this may make the media sub-critical). Mixed solvents don't seem to hurt the activity or selectivity, which is good for the industrial application of SC-FTS.

1.3.4 SC-FTS: Effects of Process Conditions and Catalyst Characteristics

Bukur's group [89] studied the influence of various process parameters on GP-FTS and SC-FTS using propane. They found that increasing conversion decreases the olefin selectivity and increases the 2-olefin selectivity for both GP-FTS and SC-FTS, though the influence is stronger in SC-FTS. In SC-FTS, temperature was shown to have a small and inconsistent effect on both the olefinicity of the product and the portion of the olefins that are internal. Increasing the syngas ratio (H_2 / CO) decreased the olefin content and increased the 2-olefin selectivity. While this affect was seen both in GP-FTS and SC-FTS, it was more pronounced in GP-FTS.

Fujimoto's group [91], on a ruthenium catalyst with hexane as the supercritical media, showed that larger pellets give a more olefinic product. Because larger pellets should mean more intra-pellet diffusion resistance, so more secondary reactions, and subsequently less olefinicity, this is surprising.

Roberts' group [94], using supercritical hexane, showed that increasing the reaction pressure increased conversion up to 65 bar. Increasing the pressure beyond that (to 80 bar) decreased the conversion. This was attributed to very high pressure leading to high density and enhanced diffusion resistance for the syngas. Haghtalab's group [105] saw a similar effect.

Fujimoto's group [95] showed that increasing the temperature in supercritical operation (cobalt on silica catalyst using hexane) increased conversion, methane selectivity, and CO_2 selectivity while decreasing propagation probability and olefinicity. Isothermally increasing conversion also increased methane and CO_2 selectivities while enhancing propagation probability and decreasing olefin content. Partially replacing hexane with nitrogen had a strong negative impact on olefin selectivity, a mild negative impact on methane selectivity, CO_2 selectivity, and propagation probability, and little or no influence on conversion.

Roberts' group [96] demonstrated that increasing temperature increases conversion and decreases propagation probability and olefinicity (with all taking a big jump between 220^{o}C and 240^{o}C). Increasing the reaction pressure increased conversion and propagation probability. Increasing the syngas ratio enhanced light product selectivity and suppressed heavy product formation. Increasing syngas rate at constant media rate also shifted the product distribution towards light compounds.

Roberts' group [97] later showed a strong relationship between pore radius and conversion in GP-FTS, but little correlation in SC-FTS. Fujimoto's group [102] showed an

increasing support pore diameter severely suppressed conversion, though at the same time methane and CO_2 selectivities were suppressed and propagation probability increased. Large pores also favored olefin selectivity.

Fujimoto's group [103] studied the effect of temperature using both pentane and hexane reaction mediums. In both cases, increasing temperature led to increased methane and CO_2 formation and suppressed propagation probability and olefinicity.

Haghtalab's group [105] showed that increasing the reaction temperature increased conversion, methane selectivity, and CO_2 selectivity. Increasing the syngas ratio increases conversion and methane selectivity while generally (and slightly) increasing CO_2 selectivity. Isothermally increasing the conversion enhances both methane and CO_2 selectivity as well.

The work that will be presented in Chapter 2 will include some of the effects of temperature on cobalt-based FTS. The work that will be presented in Chapters 4 will look at the effects of conversion level for iron for SC-FTS and GP-FTS (Chapter 4) and for SC-FTS, GP-FTS.

1.3.5 SC-FTS: Influence on Catalyst

Roberts' group [96] showed that the supercritical media maintained the catalyst's surface area and pore volume better than gas phase operation. Haghtalab's group [105] confirmed this observation, showing that SC-FTS gives less of a loss of BET surface area, catalyst pore volume, and average pore diameter during the reaction than GP-FTS.

Roberts' group [97] also demonstrated that SC-FTS does a better job of maintaining cobalt in the metallic state than GP-FTS. Additionally, the metallic cobalt in SC-FTS was hcp while the metallic cobalt from GP-FTS was fcc. This indicates that the effect of the supercritical solvent is not only on the environment around the catalyst, but upon the catalyst itself.

1.3.6 SC-FTS: Industrial Application

While recycling is done in industrial FTS, SC-FTS remains unapplied (Sasol has researched SC-FTS, but never published or presented that work). An economic comparison of SC-FTS to GP-FTS and SP-FTS has not yet been done. However, Fujimoto's group has studied the effect of using a recycled solvent [101]. This led to a significant loss in conversion (potentially due to competitive adsorption of recycled olefins) and product olefinicity (due to recycling the olefins giving them greater opportunity to be consumed). Nimir Elbashir [144] has presented work that explores the use of both temperature and pressure to effectively separate the supercritical media from both lighter and heavier reaction products an important consideration for the utilization of SC-FTS. In Chapter 5, work will be presented in which an alternate design principle is used to make the SC-FTS reactor far less expensive.

The second chapter of this dissertation will be focused on our efforts to close the SC-FTS material balance, but will also include the effect of temperature on the SC_FTS reaction performance on cobalt. The third chapter will focus on attempted activity restoration of a cobalt catalyst deactivated by GP-FTS operation, showing the capacity of the supercritical environment to alter the catalytic performance both during supercritical operation and for subsequent conventional operation. The fourth chapter will focus on the extraction and stabilization of aldehydes and methyl-ketones in SC-FTS operation, allowing a product distribution far closer to the true primary spectrum than that seen in traditional GP-FTs or SP-FTS operation. The fifth chapter will present an alternate reactor design methodology that will allow for decreased capital cost with SC-FTS utilization.

For a more detailed discussion of SC-FTS, please consult the literature review that I assisted in writing [146].

1.4 Fischer Tropsch Syncrude Processing for Fuels

1.4.1 Introduction

There are two problems in utilizing FTS for fuel synthesis: low selectivity and fuel quality. The selectivity problem being due to the unselective nature of the FT reaction: the product distribution largely follows an ASF product distribution, limiting maximum gasoline (C5-C11) selectivity to 42% [17] (at a propagation probability of 76% [16]) and diesel (C12-C18) selectivity to 22% [17] (at a propagation probability of 87% [16]). These weaknesses can be mediated by oligomerization (to shift light olefins to liquid products) and cracking (to shift the heavy waxes back to liquids) [20].

Fuel quality issues plague both the gasoline and diesel fractions. The gasoline fraction suffers from a low octane value due to low branching and aromatic content. The diesel fraction suffers from poor cold-flow properties (due to low branching) and low density (due to low aromaticity) [20].

1.4.2 Oligomerization

Olefin oligomerization is typically done using a solid acid catalyst. In general, the UOP process using SPA (Solid Phosphoric Acid) is the standard [109], though both SPA and ZSM-5 (Sasol's COD (Conversion of Olefins to Distillates) and Mobil's MOGD (Mobil Olefins to Gasoline and Distillates)) are used for Fischer Tropsch syncrude processing [111]. SPA and ZSM-5 are the only catalysts used industrially for the oligomerization of olefins derived from FTS [110].

SPA produces good gasoline but poor diesel while ZSM-5 (COD and MOGD) makes high quality diesel [111] (the size-selectivity of ZSM-5 limits the products to methyl branching

[115]). Pore sizes larger than 10nm in acid catalysts have been shown to give longer oligomerization catalyst life due to easier extraction of heavy oligomers [112]. SPA requires water in the reactor feed, is supported on quarts or kieselguhr, has an upper temperature limit of 245^{o}C, and has lower hydration limit of 110% H_3PO_4 (partially due to coking concerns) [116]. For butene oligomerization, high temperatures favor decreased branching (branched products are selectively cracked) and enhanced diesel selectivity. High moisture favors gasoline selectivity with an inconsistent effect on branching [116]. "*The highest yield of the best quality hydrogenated motor gasoline (highest degree of branching) was obtained when operating in a 'cold and wet' mode*." [116]

An issue in oligomerization is the amount of heat released (60 kJ/mol [111] or 100 kJ / mol [113]). This can make isothermal operation problematic [111], presenting opportunities for supercritical operation.

Amorphous Silica-Alumina (ASA) is a promising catalyst for oligomerization [110,111], giving a moderate density (810 g/L) to go with a kinematic viscosity of 2.8-3.6 cSt. The cetane value is low, however (28-30) [111]. The deactivation rate is .03-.04 mg C / hr-gcat in the absence of oxygenates, allowing for cycle lengths of over 100 days [111]. The catalyst can be reactivated by carbon burnoff [111]. When oxygenates are part of the feed, the product viscosity decreases, as does the catalyst life (corresponding to an increase in carbon deposition) [110]. The acids produced from these oxygenates will require removal, however, necessitating further processing (aqueous extraction) [110]. It is proposed that the weaker acid sites found in ASA make for a better oligomerization catalyst by suppressing secondary reactions such as cracking [110].

The oligomerization reaction on ASA showed excellent activity maintenance at 60 bar and irreversible deactivation at 40 bar. If this is due to clogging and coking from failure to extract heavy oligomers, this shows further potential for a supercritical media to improve the process.

An alternative to catalytic oligomerization is thermal oligomerization. Where catalytic oligomerization is done at 130^{o}C to 250^{o}C, thermal upgrading takes place at 320^{o}C to 400^{o}C. Oxygenates have minimal effect on the process. Carbon formation is low (400μg / g) and beneficial (the deposits are iron-rich and removal of this iron from the stream improves downstream processing). Skeletal isomerization does not occur, aromatics aren't made, and 1-olefins are more reactive than internal olefins. Dissociation energies suggest that the intermediate radical is formed by severance of C-C bonds, not C-H. Additionally, it is the bond between the 3 and 4 carbon (the double bond being between the 1 and 2 carbons) that is broken. The activation energy was determined to be 95 kJ / mol, though de Klerk was surprised it wasn't higher. The reaction rate was found to be low (0.1 mmol / L-sec) and the process chiefly justifiable for highly olefinic feeds producing chemicals in the naptha range or diesel fuel. [113]. Sasol researchers [114] have used SPA on a feed containing propene and benzene or toluene at 160^{o}C to 240^{o}C and 38 bar to produce a synthetic jet fuel.

1.4.3 Hydrocracking

Cracking of FT wax serves two purposes: to move the carbon in wax into the diesel fraction and to improve the diesel fraction quality by increasing branching [20]. Larger paraffins preferentially crack over shorter paraffins, allowing wax to be cracked back to diesel with minimal cracking of diesel to gasoline or gasses [117]. The distillate (diesel) yield increases as the wax conversion increases up to a wax conversion of 80% to 90%. As the wax conversion

increases beyond that, secondary cracking decreases the diesel yield [118]. Through recycling, however, the wax can be cracked to extinction without excessive secondary cracking [20]. Mild catalytic cracking of FT wax has been shown to result in a selectivity of 80% diesel, 15% naptha, and 5% gasses (consistent with random beta scisson) [20].

LTFT wax is much easier to crack than petroleum derived cracker feed due to high paraffinicity and low aromatics. This decreases coking, allowing for milder operating conditions: both lower operating pressure (35 to 70 for LTFT products versus up to 150 bar for petro-heavies) [20] and lower temperature (300^{o}C-350^{o}C for Shell's SMDS wax cracker versus >350^{o}C for petro-heavies [24]). The combination of cracking (endothermic) and olefin saturation (exothermic) makes for a nearly isothermal process [24].

Cracking can be done on either a sulfided (Co/Mo, Co/W, Ni/Mo, NiW) or unsulfided (Pt, Pd, Pt/Pd) solid acids (silica/alumina or zeolites)[20]. FT wax's cleanliness allows for unsulfided catalysts [24], which give better selectivity [118]. Hydrocracking catalysts are bifunctional, having acid sites (for isomerization and cracking) as well as metal sites (for hydrogenation and dehydrogenation) [118].

Dardas et al [120] studied the cracking of n-heptane on a Y-Type commercial zeolite under sub-critical and supercritical conditions and found that, among other things, supercritical conditions imparted much better activity maintenance, indicating potential for supercritical fluids in FT syncrude cracking.

While FTS and hydrocracking can be operated sequentially, the two reactions can also be carried out simultaneously, either by physically mixing the FTS and hydrocracking catalyst or by supporting the FTS catalyst on an acidic support (this having the theoretical advantage of preventing wax from clogging catalyst pores by cracking the wax in situ to lighter products).

Combining the two reactions is an intriguing idea, but it presents several problems. First, combining FTS and hydrocracking functionality can damage FTS performance. Botes and Bohringer [119] showed that contact between the iron and the zeolite led to migration of the alkali promoter to the zeolite, hurting activity and selectivity. Fujimoto's group [121] supported cobalt on a number of conventional and acidic supports for slurry-phase and supercritical FTS. Montmorillonite behaved like silica and alumina while the zeolites had lower conversion, higher methane selectivity, higher isomer selectivity, and suppressed wax selectivity relative to conventional supports. Second, the two reactions are done at very different temperatures [122]. Fujimoto's group [123] concluded that the two-stage process is preferable to combining the reactions in a single stage. Finally, combining the reactions decreases overall system flexibility.

Using sequential reactors, Fujimoto's group concluded that palladium was superior to platinum and that zeolites impregnated by ion exchange gave higher isomer selectivity than those loaded by impregnation [124]. Botes and Bohringer [119] concluded that low acidity ZSM-5 (a high silica to alumina ratio of 280) gave better activity maintenance than a high acidity ZSM-5 (Si/Al = 30). Fujimoto's group [125], working with β-zeolite, concluded that the optimal Si/Al ratio was 25.6. Calemma et al [20] presented work in which 0.3% Pt / ASA (35-70 bar, 330^{o}C-355^{o}C) processed a light feed (61% in the distillate range) to a diesel with excellent cold properties.

Arno de Klerk [126] studied the thermal cracking of FT wax. This was done at high temperature (460^{o}C to 490^{o}C (the activation energy was found to be 290 kJ / mol)) and at low (1 bar) and high (60 bar) pressure. The process was shown to produce a great deal of heavy diesel and light wax with little branching. Inorganics rapidly (<18 days) plugged the reactor. This process was concluded to have poor utility for fuels.

While research in upgrading FT syncrude will only be presented as future work in this dissertation, early work in integrating oligomerization and hydrocracking into FTS though a three-bed reactor has been underway by Sihe Zhang. I contributed to designing and assembling the reactor and upgrading reactions will form a part of my own efforts in the coming year.

1.5 References

[1] Wilhelm Keim: **Catalysis in C_1 Chemistry**. ISBN 90-277-1527-0

[2] Andrei Y Khodakov, Wei Chu, Pascal Fongarland: *Advances in the Development of Novel Cobalt Fischer Tropsch Catalysts for Synthesis of Long-Chain Hydrocarbons and Clear Fuels*. **Chemical Reviews** (2007): V 107, N 5, p 1692.

[3] http://stoltz.caltech.edu/litmtg/2002/may-lit-9_26_02.pdf

[4] Mark E. Dry: *The Fischer-Tropsch Process: 1950-2000*. **Catalysis Today** (2002): V 71, I 2-3, p 227.

[5] http://www.sasol.com/sasol_internet/frontend/navigation.jsp?articleTypeID =2&articleId=11200003&navid=4&rootid=4

[6] http://www.sasol.com/sasol_internet/frontend/navigation.jsp;jsessionid =AXLEOE0LMX0YPG5N4EZSFEQ?articleTypeID=2&articleId =14600001&navid=4&rootid=4

[7] http://www.busrep.co.za/index.php?fArticleId=3305588&SectionId =612&fSetId=662

[8] D.J. Wilhelm, D.R. Simbeck, A.D. Karp, R.L, Dickenson: *Syngas Production for Gas-to-Liquids Applications: Technologies, Issues, and Outlooks*. **Fuel Processing Techmology** (2001): V 71, p 139.

[9] K. Aasberg-Peterson, T.S. Christensen, I. Dybkjaer, J. Sehested, M. Ostberg, R.M. Coertzen, M.J. Keyser, A.P. Steynberg: *Synthesis Gas Production for FT Synthesis*. **Studies in Surface Science and Catalysis 152** (ISBN 978-0-444- 51354-0): Ch 4.

[10] Carlo N. Hamelinck, Adre P.C. Faaij, Herman den Uil, Harold Boerrigter: *Production of FT Transportation Fuels from Biomass: Technical Options, Process Analysis and Optimisation, and Development Potential*. **Energy** (2004): V29, p 1743.

[11] M. van den Burgt, J. Van Klinken, S. T. Sie: The Shell Middle Distillate Synthesis Process. **Paper presented at the 5th Synfuels Worldwide Symposium** (1985): Washington, DC, November 11-13

[12] M. E. Dry, A. P. Steynberg: *Commercial FT Process Applications*. **Studies in Surface Science and Catalysis 152** (ISBN 978-0-444-51354-0): Ch 5.

[13] Christopher Higman, Maarten van der Burgt: **Gasification**. ISBN 0-7506-7707-4

[14] Michiel J.A. Tijmensen, Andre P.C. Faaij, Carlo N. Hamelinck, Martijn R.M. van Hardeveld: *Exploration of the Possibilities for Production of Fischer Tropsch Liquids and Power Via Biomass Gasification*. **Biomass and Bioenergy** (2002): V 23, p129.

[15] A.P. Steynberg, R.L. Espinoza, B. Jager, A.C. Vosloo: *High Temperature Fischer-Tropsch Synthesis in Commercial Practice*. **Applied Catalysis A: General** (1999): V 186, p 41.

[16] A. P. Steynberg, M. E. Dry, B. H. Davis, B. B. Breman: *Fischer-Tropsch Reactors*. **Studies in Surface Science and Catalysis 152** (ISBN 978-0-444- 51354-0): Ch 2.

[17] M. E. Dry: Chemical *Concepts Used for Engineering Purposes*. **Studies in Surface Science and Catalysis 152** (ISBN 978-0-444-51354-0): Ch 3.

[18] R.L. Espinoza, A.P. Steynberg, B. Jager, A.C. Vosloo: *Low Temperature Fischer-Tropsch Synthesis from a Sasol Perspective*. **Applied Catalysis A: General** (1999): V 186, p 413.

[19] M. E. Dry: *FT Catalysts*. **Studies in Surface Science and Catalysis 152** (ISBN 978-0-444-51354-0): Ch 7.

[20] L. P. Dancuart, R. de Haan, A de Klerk: *Processing of Primary Fischer Tropsch Products*. **Studies in Surface Science and Catalysis 152** (ISBN 978-0-444-51354-0): Ch 6.

[21] B. Jager, R. Espinoza: *Advances in Low Temperature Fischer Tropsch Synthesis*. **Catalysis Today** (1995): V23, p17.

[22] National Association of Purchasing Management: Resources (Commodity Corner): http://www.napm-ny.org/resources/commodity.html

[23] Mark E. Dry: *Fischer–Tropsch Reactions and the Environment*. **Applied Catalysis A: General** (1999): V 189, I 2, p 185.

[24] Arno de Klerk: *Hydroprocessing Peculiarities of Fischer-Tropsch Syncrude*. **Catalysis Today** (2008): V 130, p 439.

[25] A. P. Steynberg: *Introduction to Fischer-Tropsch Technology*. **Studies in Surface Science and Catalysis 152** (ISBN 978-0-444-51354-0): Ch 1.

[26] P.W. Schaberg, P.M. Morgan, I.S. Myburgh, P.N.J. Roets, J.J Botha: *An Overview of the Production, Properties, and Exhaust Emissions Performance of Sasol Slurry Phase Distillate Diesel Fuel*. Publication unknown: http://www.sasolchevron.com/dwn/ovrview2.pdf

[27] Sasol press release: http://www.sasolchevron.com/GTLChallenge/newsroom_entry.asp?ID=5

[28] Sasol website: http://www.sasolchevron.com/GTLChallenge/the_fuel.htm

[29] US EPA Regulatory Announcement: http://www.epa.gov/otaq/regs/fuels/diesel/420f05051.htm

[30] US DHHS Agency for Toxic Substances and Disease Registry: Toxicological Profile for Fuel Oils. http://www.atsdr.cdc.gov/toxprofiles/tp75-c3.pdf

[31] Kapila Wadumesthrige, Anfeng Wang, Steven O. Salley, K. Y. Simon Ng: *Effect of Major and Minor Components of Biodiesel on the Lubricity of Petroleum and Synthetic fuel*. **AICHE 2007 Annual Meeting** (Abstract): Alternate Fuels and Enabling Technologies I.

[32] R. H. Barbour, Nigel G. Elliott, David J. Rickeard: *Understanding Diesel Lubricity*. **SAE Transactions** (2000): V109, N 4, p 1556.

[33] Sasol Website: http://sasol.investoreports.com/sasol_mm_2006/html/sasol_mm_2006_60.php

[34] M. Claeys, E. van Steen: *Basic Studies*. **Studies in Surface Science and Catalysis 152** (ISBN 978-0-444-51354-0): Ch 8.

[35] Zhi-Pan Liu, P. Hu: *A New Insight into Fischer-Tropsch Synthesis*. **Journal of the American Chemical Society** (2002): V 124, p 11568.

[36] Enrique Iglesia: *Design, Synthesis, and Use of Cobalt-Based Fischer-Tropsch Synthesis Catalysts*. **Applied Catalysis A: General** (1997): V 161, p59.

[37] Rostam J. Madon, Sebastian C. Reyes, Enrique Iglesia: *Primary and Secondary Reaction Pathways in Ruthenium-Catalyzed Hydrocarbon Synthesis*. **Journal of Physical Chemistry** (1991): V95, p 7795.

[38] Buchang Shi, Gary Jacobs, Dennis Sparks, Burtron H. Davis: *Fischer–Tropsch Synthesis: 14C Labeled 1-Alkene Conversion Using Supercritical Conditions with $Co/A1_2O_3$*. **Fuel** (2005): V 84, I 9, p 1093.

[39] Hans Schulz, Michael Claeys: *Reactions of α-Olefins of Different Chain Length Added During Fischer-Tropsch Synthesis on a Cobalt Catalyst in a Slurry Reactor*. **Applied Catalysis A: General** (1999): V 186, p 71.

[40] Gerard P. Van Der Laan, A. A. C. M. Beenackers: *Kinetics and Selectivity of the Fischer-Tropsch Synthesis: A Literature Review*. **Catalysis Reviews** (1999): V 41, I 3&4, p 255.

[41] Buchang Shi, Robert J. O'Brien, Shiqi Bao, Burtron H. Davis: *Mechanism of the Isomerization of 1-Akene During Iron-Catalyzed Fischer-Tropsch Synthesis*. **Journal of Catalysis** (2001): V 199, p 202.

[42] Burtron H. Davis: *Fischer–Tropsch synthesis: current mechanism and futuristic needs*. **Fuel Processing Technology** (2001): V 71, I 1-3, p 157.

[43] Li-Min Tau, Hussein A. Dabbagh, Burtron Davis: *Fischer-Tropsch Synthesis: Comparison of 14C Distributions When Labeled Alcohol is Added to the Synthesis Gas*. **Energy and Fuels** (1991): V 5, p 174.

[44] Burtron H. Davis: *Fischer-Tropsch synthesis: relationship between iron catalyst composition and process variables*. **Catalysis Today** (2003): V 84, I 1-2, p83.

[45] W. van Barneveld, V. Ponec: *Reactions of CHxCl4-X with Hydrogen - Relation to the Fischer-Tropsch Synthesis of Hydrocarbons*. **Journal of Catalysis** (1984): V 88, p382.

[46] Yulong Zhang, Li Hou, John W. Tierney, Irving Winder: *Acetylenes as Probes in the Fischer Tropsch Reaction*. **Topics in Catalysis** (2005): V 32, N 3-4, p 125.

[47] G. Blyholder, M. Lawless: *Hydrogen-Assisted Dissociation of CO on a Catalyst Surface*. **Langmuir** (1991): V 7, p140

[48] Oliver R. Inderwildi, Stephen J. Jenkins, David A. King: *Fischer-Tropsch Mechanism Revisited: Alternative Pathways for the Production of Higher Hydrocarbons from Synthesis Gas*. **Journal of Physical Chemistry C** (2008), V 112, N 5, p 1305

[49] Helen C. Long, Michael L. Turner, Paolo Fornasiero1, Jan Ka, Mauro Graziani1 and Peter M. Maitlis: *Vinylic Initiation of the Fischer–Tropsch Reaction over Ruthenium on Silica Catalysts*. **Journal of Catalysis** (1997): V 167, I 1, p 172.

[50] S. B. Ndlovu, N. S. Phala, M. Hearshaw-Timme, P. Beagly, J. R. Moss, M. Claeys, E. van Steen: *Some evidence refuting the alkenyl mechanism for chain growth in iron-based Fischer–Tropsch synthesis***. Catalysis Today** (2002): V 71, I 3-4, p 343.

[51] M. E. Dry: *The Fischer-Tropsch Synthesis*. **Catalysis Science and Technology Volume 1** (ISBN 3-540-10353-8): Chapter 4.

[52] G. L. Bezemer; J. H. Bitter; H. P. C. E. Kuipers; H. Oosterbeek; J. E. Holewijn,; X. Xu; F. Kapteijn; A. J. van Dillen; K. P. de Jong: *Cobalt Particle Size Effects in the Fischer-Tropsch Reaction Studied with Carbon Nanofiber Supported Catalysts***. Journal of the American Chemical Society** (2006): V 128, p 3956.

[53] Jon Wilson, Cor de Groot: *Atomic-Scale Restructuring in High-Pressure Catalysis.* **Journal of Physical Chemistry** (1995): V 99, p 7860.

[54] Fernando Morales, Bert M. Weckhuysen: *Promotion Effects in Co-Based Fischer Tropsch Catalysis*. **Catalysis** (2006): V19, p1.

[55] Gary Jacobs, Tapan K. Das, Yongqing Zhang, Jinlin Li, Guillaume Racoillet, Burtron H. Davis: *Fischer–Tropsch Synthesis: Support, Loading, and Promoter Effects on the Reducibility of Cobalt Catalysts*. **Applied Catalysis A: General** (2002): V 233, I 1-2, p263.

[56] Enrique Iglesia, Stuart L. Soled, Rocco A. Fiato, Grayson H. Via: *Bimetallic Synergy in Cobalt-Ruthenium Fischer-Tropsch Catalysts*. **Journal of Catalysis** (1993): V 143, p345.

[57] Michiaki Adachi, Kiyotaka Yoshii, Yi Zhuo Han, Kaoru Fujimoto: *Fischer-Tropsch Synthesis with Supported Cobalt Catalyst. Promoting Effects of Lanthanum Oxide for Cobalt / Silica Catalyst*. **Bulletin of the Chemical Society of Japan** (1996): V 69, p 1509.

[58] Hans Schulz: *Short History and Present Trends of Fischer–Tropsch Synthesis*. **Applied Catalysis A: General** (1999): V 186, I 1-2, p 3.

[59] F. Rohr, O. A. Lindvag, A Holmen, E. A. Blekkan: *Fischer-Tropsch Synthesis Over Cobalt Catalysts Suported on Zirconia-Modified Alumina*. **Catalysis Today** (2000): V 58, p 247.

[60] G.L. Bezemer, P.B. Radstake, U. Falke, H. Oosterbeek, H.P.C.E. Kuipers, A.J. van Dillen, and K.P. de Jong: *Investigation of promoter effects of manganese oxide on carbon nanofiber-supported cobalt catalysts for Fischer–Tropsch synthesis*. **Journal of Catalysis** (2006): V 237, I 1, p 152.

[61] Martin J. Keyser, Raymond C. Everson, Rafael L. Espinoza: *Fischer–Tropsch Studies with Cobalt–Manganese Oxide Catalysts: Synthesis Performance in a Fixed Bed Reactor*. **Applied Catalysis A: General** (1998): V 171, I 1, p 99.

[62] A. M. Hilmen, E. Bergene, O. A. Lindvåg, D. Schanke, S. Eri, A. Holmen: *Fischer–1 Tropsch Synthesis on Monolithic Catalysts of Different Materials*. **Catalysis Today** (2001): V 69, I 1-4, p 227.

[63] A.-M. Hilmen, E. Bergene, O.A. Lindvåg, D. Schanke, S. Eri, A. Holmen: *Fischer–Tropsch Synthesis on Monolithic Catalysts with Oil Circulation*. **Catalysis Today** (2005): V 105, I 3-4, p 357.

[64] Jean-Sébastien Girardon, Anatoly S. Lermontov, Léon Gengembre, Petr A. Chernavskii, Anne Griboval-Constant, Andrei Y. Khodakov: *Effect of Cobalt Precursor and Pretreatment Conditions on the Structure and Catalytic Performance of Cobalt Silica-Supported Fischer–Tropsch Catalysts*. **Journal of Catalysis** (2005): V 230, I 2, p 339.

[65] Shouli Sun, Noritatsu Tsubak, Kaoru Fujimoto: *The Reaction Performances and Characterization of Fischer–Tropsch Synthesis Co/SiO_2 Catalysts Prepared from Mixed Cobalt Salts*. **Applied Catalysis A: General** (2000): V 202, I 1, p 121.

[66] Martin Kraum, Manfred Baerns: Fischer–Tropsch Synthesis: *The Influence of Various Cobalt Compounds Applied in the Preparation of Supported Cobalt Catalysts on their Performance*. **Applied Catalysis A: General** (1999): V 186, I 1-2, p 189.

[67] D. J. Duvenhage, N. J. Coville: *Fe:Co/TiO2 Bimetallic Catalysts for the Fischer–Tropsch Reaction Part 2. The Effect of Calcination and Reduction Temperature*. **Applied Catalysis A: General** (2002): V233, I 1-2, p63.

[68] E. Iglesia, S. L. Soled, J. E. Baumgartner, S. C. Reyes*: Synthesis and Catalytic Properties of Eggshell Cobalt Catalysts for the Fischer-Tropsch Synthesis*. **Journal of Catalysis** (1995): V 153, I 1, p 108.

[69] Azzeddine Lekhal, Benjamin J. Glasser, Johannes G. Khinast*: Impact of Drying on the Catalyst Profile in Supported Impregnation Catalysts*. **Chemical Engineering Science** (2001): V 56, I 15, p 4473.

[70] Thomas Riedel, Michael Claeys, Hans Schulz, Georg Schaub, Sang-Sung Nam, Ki-Won Jun, Myoung-Jae Choi, Gurram Kishan, Kyu-Wan Lee: *Comparative Study of Fischer–Tropsch Synthesis with H_2/CO and H_2/CO_2 Syngas using Fe- and Co-Based Catalysts*. **Applied Catalysis A: General** (1999): V 186, I 1-2, p201.

[71] Jian-Gang Chen, Hong-Wei Xiang, Hai-Yan Gao, Yu-Han Sun: *Study on Deactivation of Co/ZrO_2/SiO_2 Catalyst for Fischer Tropsch Synthesis*. **Reaction Kinetics Catalysis Letters** (2001): V 73, N 1, p 169.

[72] Tapan K. Das, Gary Jacobs, Patricia M. Patterson, Whitney A. Conner, Jinlin Li, Burtron H. Davis: *Fischer–Tropsch Synthesis: Characterization and Catalytic Properties of Rhenium Promoted Cobalt Alumina Catalysts*. **Fuel** (2003): V 82, I 7, p 805.

[73] Gary Jacobs, Karuna Chaudhari, Dennis Sparks, Yongqing Zhang, Buchang Shi, Robert Spicer, Tapan K. Das, Jinlin Li, Burtron H. Davis: *Fischer–Tropsch Synthesis: Supercritical Conversion Using a Co/Al_2O_3 Catalyst in a Fixed Bed Reactor*. **Fuel** (2003): V 82, I 10, p 1251.

[74] Wilfried Ngantsoue-Hoc, Yongqing Zhang, Robert J. O'Brien, Mingsheng Luo, Burtron H. Davis: *Fischer−Tropsch Synthesis: Activity and Selectivity for Group I Alkali Promoted Iron-Based Catalysts*. **Applied Catalysis A: General** (2002): V 236, I 1-2, p 77.

[75] Mingsheng Luo, Burtron H. Davis: *Fischer–Tropsch Synthesis: Group II Alkali- Earth Metal Promoted Catalysts*. **Applied Catalysis A: General** (2003): V 246, I 1, p 171.

[76] Robert J. O'Brien, Liguang Xu, Robert L. Spicer, Shiqi Bao, Diane R. Milburn and Burtron H. Davis: *Activity and Selectivity of Precipitated Iron Fischer-Tropsch Catalysts*. **Catalysis Today** (1997): V 36, I 3, p 325.

[77] Senzi Li, Sundaram Krishnamoorthy, Anwu Li, George D. Meitzner, Enrique Iglesia: *Promoted Iron-Based Catalysts for the Fischer–Tropsch Synthesis: Design, Synthesis, Site Densities, and Catalytic Properties*. **Journal of Catalysis** (2002): V 206, I 2, p 202.

[78] Mingsheng Luo, Robert O'Brien, Burtron H. Davis: *Effect of Palladium on Iron Fischer–Tropsch Synthesis Catalysts*. **Catalysis Letters** (2005): V98, N 1, p 17.

[79] Hien N. Pham, Abhaya K. Datye: *The Synthesis of Attrition Resistant Slurry Phase Iron Fischer–Tropsch Catalysts*. **Catalysis Today** (2000): V 58, I 4, p 233.

[80] Robert J. O'Brien, Liguang Xu, Robert L. Spicer, Burtron H. Davis: *Activation Study of Precipitated Iron Fischer-Tropsch Catalysts*. **Energy and Fuels** (1996): V 10, I 4, p 921.

[81] Burtron H. Davis: *Fischer–Tropsch Synthesis: Reaction Mechanisms for Iron Catalysts*. **Catalysis Today** (2009): V 141, I 1-2, p 25-33.

[82] Dragomir B. Bukur, Chokkaram Sivaraj: *Supported Iron Catalysts for Slurry Phase Fischer–Tropsch Synthesis*. **Applied Catalysis A: General** (2002): V 231, I 1-2, p201.

[83] Gerard P. van der Laan, Antonie A. C. M. Beenackers: *Intrinsic Kinetics of the Gas–Solid Fischer–Tropsch and Water Gas Shift Reactions Over a Precipitated Iron Catalyst*. **Applied Catalysis A: General** (2000): V 193, I 1-2, p39.

[84] M. Luo, S. Bao, T. Das, B.H. Davis: *Fischer-Tropsch Synthesis: Is a Single Site Responsible for FTS and WGS on Iron Catalysts?* **North American Catalysis Society** (2007): 20th North American Meeting (poster session).

[85] Kohshiroh Yokota, Kaoru Fujimoto: *Supercritical Phase Fischer-Tropsch Synthesis Reaction*. **Fuel** (1989): V 68, I 2, p255.

[86] Kohshiroh Yokota, Kaoru Fujimoto: *Supercritical-Phase Fischer-Tropsch Synthesis Reaction. 2. The Effective Diffusion of Reactant and Products in the Supercritical-Phase Reaction*. **Industrial and Engineering Chemistry Research** (1991): V 30, I 1, p 95.

[87] Kohshiroh Yokota, Yoshio Hanakata, Kaoru Fujimoto: *Supercritical-Phase Fischer-Tropsch Synthesis Reaction. 3: Extraction Capability of Supercritical Fluids*. **Fuel** (1991): V 70, I 8, p 989.

[88] Xiaosu Lang, Aydin Akgerman, Dragomir B. Bukur: *Steady State Fischer-Tropsch Synthesis in Supercritical Propane*. **Industrial and Engineering Chemistry Research** (1995): V 34, I 1, p 72.

[89] Dragomir B. Bukur, Xiaosu Lang, Aydin Akgerman, Zhentao Feng: *Effect of Process Conditions on Olefin Selectivity during Conventional and Supercritical Fischer-Tropsch Synthesis*. **Industrial and Engineering Chemistry Research** (1997): V 36, N 7, p 2580.

[90] Shirun Yan, Li Fan, Zhixin Zhang, Jinglai Zhou, Kaoru Fujimoto: *Supercritical- Phase Process for Selective Synthesis of Heavy Hydrocarbons from Syngas on Cobalt Catalysts*. **Applied Catalysis A: General** (1998): V 171, p 247.

[91] Li Fan, Kaoru Fujimoto: *Fischer-Tropsch Synthesis in Supercritical Fluid: Characteristics and Application*. **Applied Catalysis A: General** (1999): V 186, p 343.

[92] Noritatsu Tsubaki, Kiyotaka Yoshii, Kaoru Fujimoto: *Anti-ASF Distribution of Fischer-Tropsch Hydrocarbons in Supercritical-Phase Reactions*. **Journal of Catalysis** (2002): V 207, p 371.

[93] Gary Jacobs, Karuna Chaudhari, Dennis Sparks, Yongqing Zhang, Buchang Shi, Robert Spicer, Tapan K. Das, Jinlin Li, Burtron H. Davis: *Fischer–Tropsch Synthesis: Supercritical Conversion Using a Co/Al_2O_3 Catalyst in a Fixed Bed Reactor*. **Fuel** (2003): V 82, I 10, p 1251.

[94] Xiwen Huang, Christopher B. Roberts: *Selective Fischer-Tropsch Synthesis Over an Al_2O_3 Supported Cobalt Catalyst in Supercritical Hexane*. **Fuel Processing Technology** (2003): V 83, p 81.

[95] Wensheng Linghu, Xiaohong Li, Kenji Asami, Kaoru Fujimoto: *Supercritical Phase Fischer-Tropsch Synthesis over Cobalt Catalyst*. **Fuel Processing Technology** (2004): V 85, p 1121.

[96] Xiwen Huang, Nimir O. Elbashir, Christopher B. Roberts: *Supercritical Solvent Effects on Hydrocarbon Product Distributions from Fischer Tropsch Synthesis Over an Alumina-Supported Cobalt Catalyst*. **Industrial and Engineering Chemistry Research** (2004): V 43, p 6369.

[97] Nimir O. Elbashir, P. Dutta, A. Manivannan, M. S. Seehra, Christopher B. Roberts: *Impact of Cobalt-Based Catalyst Characteristics on the Performance of Conventional Gas-Phase and Supercritical-Phase Fischer Tropsch Synthesis*. **Applied Catalysis A: General** (2005): V 285, p 169.

[98] Nimir O. Elbashir, Christopher B. Roberts: *Enhanced Incorporation of α-Olefins in the Fischer-Tropsch Synthesis Chain-Growth Process Over an Alumina-Supported Cobalt Catalyst in Near-Critical and Supercritical Hexane Media*. **Industrial and Engineering Chemistry Research** (2005): V 44, p 505.

[99] Dragomir Bukur, Xiaosu Lang, Lech Nowicki: *Comparative Study of an Iron Fischer Tropsch Catalyst Performance in Stirred Tank Slurry and Fixed-Bed Reactors*. **Industrial and Engineering Chemistry Research** (2005): V 44, p 6038.

[100] Buchang Shi, Gary Jacobs, Dennis Sparks, Burtron H. Davis: *Fischer-Tropsch Synthesis: 14C Labeled 1-Alkene Conversion Using Supercritical Conditions with Co / Al_2O_3*. **Fuel** (2005): V 84, p 1093.

[101] Wen-Sheng Linghu, Xiao-Hong Li, Kenji Asami, Kaoru Fujimoto: *Process Design and Solvent Recycle for the Supercritical Fischer-Tropsch Synthesis*. **Energy and Fuels** (2006): V 20, p 7.

[102] Xiaohao Liu, Wen-Sheng Linghu, Xiao-Hong Li, Kenji Asami, Kaoru Fujimoto: *Effect of Solvent on Fischer Tropsch Synthesis*. **Applied Catalysis A: General** (2006): V 303, p 251.

[103] Wen-Sheng Linghu, Xiao-Hong Li, Kaoru Fujimoto: *Supercritical and Near-Critical Fischer-Tropsch Synthesis: Effects of Solvents*. **Journal of Fuel Chemistry and Technology** (2007): V 35, I 1, p 51.

[104] Abdullah Irankhah, All Haghtalab, Ebrahim Vasheghani Farahani, Kambiz Sadaghianizadeh: *Fischer-Tropsch Reaction Kinetics of Cobalt Catalyst in Supercritical Phase*. **Journal of Natural Gas Chemistry** (2007): V 16, I 2, p 115.

[105] Abdullah Irankhah, All Haghtalab: *Fischer-Tropsch Synthesis Over Co-Ru / γ-Al2O3 Catalyst in Supercritical Media*. **Chemical Engineering Technology** (2008): V 31, N 4, p 525.

[106] TANG Haodong, LIU Huazhang, YANG Xiazhen, LI Ying: *Supercritical Phase Fischer-Tropsch Synthesis Reaction over Highly Active Fused Iron Catalyst at Low Temperature*. **Journal of Chemical Engineering of Chinese Universities** (2008): V 22, N 2, p 259.

[107] Jeremiah Benoit, Kanchan Mondal, Tomasz Wiltowski: *Supercritcal Phase Fischer Tropsch Synthesis from Coal Derived Syngas*. **AIChE Annual Meeting** (2008): Presentation 330d.

[108] Ed Durham, Sihe Zhang, Christopher B. Roberts*: Supercritical Reactivation of Fischer Tropsch Catalysts*. **AIChE Annual Meeting** (2008): Presentation 678d.

[109] Arno de Klerk, Dan J. Engelbrecht, Herman Boikanyo: *Oligomerization of Fischer−Tropsch Olefins: Effect of Feed and Operating Conditions on Hydrogenated Motor-Gasoline Quality*. **Industrial and Engineering Chemistry Research** (2004): V 43, I 23, p 7749.

[110] Arno de Klerk: *Effect of Oxygenates on the Oligomerization of Fischer−Tropsch Olefins over Amorphous Silica−Alumina*. **Energy and Fuels** (2007): V 21, I 2, p 625.

[111] Arno de Klerk: *Oligomerization of Fischer-Tropsch Olefins to Distillates Over Amorphous Silica-Alumina*. **Energy and Fuels** (2006): V 20, I 5, p 1799.

[112] Arno de Klerk: *Oligomerization of 1-Hexene and 1-Octene Over Solid Acid Catalysts*. **Industrial and Engineering Chemistry Research** (2005): V 44, I 11, p 3887.

[113] Arno de Klerk: *Thermal Upgrading of Fischer-Tropsch Olefins*. **Energy and Fuels** (2005): V 19, I 4, p 1462.

[114] Tebogo M. Sakuneka, Arno de Klerk, Reinier J. J. Nel, Andrew D. Pienaar: *Synthetic Jet Fuel Production by Combined Propene Oligomerization and Aromatic Alkylation over Solid Phosphoric Acid*. **Industrial and Engineering Chemistry Research** (2008): V 47, I 6, p 1828.

[115] Mark E. Dry: *High Quality Diesel via the Fischer-Tropsch Process – a Review*. **Journal of Chemical Technology & Biotechnology** (2002): V 77, I 1, p 43.

[116] Arno de Klerk, Dieter O. Leckel, Nicolaas Prinsloo: *Butene Oligomerization by Phosphoric Acid Catalysis: Seperating the Effects of Temperature and Catalyst Hydration on Product Selectivity*. **Industrial and Engineering Chemistry Research** (2006): V 45, p 6127.

[117] John Abbot, Paul R. Dunstan: *Catalytic Cracking of Linear Paraffins: Effects of Chain Length*. **Industrial and Engineering Chemistry Research** (1997): V 36, p 76.

[118] V. Calemma, S. Correra, C Perego, P. Pollesel, L. Pellegrini: *Hydroconversion of Fischer-Tropsch Waxes: Assessment of the Operation Conditions Effect by Factorial Design Experiments*. **Catalysis Today** (2005): V 106, p 282.

[119] F. G. Botes, W. Bohringer: *The Addition of HZSM-5 to the Fischer Tropsch Process for Improved Gasoline Production*. **Applied Catalysis A: General** (2004): V 267, p 217.

[120] Zissis Dardas, Murat G. Süer, Yi. H. Ma, William R. Moser: *A Kinetic Study of n-Heptane Catalytic Cracking over a Commercial Y-Type Zeolite under Supercritical and Subcritical Conditions*. **Journal of Catalysis** (1996): V 162, p 327.

[121] Chawalit Ngamcharussrivichai, Xiaohao Liu, Xiaohong Li, Tharapong Vitidsant, Kaoru Fujimoto: *An active and selective production of gasoline-range hydrocarbons over bifunctional Co-based catalysts*. **Fuel** (2007): V 86, p 50.

[122] Guillermo Calleja, Antonio de Lucas, Rafael van Grieken: *Co/HZSM-5 Catalyst for Syngas Conversion: Influence of Process Variables*. **Fuel** (1995): V 74, N 3, p 445.

[123] Xiaohong Li, Xiaohao Liu, Zhong-Wen Liu, b, Kenji Asami, Kaoru Fujimoto*: Supercritical Phase Process for Direct Synthesis of Middle Iso-Paraffins from Modified Fischer–Tropsch Reaction*. **Catalysis Today** (2005): V 106, p 154.

[124] Zhong-Wen Liu, Xiaohong Li, Kenji Asami, Kaoru Fujimoto: *Syngas to iso-paraffins over Co/SiO2 combined with metal/zeolite catalysts*. **Fuel Processing Technology** (2007): V 88, p 165.

[125] Zhong-Wen Liu, Xiaohong Li, Kenji Asami, Kaoru Fujimoto*: High Performance Pd/beta Catalyst for the Production of Gasoline-Range Iso-Paraffins via a Modified Fischer–Tropsch Reaction*. **Applied Catalysis A: General** (2006): V 300, p 162.

[126] Arno de Klerk: *Thermal Cracking of Fischer-Tropsch Waxes*. **Industrial and Engineering Chemistry Research** (2007): V 46, p 5516.

[127] Burtron H. Davis: *Fischer Tropsch Mechanisms … Storch is Correct?*. **Storch Award** (2002): Presentation.

[128] Kenneth Agee, Rafael Espinoza: *Future Role and Characteristics of the Fischer-Tropsch Technology*. **Presentation - AIChE Spring Meeting** (2010): Coal, Biomass, and Natural Gas to Liquids I, 10a.

[129] Arno de Klerk: *Can Fischer-Tropsch Syncrude Be Refined to On-Specification Diesel Fuel?* **Energy & Fuels** (2009): V 23, p 4593-4604.

[130] Arno de Klerk: *Fischer Tropsch Refining*. **PhD Thesis**, University of Pretoria, Pretoria, South Africa, 2008.

[131] Mingkun Zhuo, Kong Fei Tan, Armando Borgna, Mark Saeys: Density Functional Theory Study of the CO Insertion Mechanism for Fischer Tropsch Synthesis over Co Catalysts. **Journal of Physical Chemistry C** (2009): V 133, p 8357-8365.

[132] Xiaoping Dai, Changchun Yu: *H_2-Induced CO Adsorption and Dissociation Over Co/Al_2O_3 Catalyst*. **Journal of Natural Gas Chemistry** (2008): V 17, p 365-368.

[133] Robert C. Brady, R. Pettit: *On the Mechanism of the Fischer-Tropsch Reaction. The Chain Propagation Step*. **Journal of the American Chemical Society** (1981): V103, N 5, p 1287-1289.

[134] Cathrin Welker, Noko S. Phala, John R. Moss, Michael Claeys, Eric van Steen: *Theoretical Feasibility of CO-Activation and Fischer Tropsch Chain Growth on Mono and Diatomic Ru Complexes*. **Journal of Molecular Catalysis A: Chemical** (2008): V 288, p 75-82.

[135] J. Gaube, H. F. Klein: *Studies on the Reaction Mechanism of the Fischer– Tropsch Synthesis on Iron and Cobalt*. **Journal of Molecular Catalysis A: Chemical** (2008): V 283, I 1-2, p 60-68.

[136] J. Patzlaff, Y. Liu, C. Graffmann, J. Gaube: *Studies on Product Distributions of Iron and Cobalt Catalyzed Fischer–Tropsch Synthesis*. **Applied Catalysis A: General** (1999): V 186, I 1-2, p 109-119.

[137] E. W. Kuipers, C. Scheper, J. H. Wilson, I. H. Vinkenburg, H. Oosterbeek: *Non-ASF Product Distributions Due to Secondary Reactions during Fischer–Tropsch Synthesis*. **Journal of Catalysis** (1996): V 158, I 1, p288-300.

[138] I. Puskas, R.S. Hurlbut: *Comments About the Causes of Deviations from the Anderson–Schulz–Flory Distribution of the Fischer–Tropsch Reaction Products*. **Catalysis Today** (2003): V 84, p 99–109.

[139] Cornelius Mduduzi Masuku, Diane. Hildebrandt and David Glasser: *Olefin Pseudo-Equilibrium in the Fischer-Tropsch Reaction*. **AIChE Spring Meeting** (2010): Presentation 33c.

[140] Xiaojun Lu, Diane Hildebrandt and David Glasser: *A Thermodynamic Approach to the Olefin Products Distribution in Fischer-Tropsch Synthesiss*. **AIChE Spring Meeting** (2010): Presentation 10c.

[141] O. Ducreux, J. Lynch, B. Rebours, M. Roy, P. Chaumette: *In situ characterization of cobalt based Fischer-Tropsch catalysts: a new approach to the active phase*. **Studies in Surface Science and Catalysis V119 - Natural Gas Conversion V** (ISBN 978-0444829672): p 125.

[142] Xiaowei Zhu, Diane Hildebrandt and David Glasser: *A Study of Radial Heat Transfer in a Tubular Fischer-Tropsch Synthesis Reactor*. **Presentation - AIChE Spring Meeting** (2010): Coal, Biomass, and Natural Gas to Liquids I, 10b.

[143] William H. Zimmerman, Joseph A. Rossin, and Dragomir B. Bukur: *Effect of Particle Size on the Activity of a Fused Iron Fischer-Tropsch Cata1yst*. **Industrial and Engineering Chemistry Research** (1989): V 28, p 406-413.

[144] N. O. Elbashir, B. Bao, M. M El-Halwagi. *An Approach to the design of Advanced Fischer-Tropsch Rreactor for Operation in Near-Critical and Supercritical Phase Media*. In: Alfadalla HE, Reklaitis GV, El-Halwagi MM, editors. **Advances in Gas Processing: Proceedings of the 1st Annual Symposium on Gas Processing Symposium, Vol. 1.** Amsterdam: Elsevier, 2009: 423-433.

[145] Muthu K. Gnanamani, Robert A. Keogh, Wilson D. Shafer, Buchang Shi, Burtron H. Davis: *Fischer–Tropsch Synthesis: Deuterium Labeled Ethanol Tracer Studies on Iron Catalysts*. **Applied Catalysis A: General** (2010): V 385, p 46-51.

[146] Nimir O. Elbashir, Dragomir B. Bukur, Ed Durham, Christopher B. Roberts: *Advancement of Fischer-Tropsch Synthesis Via Utilization of Supercritical Fluid Reaction Media*. **AIChE Journal** (2010): V 56, p 997-1015.

[147] Eric van Steen, Michael Claeys, Mark E. Dry, Jan van de Loosdrecht, Elvera L. Viljoen, Jacobus L. Visagie: Stability of Nanocrystals: *Thermodynamic Analysis of Oxidation and Re-reduction of Cobalt in Water/Hydrogen Mixtures*. **Journal of Physical Chemistry B** (2005): V 109, p 3575.

Chapter 2

Supercritical Fischer Tropsch Synthesis Material Balance

2.1 Background

The use of Supercritical Fluids as a media for the Fischer Tropsch reaction has a 20 year history, dating back to Kaoru Fujimoto's group's seminal paper [1] in 1989. In the decades since, a number of research groups have done further research, demonstrating a decreased methane [1-6] and CO_2 [3] selectivity while enhancing the selectivity of primary products [3,7-10] relative to gas phase FTS. The verdict is mixed regarding catalytic activity (conversion) and propagation probability (alpha). A more thorough understanding of these benefits requires that the material balance be closed, with all of the carbon, hydrogen, and oxygen accounted for.

In gas-phase Fischer Tropsch (GP-FTS), the syngas feed is passed through a fixed catalyst bed, where the highly exothermic reaction occurs [16]. In supercritical Fischer Tropsch (SC-FTS), the syngas is mixed with a solvent (often hexane in research, though in industrial application it would be a product cut), which is passed through the fixed catalyst bed now maintained at a higher pressure (often such that the syngas partial pressure is the same as in GP-FTS). This solvent combined with the higher pressure gives a dense reaction media, resulting enhanced heavy product extraction and heat dissipation [3].

While the presence of the solvent presents a number of performance advantages, it also presents an analytical challenge, particularly in closing the material balance. Using hexane at the

typical rate of 1 mL hexane per 50 SmL syngas gives a molar ratio of 3.5 and mass ratio of 28.5 (media / syngas). The purpose of this work is to close the material balance for SC-FTS to allow us to better quantify the performance advantages that have been seen with SC-FTS and to prepare for our future work.

A simplification of the reactor system used in this study is as follows:

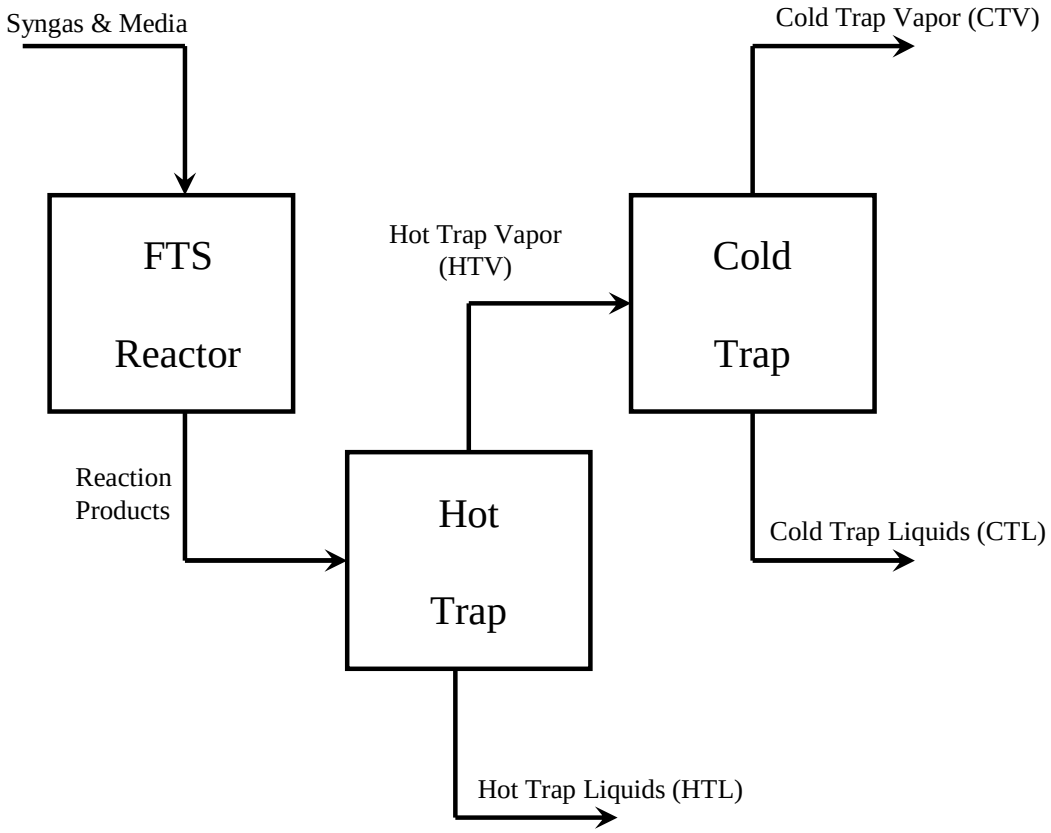

Figure 2.1 A simplified schematic of the SC-FTS reactor system

There is one feed stream and there are three product streams. Closing the material balance requires adequate characterization of all four streams.

The composition of the syngas is known from the supplier and confirmed by TCD analysis. The rate is controlled by a mass flow controller, whose accuracy is confirmed prior to and during each run. Consequently, the syngas feed is fully characterized. The media is a

paraffin, which can be assumed to be inert [12], allowing it to be ignored in the analysis. The media is delivered by a highly accurate volumetric pump.

The Hot Trap Liquid stream (HTL) can be ignored in this analysis, provided that the temperature in the hot trap is high enough that VLE partitioning occurs in the wax range ($>C_{20}$). The wax production can then be estimated by extrapolating the diesel range (C10 – C20) production to infinite carbon number (via the ASF model), leaving only the Cold Trap Vapor and Cold Trap Liquid streams needing to be characterized. For SC-FTS operation, condensation in the hot trap occurs to a smaller degree than in GP-FTS and begins at higher carbon numbers (see Figure 4.3 and 4.6 for SC-FTS and Figure 4.4 for GP-FTS).

The Cold Trap Vapor stream (CTV) is analyzed by automatic injection to a TCD GC. The areas from the chromatogram are converted to concentrations using the component's molar response factor (RF_n = area / moles injected). The response factors for the various components are determined by using the same injection procedure with unreacted syngas and other standard gasses. While this determines the concentration of the various components in the CTV stream, the stream rate remains unknown. To that end, the syngas used includes a small concentration of N_2 (typically 1% to 2%). Because the nitrogen is inert in the process, it can be used to determine the rate of the CTV stream. This method is used, with confirmation from direct rate measurement, to determine the rate of the CTV stream, allowing the stream to be fully characterized.

Water partitions between the CTV stream and the CTL stream and is difficult to quantify in both. However, the rate of water production can be estimated by assuming that all of the oxygen that enters the system leaves as CO, CO_2, or H_2O. As the CO and CO_2 in the CTV

stream are quantified, the H_2O production rate is easily estimated. This leaves only the Cold Trap Liquid stream (CTL) to be characterized.

The quality of the balance to this point (syngas feed, cold trap vapor, and water production having been quantified) can be tested by calculating the carbon and hydrogen that remain unaccounted for. This carbon and hydrogen should be almost entirely contained in CH_2 groups, so the ratio of unaccounted for H to unaccounted for C should be slightly greater than 2. If it proves to be so, the analysis to this point can be trusted.

The cold trap liquid (CTL) stream consists of the media (minus what is lost to the cold trap vapor stream and the hot trap liquids) and produced hydrocarbons (produced water being ignored as it has already been quantified). Dietz [11] has demonstrated that, for hydrocarbons with no heteroatoms, the mass response factor (RF_m = GC area / mass of component injected) is essentially constant for all hydrocarbons. This allows the relative concentrations of the produced liquids to be easily determined (the C6 production cannot be quantified because of the media, but it can be from the C5's and C7's). The actual production rate is, however, not resolved in this way.

The total rate of the cold trap liquids is essentially known, as it should be nearly identical to the hexanes inlet rate. An internal standard could be employed in the same way as nitrogen is to determine the concentration of generated hydrocarbons in the media. In fact, because we have used hexanes (a mixture of C6 hydrocarbons including n-hexane, methyl-pentane, methyl-cyclopentane, and other components) instead of hexane, several potential internal standards are already present in the media. Unfortunately, the change in their peak areas is too small to be accurately quantified, making an internal standard of that type infeasible.

An external standard was used to characterize the Cold Trap Liquid stream (CTL). A series of standards of representative compounds were made to determine the mass response factor of the FID GC used to analyze this stream. This factor was then used to attempt to characterize the CTL stream.

Prior to beginning experimental work, a series of simulations were done in Hysis (Peng Robinson EOS) using a typical GP-FTS SC-FTS reactor effluent to determine if the hot trap (typically used to condense heavy waxes) could be used to effectively separate the diesel and wax (HTL) from the gas, gasoline, and media (HTV) for SC-FTS. C11+ purity (the concentration of C11+ components in the HTL) was plotted against C11+ recovery (the fraction of the C11+ components fed to the hot trap recovered in the HTL) at various pressures. Ideally, both would be 100%. The results of these simulations are shown in Figures 2.2 and 2.3 below.

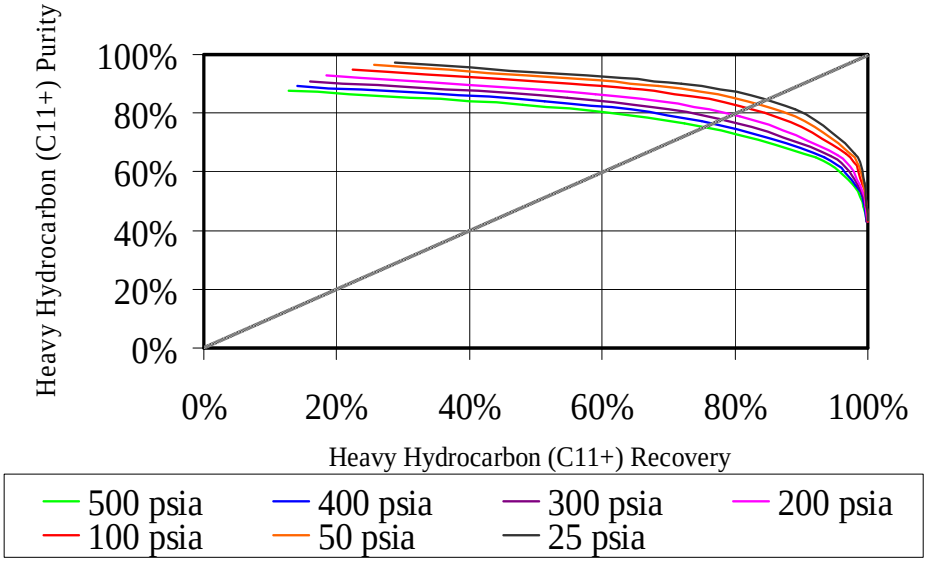

Figure 2.2 Hot trap simulation for gas-phase FTS to determine the possibility of using the hot trap to separate produced diesel and wax from the lighter products.

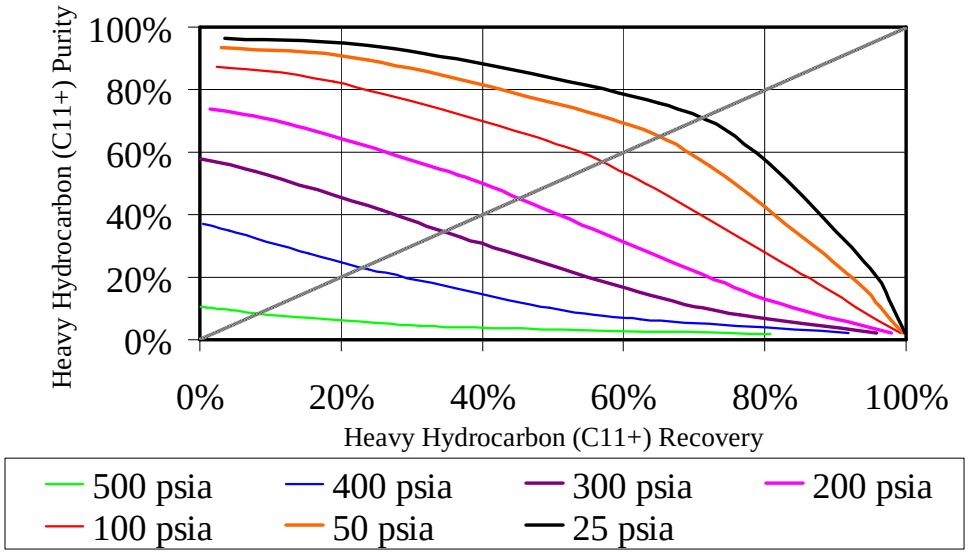

Figure 2.3 Hot trap simulation for Supercritical FTS to determine the viability of using the hot trap to separate produced diesel and wax from the lighter products and media

From the above, some conclusions can be drawn. First, low pressure enhances the effectiveness of the hot trap separation for both GP-FTS and SC-FTS. Second, under GP-FTS conditions, the hot trap can achieve both a relatively high purity and recovery (over 80%) of the diesel and wax while, under SC-FTS conditions, no such separation is possible.

This result set the stage for the experimental work to be discussed in this chapter, in which the procedure discussed above (external standard for the CTL stream) is to be used to attempt to close the SC-FTS material balance.

2.2 **Experimental**

A diagram of the reactor system (excluding minor equipment like check valves) used in this study is as follows:

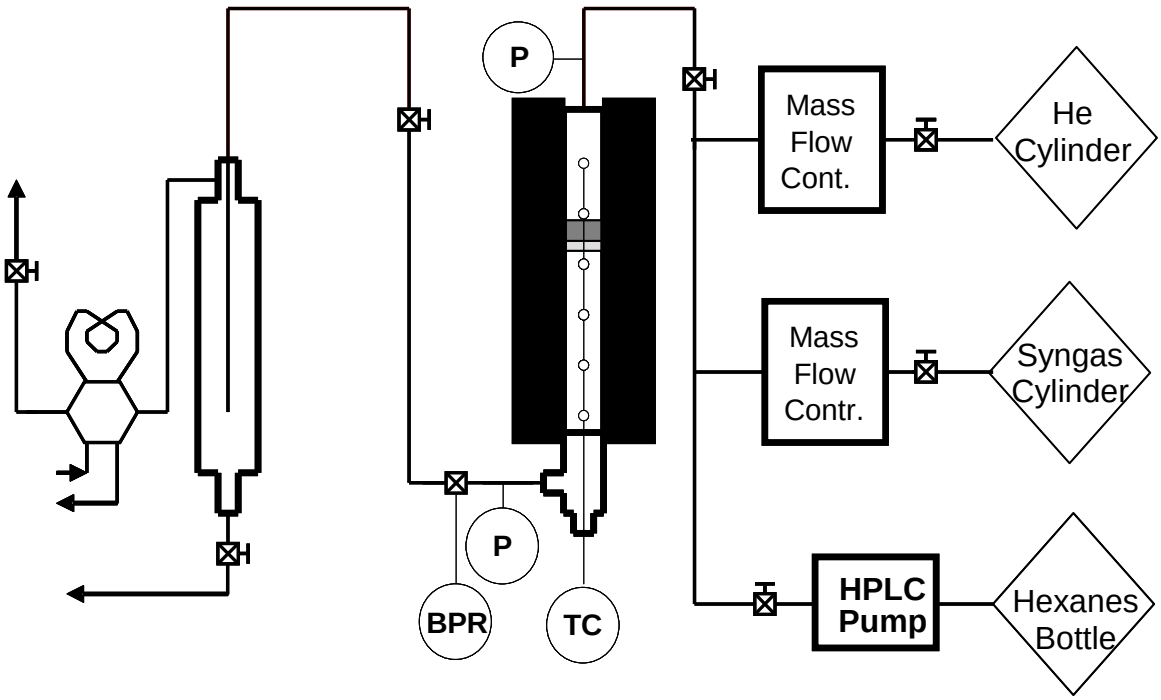

Figure 2.4 Diagram of the reactor system as used in this study

Syngas and helium (for startup and shut-down) were fed to the system through mass flow controllers and mixed (when appropriate) with hexanes fed through a positive displacement HPLC pump. This mixture then passed through heated tubing to the reactor in a split tube furnace. From the reactor, the effluent passed through heated tubing to the BPR (Back Pressure Regulator, used to control the reactor pressure), and on through heated tubing to the cold trap (cooled by circulating cold water in tubing outside its shell). The liquid that accumulated in the cold trap (CTL) was manually collected periodically for injection onto the FID GC. The gasses from the cold trap (CTV) passed through a 6-way injection valve, where they were periodically injected to the TCD GC. From there, the CTV stream passed through the WTM (Wet Test Meter: used to measure gas actual volumetric flow rates) and was then vented to the fume hood.

The reactor in this system is an HIP microreactor with a length of 10 inches and an ID of 0.5 inches. The upper half has been reamed out to an ID of 0.625 inches. A stainless steel filter

disk rests on the rim between the larger and smaller ID sections, with the catalyst resting upon the disk with glass wool both upstream and downstream of the catalyst bed to immobilize it. The reactor thermocouple is a 6-point profile thermocouple (Omega Engineering PP6-36-K-G-18).

The media used in this study was ACS Grade Hexanes purchased from Fisher Scientific in bulk and then transferred to 4 liter bottles. The syngas used was 67% H_2, 2% N_2, and 31% CO purchased as a certified standard from Airgas. A calibration gas (20% H_2, 5% N_2, 10% CO, 10% CH_4, 10% CO_2, and 1% C_2H_6) was purchased as a certified standard from Airgas. Pure gasses used for GC calibration were UHP grade from Airgas.

The cold trap vapor stream was analyzed by automatic injection (50 μL loop) onto a Varian 3800 GC with a TCD detector. The column in the TCD GC is a Haysep DB 100/120 (Alltech part number 2836PC). The cold trap liquid stream was analyzed by manual injection (0.3 μL) onto a Varian 3300 GC with an FID detector. The column in the FID GC is a DB-5 (Agilent 125-5032). Both GC's use UHP helium as the carrier gas and all chromatogram analysis is done using Varian's Star Workstation.

The catalyst used was 0.8g (in calcined form) of a 20% cobalt on alumina industrial catalyst. The catalyst was loaded into the reactor pre-calcined and reduced in situ at 320^{o}C for 4 hours in 50 SCCM H_2 at flowing pressure. At the end of the reduction, the hydrogen was displaced with helium. While flowing helium, the temperature was lowered to the initial reaction temperature (240^{o}C) and the pressure boosted to the reaction pressure (85 bar). Hexanes flow was then initiated, helium flow stopped, and syngas flow initiated (initiating the reaction). During the two week run, the temperature was varied in the following "random" order: 240^{o}C, 250 ^{o}C, 230 ^{o}C, 260 ^{o}C, 220 ^{o}C.

Selectivities in this dissertation are defined as shown below in Table 2.1 below.

Table 2.1 Selectivity definitions

Selectivity	Iron-Based Catalyst
CO_2	CO_2 produced / CO consumed
CH_4 (Cobalt)	CH_4 produced / CO consumed
CH_4 (Iron)	CH_4 produced / (CO consumed – CO_2 produced)
C3 Olefin Selectivity	Propene produced / (Propene produced + Propane produced)

2.3 Results

The response factors for the syngas components (H_2, N_2, CO) were determined by injecting syngas onto the TCD GC. The primary purpose of the calibration gas was to determine the response factors for methane, CO_2, and ethane. However, this calibration gas also includes the syngas components, and these different compositions gave somewhat different response factors. To further study this, when available, pure components were injected onto the TCD GC. The following data summarizes the results that were seen for hydrogen (Figure 2.5), nitrogen (Figure 2.6), and carbon monoxide (Figure 2.7):

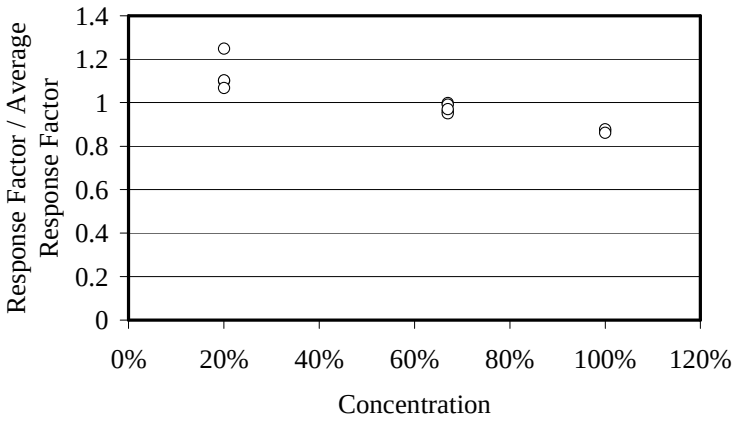

Figure 2.5 Variance in hydrogen TCD response factor with concentration.

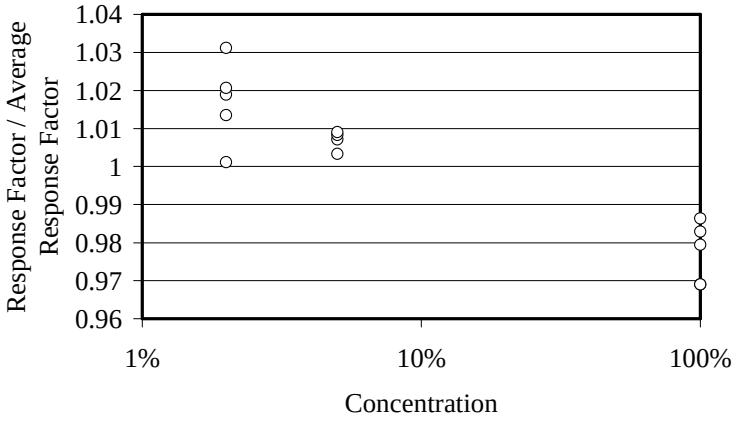

Figure 2.6 Variance in nitrogen TCD response factor with concentration

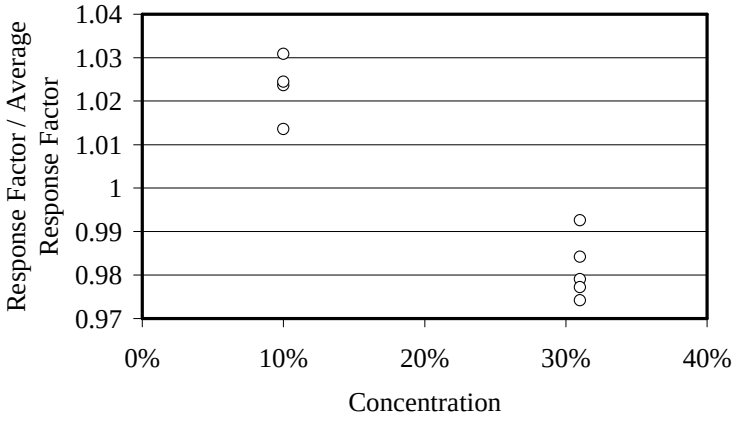

Figure 2.7 Variance in carbon monoxide TCD response factor with concentration

The response factors consistently decrease with increasing concentration. The change is largest for hydrogen (which has the lowest response factor), but not insignificant for carbon monoxide. While this discovery is apparently not new, it does indicate that the area ratio method of utilizing the internal standard (which assumes constant response factor) induces error. In

subsequent work, the variation in hydrogen response factor with hydrogen concentration has always been reproduced; the variation in CO and N_2 response factors have been less consistent.

Upon fixing this problem, the material balance was calculated. By subtracting the carbon and hydrogen in CTV stream and in the produced water from that in the syngas, a value is found for the unaccounted for carbon and hydrogen. Because these atoms should be in the CTL and HTL streams where they would primarily be in $(CH_2)_n$ groups, the atomic ratio of this unaccounted for hydrogen to unaccounted for carbon should be slightly greater than two. The results of this analysis are shown in Figure 2.2 below.

Table 2.2 Ratio of H and C unaccounted for after TCD analysis. A value slightly greater than 2 supports the accuracy of the TCD analysis.

Temperature (^oC)	H / C
220	2.09
230	2.07
240	2.1
250	2.1
260	2.0

With the possible exception of the data at 260^oC, at each temperature the ratio is slightly greater than two, indicating that the analysis thus far (including the syngas feed, CTV stream, and the produced water estimate) is accurate. This leaves only the CTL stream to characterize. Doing so, the excess carbon and hydrogen from the system can be calculated (Excess Carbon = 1 – Carbon Out / Carbon In). The results of this analysis are shown in Table 2.3 below.

Table 2.3 Excess C and H from overall SC-FTS material balance. If the material balance were perfect, the excess carbon and hydrogen would be zero.

Temperature (^{o}C)	Excess Carbon	Excess Hydrogen
220	6.7%	5.8%
230	9.7%	7.5%
240	-3.9%	0.5%
250	7.2%	7.0%
260	8.1%	8.4%

At four of the five temperatures studied, the material balance showed more hydrocarbons produced than syngas had been fed. Cracking of the media is unlikely because paraffins should be inert under FTS conditions [12] and there is no trend with temperature. Consequently, the problem is likely analytical. Specifically, since completing this study a water-cooled heat exchanger has been added to the fixed-bed system immediately prior to the cold trap. Condensation of heavy products and the media require a great deal of heat removal, which I no longer believe to have been completed satisfactorally, leading to losses of media to the CTV stream. This led to inflated concentrations of products in the CTL stream

. In addition to improving the product condensation in the system, the analytical procedures have been improved to measure the concentration of the media in the cold trap vapor stream and more careful cold trap liquids collection is now done to directly measure the rate. In determining liquid response factors, both the concentration and injection volume were varied. The data generated is plotted in Figure 2.7 below.

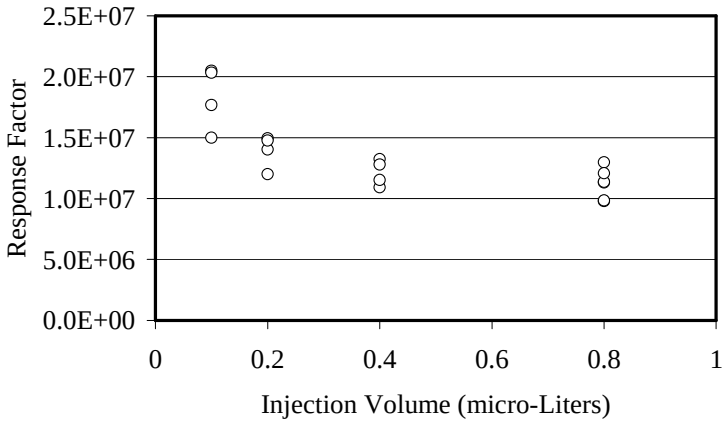

Figure 2.8 1-Octene FID Response factor at various standard concentrations and nominal injection volumes.

The above indicates that there is a dependence of the response factor on the injection volume, with the behavior being what would be expected if the true injection volume were larger than the nominal one by a constant value (which becomes increasingly significant as the injection volume decreases). As the injection volume needed to be adjusted during the run, this complicated the analysis and demonstrated the need for consistency in this area.

Since completion of this study, we have begun practicing a new method of liquid analysis. SC-FTS liquid samples are analyzed twice: first as collected, second with a known concentration of C14 added. This allows the C14 to be used as an internal standard, to determine the response factor and analyze the product in the same GC injection.

Looking now at the selectivity of carbon to the various products at the different temperatures, some clear trends emerge:

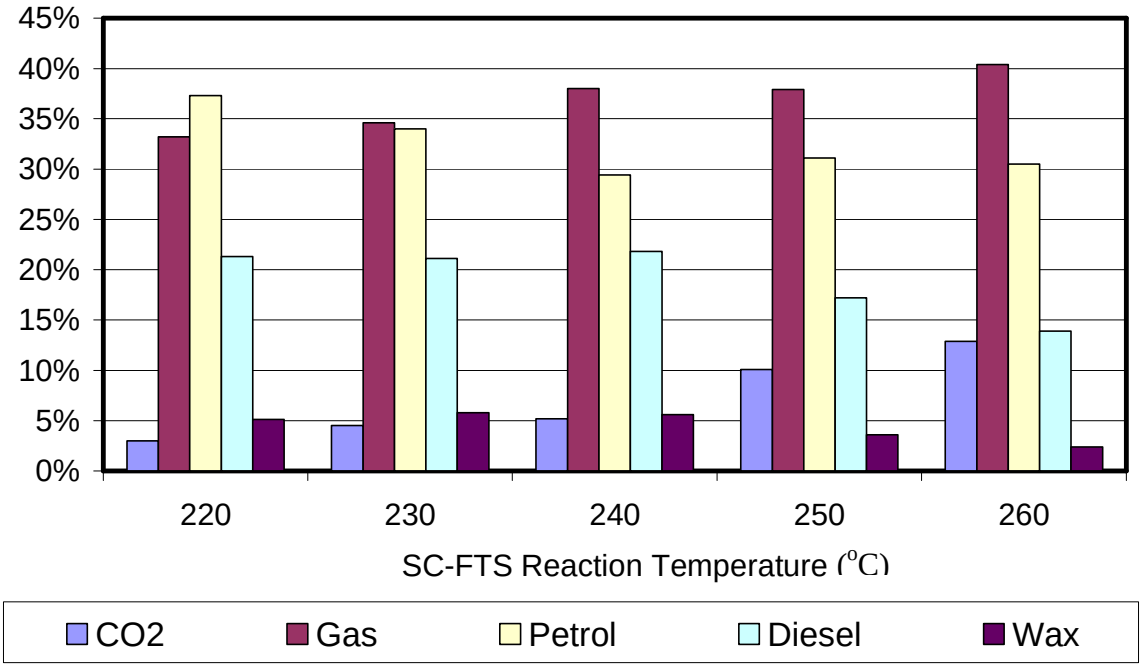

Figure 2.9 Carbon Selectivity for various FT products at various temperatures under SC-FTS conditions.

With increasing temperature, the oxygen disposal shifts towards CO_2 and the overall product distribution shifts more towards light products. It should be noted that, in switching from SC-FTS to GP-FTS the CO_2 selectivity has been shown to increase [3] and some research groups have seen enhanced light product selectivity [13-15]). This indicates that SC-FTS behaves in some ways like GP-FTS at a lower temperature, supporting the contention that SC-FTS improves heat management due to its higher density.

2.4 Conclusions

A number of unexpected problems were encountered in attempting to close the SC-FTS material balance, including the variability in TCD response factors and the influence of FID injection volume.

It should be noted, however, that the material balance numbers reported above are optimistic. First, they do not include the light oxygenates that are more soluble in the produced water (which was not analyzed) than the organic phase. Second, the ASF plot should be extrapolated to an infinite carbon number to capture the waxes produced that are too heavy to stay dissolved in the organic liquid phase or to elute from the FID column (this was not done).

The improvements made in the reactor system and our analytical procedures as outlined in this chapter have allowed us to more accurately close the material balance, which will be very important in the work that will be outlined in Chapter 6 (Future Work).

2.5 References

[1] Kohshiroh Yokota**,** Kaoru Fujimoto: Supercritical phase Fischer-Tropsch synthesis reaction. **Fuel** (1989): V 68, I 2, p 255.

[2] Nimir O. Elbashir, P. Dutta, A. Manivannan, M. S. Seehra, Christopher B. Roberts: *Impact of Cobalt-Based Catalyst Characteristics on the Performance of Conventional Gas-Phase and Supercritical-Phase Fischer Tropsch Synthesis*. **Applied Catalysis A: General** (2005): V 285, p 169.

[3] Gary Jacobs, Karuna Chaudhari, Dennis Sparks, Yongqing Zhang, Buchang Shi, Robert Spicer, Tapan K. Das, Jinlin Li, Burtron H. Davis: *Fischer–Tropsch Synthesis: Supercritical Conversion Using a Co/Al_2O_3 Catalyst in a Fixed Bed Reactor*. **Fuel** (2003): V 82, I 10, p 1251.

[4] Shirun Yan, Li Fan, Zhixin Zhang, Jinglai Zhou, Kaoru Fujimoto: *Supercritical-Phase Process for Selective Synthesis of Heavy Hydrocarbons from Syngas on Cobalt Catalysts*. **Applied Catalysis A: General** (1998): V 171, p 247.

[5] Xiwen Huang, Christopher B. Roberts: *Selective Fischer-Tropsch Synthesis Over an Al_2O_3 Supported Cobalt Catalyst in Supercritical Hexane*. **Fuel Processing Technology** (2003): V 83, p 81.

[6] TANG Haodong, LIU Huazhang, YANG Xiazhen, LI Ying: *Supercritical Phase Fischer-Tropsch Synthesis Reaction over Highly Active Fused Iron Catalyst at Low Temperature*. **Journal of Chemical Engineering of Chinese Universities** (2008): V 22, N 2, p 259.

[7] Kohshiroh Yokota, Yoshio Hanakata, Kaoru Fujimoto: *Supercritical-Phase Fischer-Tropsch Synthesis Reaction. 3: Extraction Capability of Supercritical Fluids*. **Fuel** (1991): V 70, I 8, p 989.

[8] Xiwen Huang, Christopher B. Roberts: *Selective Fischer-Tropsch Synthesis Over an Al_2O_3 Supported Cobalt Catalyst in Supercritical Hexane*. **Fuel Processing Technology** (2003): V 83, p 81.

[9] Xiaosu Lang, Aydin Akgerman, Dragomir B. Bukur: *Steady State Fischer-Tropsch Synthesis in Supercritical Propane*. **Industrial and Engineering Chemistry Research** (1995): V 34, I 1, p 72.

[10] Dragomir B. Bukur, Xiaosu Lang, Aydin Akgerman, Zhentao Feng: *Effect of Process Conditions on Olefin Selectivity during Conventional and Supercritical Fischer-Tropsch Synthesis*. **Industrial and Engineering Chemistry Research** (1997): V 36, N 7, p 2580.

[11] WA Dietz: *Response Factors for Gas Chromatographic Analyses*. **Journal of Gas Chromatography** (1967): V 5, p 68.

[12] M. Claeys, E. van Steen: *Basic Studies*. **Studies in Surface Science and Catalysis 152** (ISBN 978-0-444-51354-0): Ch 8.

[13] Xiwen Huang, Christopher B. Roberts: *Selective Fischer-Tropsch Synthesis Over an Al_2O_3 Supported Cobalt Catalyst in Supercritical Hexane*. **Fuel Processing Technology** (2003): V 83, p 81.

[14] Xiwen Huang, Nimir O. Elbashir, Christopher B. Roberts: *Supercritical Solvent Effects on Hydrocarbon Product Distributions from Fischer Tropsch Synthesis Over an Alumina-Supported Cobalt Catalyst*. **Industrial and Engineering Chemistry Research** (2004): V 43, p 6369.

[15] Nimir O. Elbashir, P. Dutta, A. Manivannan, M. S. Seehra, Christopher B. Roberts: *Impact of Cobalt-Based Catalyst Characteristics on the Performance of Conventional Gas-Phase and Supercritical-Phase Fischer Tropsch Synthesis*. **Applied Catalysis A: General** (2005): V 285, p 169.

[16] Mark E. Dry: *Practical and Theoretical Aspects of the Catalytic Fischer-Tropsch Process*. **Applied Catalysis A: General** (1996): V 138, I 2, p 319-344.

Chapter 3

Supercritical Activity Restoration for Fischer Tropsch Synthesis

3.1 Abstract

Previous research has demonstrated that supercritical phase Fischer Tropsch Synthesis (SC-FTS) using hexanes as the solvent medium offers superior activity maintenance to gas-phase Fischer Tropsch Synthesis (GP-FTS) [1]. This has prompted an investigation into whether supercritical media can reactivate a catalyst used in GP-FTS. To that end, an experiment was conducted in which a series of GP-FTS periods of approximately 2 days each were performed, separated by periods of catalyst reactivation using supercritical hexanes as well as SC-FTS.

It was found that the supercritical hexanes media and SC-FTS reactivations periods were effective in restoring lost catalyst activity and selectivity, though not completely. GP-FTS was demonstrated to have detrimental effects on subsequent SC-FTS operation while SC-FTS operation showed beneficial effects on subsequent GP-FTS operation, particularly with the SC-FTS reactivations reducing the methane selectivity in subsequent GP-FTS periods. The CO_2 selectivity in SC-FTS operation is consistently lower than that in GP-FTS operation while the olefin selectivity into the diesel range is higher with SC-FTS. While the propagation probability was initially higher in SC-FTS than GP-FTS, with increasing time on stream the propagation probability values converged.

3.2 Background

Fischer Tropsch Synthesis (FTS) is a mature process for the production of hydrocarbons from syngas (carbon monoxide and hydrogen). Industrially, FTS is operated in two modes: high temperature (HTFT) and low temperature (LTFT). HTFT (~ 340^{o}C) is performed in a fluidized bed reactor on a fused iron catalyst for synthesizing primarily gasoline and light olefins. LTFT (200^{o}C-250^{o}C) is typically conducted in a fixed bed reactor or slurry bed reactor on an impregnated cobalt or precipitated iron catalyst for synthesizing primarily diesel and wax [2]. Subsequent discussion of FTS in this paper will be exclusively related to LTFT.

FTS is a polymerization process that appears to follow an ASF mechanism, making it unselective. Consequently, a broad product spectrum from methane to heavy wax is produced, including different types of hydrocarbons (n-alkanes, n-alkenes, oxygenates, and methyl-branched compounds). FTS is also a highly exothermic process [2]:

$$CO + 2H_2 \rightarrow (CH_2) + H_2O + 146\ kJ$$

Managing the heat released by the reaction is a major influence on reactor design [2].

Sasol originally utilized a fixed-bed reactor (GP-FTS) for LTFT. These reactors have a diameter of 3m and include 2050 tubes with a length of 12m and an ID of 5cm, resulting in a capacity of 900 BPD [3]. The exothermic nature of the reaction requires a high velocity in narrow tubes, resulting in a large number of tubes and a high pressure drop (3 to 7 bar) [3]. Localized overheating still occurs [4], leading to increased methane formation [2]. Additionally, wax accumulates in the catalyst pores [4], leading to diffusion resistance. This diffusion resistance both decreases the conversion and increases the methane selectivity [5]). Despite these limitations, fixed bed FTS still garners significant attention, including Shell's SMDS (Shell Middle Distillate Synthesis) process, which utilizes a fixed-bed reactor design [6].

To overcome these limitations, Sasol developed their slurry-bed reactor. This reactor utilizes a heavy wax liquid media and operates like a CSTR, producing high temperature uniformity [3]. The pressure drop across the reactor is much lower and economies of scale are much better than fixed-bed operation. Some challenges in slurry bed FTS are separation of the wax from the catalyst [3], catalyst attrition [3], and development cost and economic risk [7].

A third option that has not been utilized industrially is the use of a supercritical medium for Fischer Tropsch Synthesis (SC-FTS). Supercritical fluids are miscible with gasses and their high, liquid-like density leads to improved heat dissipation properties and excellent liquid product extraction relative to a gas phase medium.

Most research into SC-FTS has compared it with GP-FTS. SC-FTS has been consistently shown to suppress methane formation [1,4,5,8,9,10] and has been demonstrated to suppress CO_2 formation [4,11]. While little difference is usually seen between GP-FTS and SC-FTS in light hydrocarbon olefin selectivity, SC-FTS has been consistently shown to enhance the maintenance of olefin selectivity into higher carbon numbers [4,9,12,13,14]. The literature, however, is inconsistent regarding the effects of SC-FTS operation on conversion. Additionally, some researchers have observed an enhanced propagation probability or diesel and wax selectivity in SC-FTS [1,9,15] relative to GP-FTS while others have reported no difference [4,16,17] .

Yokota and Fujimoto [16] determined activation energies for both GP-FTS and SC-FTS and found that SC-FTS had a lower activation energy than GP-FTS; suppressed activation energy corresponds to diffusion restrictions [18].

Kaoru Fujimoto's group [12] has demonstrated the capacity of the supercritical media to extract hydrocarbon products in two ways: (1) by determining the portion of products remaining on the catalyst at the completion of a GP-FTS and SC-FTS run and (2) by pre-impregnating a

catalyst with wax and attempting to extract it with a gas phase and a supercritical phase media. In both cases, supercritical hexane gave much better hydrocarbon extraction than nitrogen of the same temperature and pressure. Kaoru Fujimoto's [5] group also demonstrated that SC-FTS gives a more uniform syngas composition within the catalyst than GP-FTS.

Earlier work in our group [1] has demonstrated that SC-FTS offers much better activity maintenance and methane selectivity than GP-FTS on a cobalt-based catalyst. In GP-FTS, the conversion dropped from 70% to 40% in under 200 hours time on stream while, in SC-FTS, there was no loss in conversion after 250 hours time on stream. GP-FTS gave a methane selectivity of 20% to 40% (230^{o}C to 250^{o}C), while SC-FTS gave a methane selectivity approximately half of that. This led us to design an experiment to test whether a period in which the catalyst was exposed to a supercritical environment could restore lost activity and selectivity for subsequent GP-FTS operation. Preliminary results are presented elsewhere [19].

3.3 Experimental

A schematic of the reactor system is shown in Figure 3.1 below.

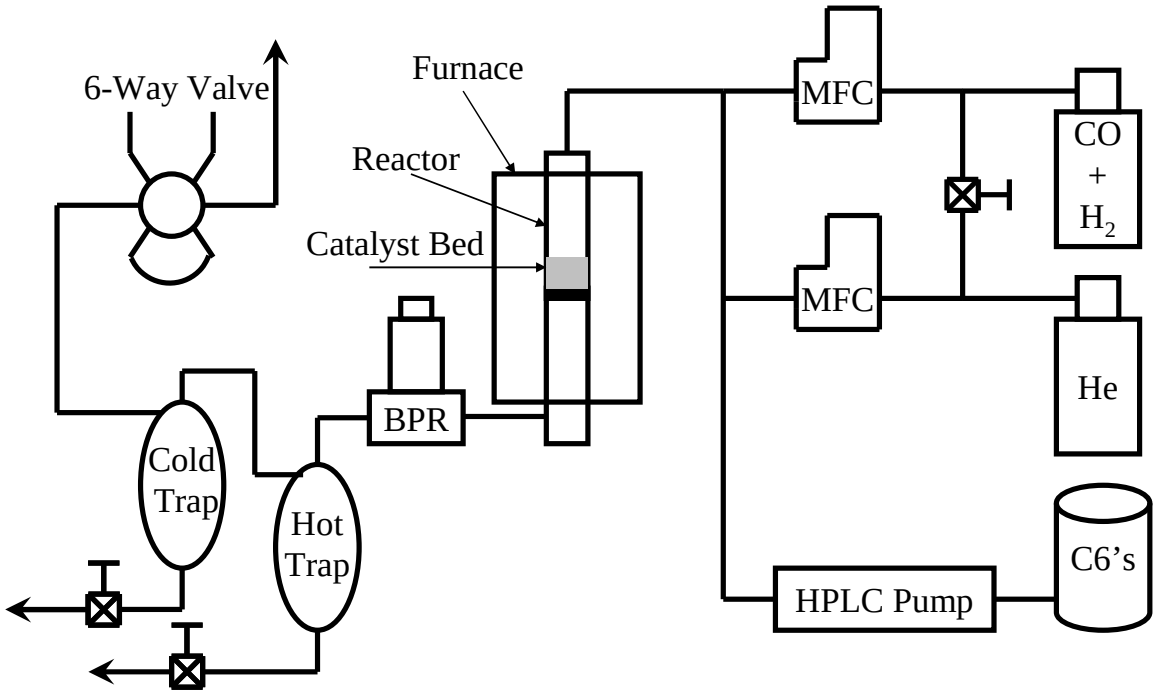

Figure 3.1 Schematic of the fixed bed reactor system used in this study. Syngas is metered through a thermal mass flow controller and mixed with hexanes delivered through an HPLC pump. The ID in the upper half of the reactor was increased, creating a lip halfway down the reactor, on which a porous silica frit rests. The catalyst bed sits upon the frit. The reactor is in a downflow configuration within a split-tube furnace. The Back Pressure Regulator (BPR) maintains the reactor pressure. The hot trap is used to condense heavy products and the cold trap used to condense all but the permanent gasses. The cold trap vapor stream flows to the 6-way valve where it is automatically injected to the TCD GC. The cold trap liquids are manually collected for manual injection to the FID GC.

Syngas is metered through a mass flow controller (MFC) and mixed with hexanes delivered through an HPLC pump. The upper half of the reactor was reamed out to increase the ID, creating a lip halfway down the reactor on which a porous silica frit rests. The catalyst bed sits upon the frit, immobilized by glass wool. The reactor is in a downflow configuration within a split-tube furnace. The back pressure regulator (BPR) maintains the reactor pressure. The hot trap is used to condense heavy products and the cold trap used to condense all but the permanent

gasses. The cold trap vapor stream flows to the 6-way valve where it is automatically injected to the TCD GC. The cold trap liquids are manually collected for manual injection to the FID GC.

Gas Analysis was carried out by online injection to a Varian 3800 GC with a TCD detector and a Hayesep column (Grace Davison 2836PC). Liquid analysis was carried out by manual injection to a Varian 3300 GC with an FID detector and a DB-5 column (Agilent 125-5032).

The syngas was purchased pre-mixed from Airgas (Certified Standard) with 2% N_2 (internal standard) and a syngas ratio (H_2/CO) of 2.15. The helium is UHP grade and is used for pressure testing, startup, and shut-down. The hexanes was purchased in bulk from Fisher Scientific.

The catalyst was 0.75g of 20% cobalt on alumina industrial catalyst diluted with an equal mass of blank alumina. Reduction was done in situ using 50 SCCM hydrogen at 320^{o}C and atmospheric pressure for 4 hours.

The reaction temperature was maintained at 240^{o}C. Under gas phase operation, the syngas rate was 50 SCCM and the reactor pressure set at 15 bar. Under supercritical operation, the syngas rate was 50 SCCM, the hexanes rate 1 mL/min, and the reactor pressure set at 65 bar to give a constant syngas partial pressure under both sets of conditions.

Switching between gas phase and supercritical operation was done by initiating hexanes and shutting off syngas flow. When the reactor had been purged, the hexanes rate was boosted to 4 mL/min and the reactor pressure increased. When the reactor pressure reached 65 bar, the hexanes rate was reduced to 1 mL/min. After 4 hours, the liquid was collected (including gas phase products) and syngas flow restarted.

Switching back to gas phase operation was done by stopping the syngas flow and reducing the reactor pressure to 15 bar. Syngas flow was then restarted and hexanes flow stopped.

The timeline for the study is shown in Figure 3.2 below.

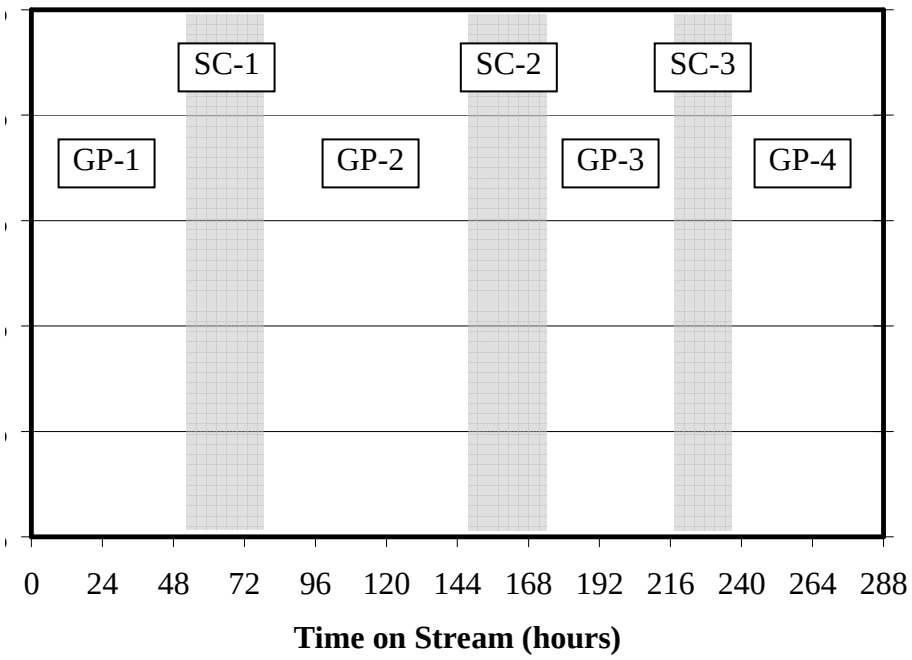

Figure 3.2 Schematic of the experimental procedure. Unshaded periods correspond to GP-FTS, shaded portions correspond to SC-hexane flushing and SC-FTS operation.

The shaded regions correspond to times in which the catalyst is either being extracted with supercritical hexanes or SC-FTS is taking place (heretofore referred to as washings). The unshaded portions correspond to GP-FTS operation.

No data was collected during the third period of SC-FTS operation due to difficulties in temperature control.

3.4 Results

CO and H_2 conversion for this study are shown in Figure 3.3 below.

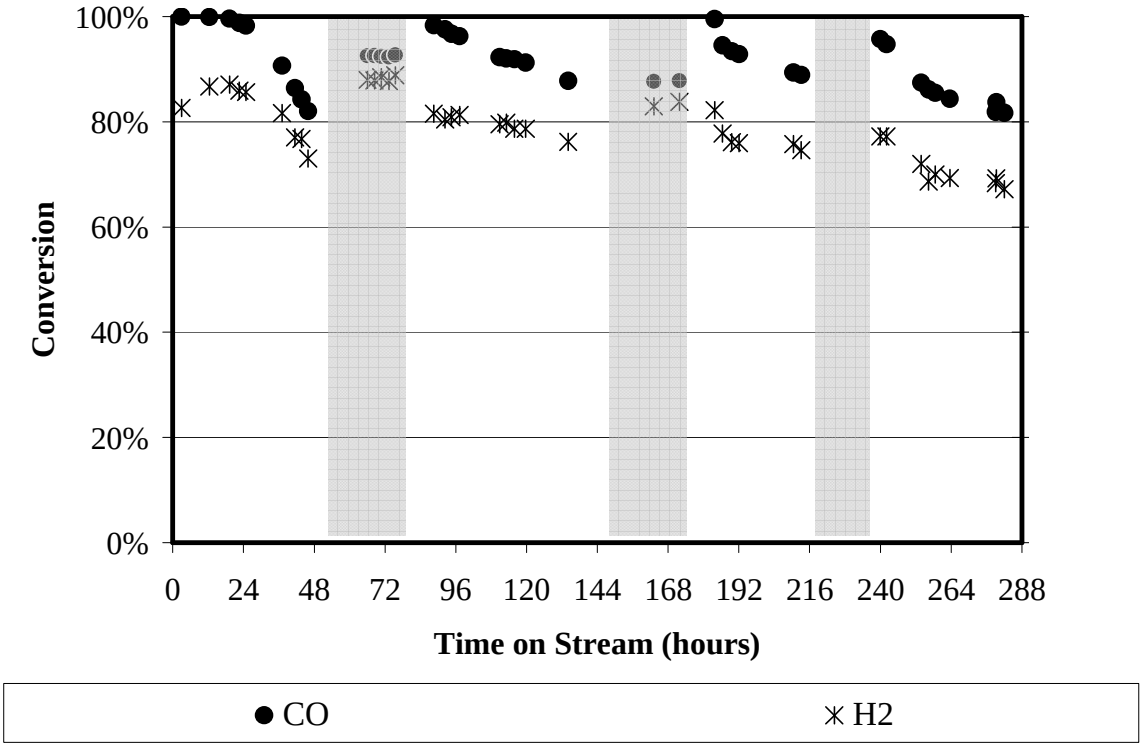

Figure 3.3 CO and H_2 conversion –v– time-on-stream

It is clear that the supercritical washings showed a strong capacity to restore lost activity as the CO conversion increased after each supercritical washing to nearly 100%. Additionally, during the first GP-FTS period the rate of activity loss was high. In the subsequent GP-FTS periods, the deactivation rate was significantly moderated. The conversion is higher during the first SC-FTS portion than the second, indicating that GP-FTS operation damaged the catalyst for SC-FTS operation. As conversion did not increase during SC-FTS operation, it is concluded that increasing the washing time would not have led to greater reactivation. SC-FTS gave a higher usage ratio (consumption rate of H_2 / consumption rate of CO) than GP-FTS.

The methane selectivity is shown in Figure 3.4 below.

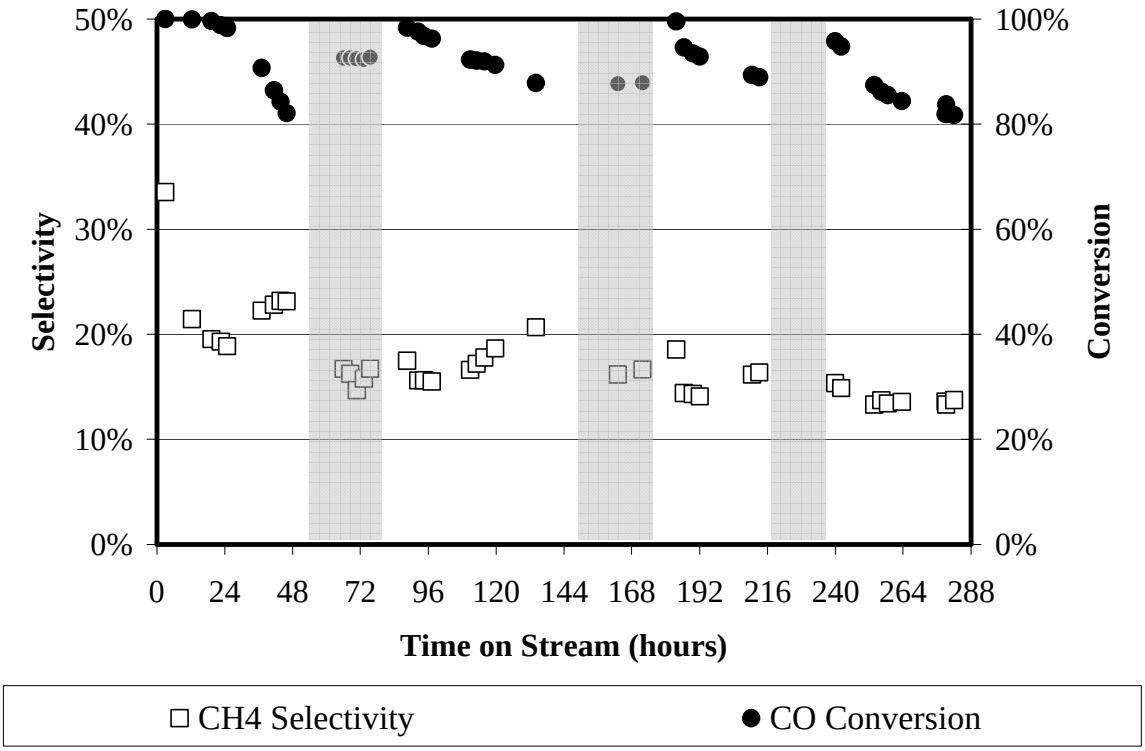

Figure 3.4 Methane selectivity –v– time-on-stream (CO conversion shown for comparison)

During each of the GP-FTS periods, the methane selectivity first dropped with increasing time on stream, then reached a minimum, followed by a modest increase with further time on stream. Since the syngas ratio is higher than the usage ratio, high conversion results in an inflated syngas ratio near the reactor exit, thereby promoting methanation. We attribute the drop in methane selectivity early in each GP-FTS period to the drop in conversion moderating the syngas ratio near the bed exit. As time passes during a GP-FTS portion, the catalyst pores will fill with wax. This leads to diffusion resistance, which promote methanation [5]. This is a reasonable explanation for the minimum and subsequent increase of the methane selectivity seen in each GP-FTS period.

The methane selectivity is 16% in both the first and second SC-FTS portions. However, for GP-FTS operation, the methane selectivity drops after each washing stage. Our group has

run GP-FTS for extended periods without washing stages and have not observed this drop in methane selectivity [1]. Consequently, this leads us to believe that the supercritical washings are acting to decrease the methane selectivity in subsequent GP-FTS operation.

The CO_2 selectivity is shown in Figure 3.5 below.

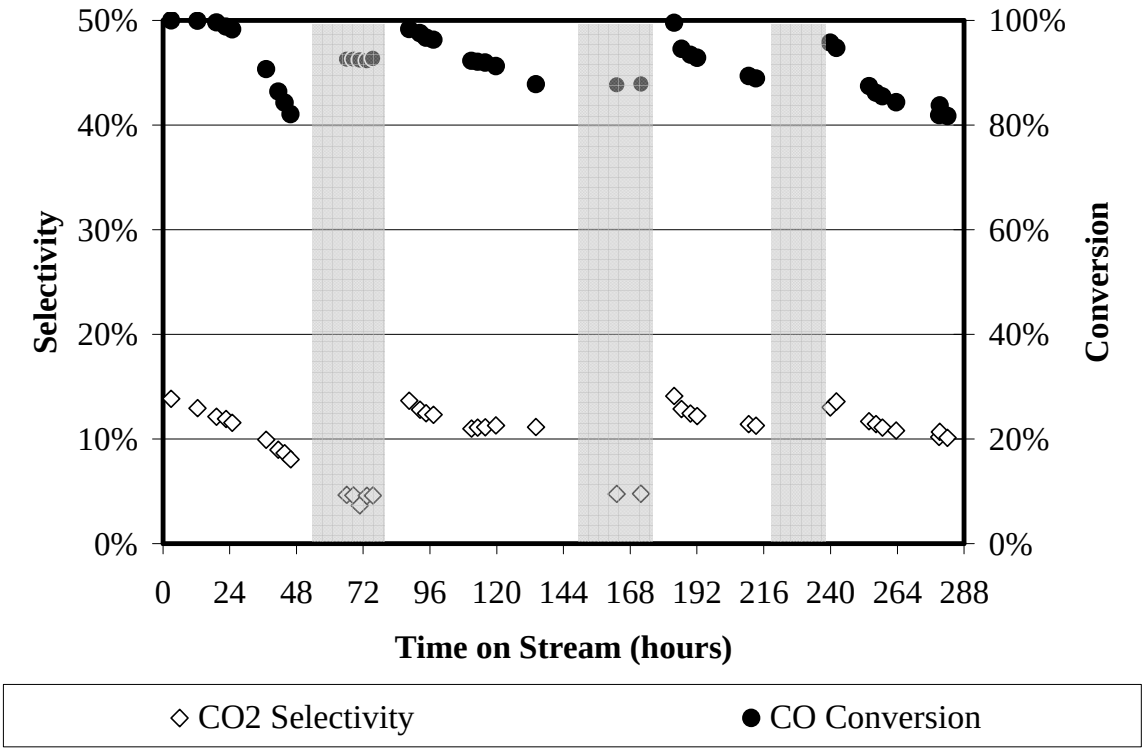

Figure 3.5 CO_2 selectivity –v– time-on-stream (CO conversion shown for comparison)

The CO_2 selectivity during GP-FTS operation is higher than during SC-FTS operation. During GP-FTS, the CO_2 selectivity decreases with time on stream, but the corresponding drop in conversion is at least partly responsible for the decrease in CO_2 selectivity.

The propene selectivity [propene / (propene + propane)] is shown in Figure 3.6 below.

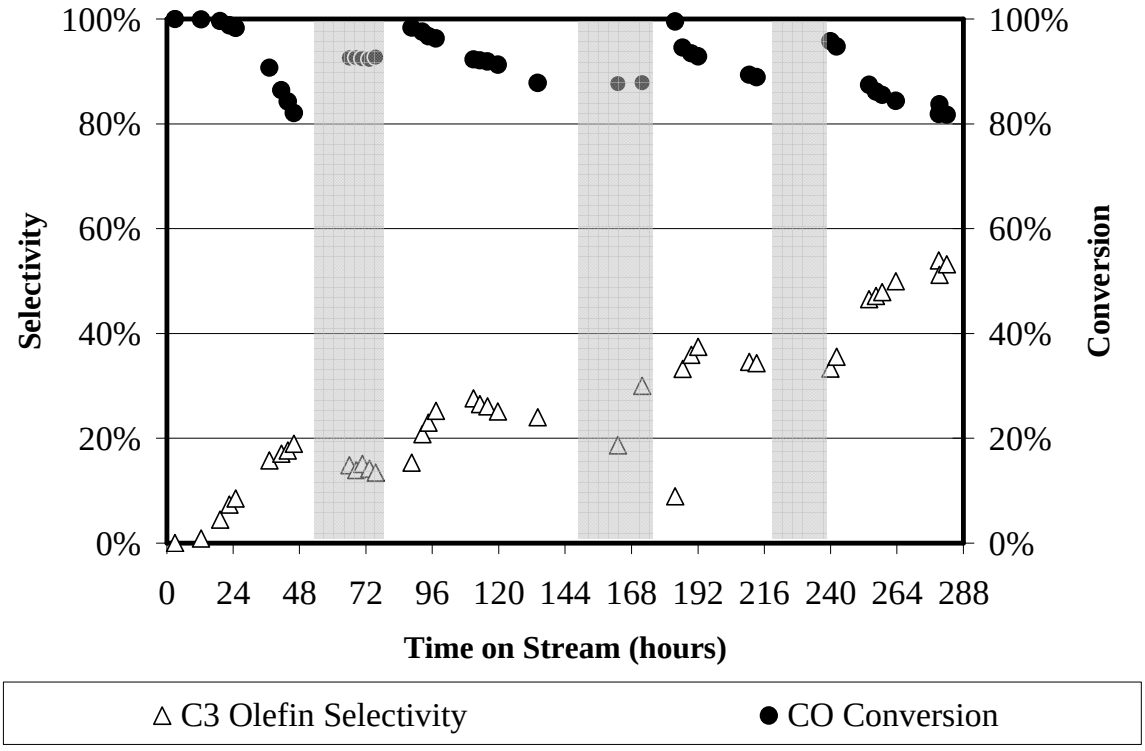

Figure 3.6 Propene selectivity –v– time-on-stream (CO conversion shown for comparison)

During GP-FTS operation, the C3 olefin selectivity increases with decreasing conversion (hydrogenation being a secondary reaction). However, during the 2nd and 3rd GP-FTS portions, the C3 olefin selectivity reached a maximum and began to decrease with increasing TOS (and associated decrease in conversion), an observation analogous to that seen with the methane selectivity). This may be due to wax buildup leading to diffusion limitations. Comparing the GP-FTS gas analysis, the later periods show higher C3 olefin selectivity, even adjusting for conversion. This may be due either to the washings themselves or increasing time on stream.

The liquid product analysis is shown in Table 3.1 below.

Table 3.1 Propagation Probability (α) and the olefin selectivity for the C7 – C12 range for each portion of the experiment. The C3 olefin selectivity is shown for comparison.

	Propagation Probability	C3 Olefin Selectivity	C7 – C12 Olefin Selectivity
GP-1	73%	10%	3%
SC-1	80%	14%	11%
GP-2	73%	26%	4%
SC-2	78%	21%	13%
GP-3	78%	35%	5%
SC-3	-	-	-
GP-4	77%	50%	9%

As was discussed earlier, there is little difference in the C3 olefin selectivity between GP-FTS and SC-FTS operation. However, the C7-C12 olefin selectivity is greatly enhanced in supercritical operation, indicating that SC-FTS gives a better maintenance of the olefin selectivity into high carbon numbers. As was noted above, this is a common observation, and one that we have also observed on an iron catalyst [11].

At low time on stream, SC-FTS gave a higher propagation probability than GP-FTS. This is in keeping with the observation that some researchers have made of SC-FTS giving enhanced heavy product selectivity [1,9,14]. However, the propagation probability for GP-FTS and SC-FTS converged as the experiment continued, in keeping with the observations of other researchers who reported no difference in the overall product distribution between GP-FTS and SC-FTS [4,16,17]. An explanation for this observation is that the catalyst bed may require significant time on stream to build sufficient thermal mass to effectively manage the heat released by the reaction.

3.5 Conclusions

In this work, we have confirmed the capacity of a supercritical hexanes environment to restore activity lost during GP-FTS operation. Additionally, the SC-FTS washings benefited subsequent GP-FTS selectivity, decreasing the methane selectivity and increasing the C3 olefin selectivity. While GP-FTS operation decreased the conversion in subsequent SC-FTS periods, it showed no effect on the selectivity.

A critical observation in this study involves the decrease in GP-FTS methane selectivity after each supercritical washing period. In earlier work in our group in which GP-FTS was continued for over 150 hours time on stream this decrease in methane selectivity was not observed [1], indicating that it is the SC-FTS washing and not the time on stream that is the cause of the decreased methane selectivity. This is in keeping with the observation that SC-FTS gives a different oxidation state and crystalline structure for cobalt than does GP-FTS [1]. It has previously been shown that a waxed up LTFT catalyst can have its activity temporarily enhanced by exposure to a liquid solvent [20]. That this effect would also be seen when using a supercritical environment is expected. However, the effects of the SC-FTS washings on the methane selectivity indicate that more than extraction, like modification of the catalyst oxidation / crystalline state, is taking place.

3.6 References

[1] Nimir O. Elbashir, P. Dutta, A. Manivannan, M. S. Seehra, Christopher B. Roberts, Appl. Catal., A 285 (2005) 169-180.

[2] Mark E. Dry, Appl. Catal., A 138 (1996) 319-344.

[3] B. Jager, R. Espinoza, Catal. Today 23 (1995) 17-28.

[4] Gary Jacobs, Karuna Chaudhari, Dennis Sparks, Yongqing Zhang, Buchang Shi, Robert Spicer, Tapan K. Das, Jinlin Li, Burtron H. Davis, Fuel 82 (2003) 1251- 1260.

[5] Shirun Yan, Li Fan, Zhixin Zhang, Jinglai Zhou, Kaoru Fujimoto, Appl. Catal., A 171 (1998) 247-254.

[6] Shell in Malaysia website: http://www.shell.com.my/home/content/mys/products_services/solutions_for_businesses/smds/smds_process.html Accessed 04/16/2010.

[7] Kenneth Agee, Rafael Espinoza, AIChE Spring Meeting (2010) Presentation10a.

[8] Kohshiroh Yokota, Kaoru Fujimoto, Fuel 68 (1989) 255-256.

[9] Xiwen Huang, Christopher B. Roberts, Fuel Process. Technol. 83 (2003) 81-99.

[10] TANG Haodong, LIU Huazhang, YANG Xiazhen, LI Ying, J. Chem. Eng. Chin. 22 (2008) 259.

[11] Ed Durham, Sihe Zhang, Christopher B. Roberts, Preprints of Symposia - American Chemical Society: Division of Fuel Chemistry (2010).

[12] Kohshiroh Yokota, Yoshio Hanakata, Kaoru Fujimoto, Fuel 70 (1991) 989-994.

[13] Xiaosu Lang, Aydin Akgerman, Dragomir B. Bukur, Ind. Eng. Chem. Res. 34 (1995): V 34, I 1, p 72-77.

[14] Dragomir B. Bukur, Xiaosu Lang, Aydin Akgerman, Zhentao Feng, Ind. Eng. Chem. Res. 36 (1997) 2580-2587.

[15] Xiwen Huang, Nimir O. Elbashir, Christopher B. Roberts, Ind. Eng. Chem. Res. 43 (2004) 6369-6381.

[16] Kohshiroh Yokota, Kaoru Fujimoto, Ind. Eng. Chem. Res. 30 (1991) 95-100.

[17] Dragomir Bukur, Xiaosu Lang, Lech Nowicki, Ind. Eng. Chem. Res. 44 (2005) 6038-6044.

[18] William H. Zimmerman, Joseph A. Rossin, and Dragomir B. Bukur, Ind. Eng. Chem. Res. 28 (1989) 406-413.

[19] Ed Durham, Mahesh Bordawekar, Christopher B. Roberts, Preprints of Symposia - American Chemical Society: Division of Fuel Chemistry (2007).

[20] M. E. Dry, The Fischer-Tropsch Synthesis, in: John R Anderson, Michael Boudart (eds.), Catalysis Science and Technology Volume 1, Springer-Verlag, Berlin 1981, pp159-255.

Chapter 4

Diesel-Length Aldehydes and Ketones via Supercritical Fischer Tropsch Synthesis on an Iron Catalyst

4.1 Abstract

Use of an iron-based catalyst (1 Fe : 0.01 Cu : 0.02 K by mole with and without 0.1 Zn) for Fischer Tropsch Synthesis with a supercritical hexanes reaction media resulted in a significant selectivity towards diesel length aldehydes and methyl-ketones. Varying the residence time indicated that aldehydes are primary products that are converted by secondary reactions to olefins. Additionally, incorporation studies showed that octyl aldehyde and octyl alcohol incorporated into growing chains while the octyl olefin did not. The results of this work support n-alkanes and aldehydes as primary products, olefins as both primary and secondary products, CH_4 and CO_2 as secondary products, and an oxygenate mechanism for propagation.

4.2 Introduction

Fischer Tropsch Synthesis (FTS) is a process for converting syngas ($CO + H_2$) to fuels and chemicals. FTS can be performed at high temperature (HTFT) on an iron catalyst for the production of gasoline and light olefins or at low temperature (LTFT) on either an iron or cobalt catalyst for the production of diesel and wax [1]. Iron is cheaper [1] and less active [2] than cobalt. Iron offers Water-Gas Shift activity, allowing for a lower usage ratio (the ratio of the rate

of consumption of H_2 to the rate of consumption of CO) and a broader range of the syngas ratio (the ratio of the feed rate of H_2 to the feed rate of CO) at the cost of a higher CO_2 selectivity [3]. Iron also provides greater resistance to poisoning by sulfur, but inferior resistance to coking and attrition [3]. Iron gives a more olefinic product and suppressed methane formation [4].

Sasol's original LTFT reactor design utilized a fixed bed, as does a Shell design [5]. This form of operation is Gas Phase Fischer Tropsch (GP-FTS). To overcome the limitations of GP-FTS (poor extraction of products and heat from the catalyst, high pressure drop, and poor economies of scale), Sasol developed their slurry bed reactor (SP-FTS) [5]. Kaoru Fujimoto's group [6] pioneered the use of a supercritical fluid as the reaction medium for fixed bed LTFT (SC-FTS) to mitigate some of the problems seen in GP-FTS. A number of benefits have been seen in SC-FTS relative to GP-FTS, including suppressed methane formation [6-12], CO_2 formation [8,12] and improved activity maintenance [10]. Additionally, many researchers have seen an enhancement in the olefin selectivity into higher carbon numbers [8-9,12-15]. This can be explained by the supercritical media having a high capacity to extract and stabilize products that would otherwise undergo secondary reactions (such as olefin hydrogenation to paraffins).

The mechanism of the Fischer Tropsch reaction is still a matter of contention, with Claeys and van Steen listing four pathways [16]: the alkyl mechanism, the alkenyl mechanism (associated with Maitlis), the enol mechanism (associated with Storch), and the CO insertion mechanism (via coordination chemistry and homogenous catalysis). Three key aspects of any Fischer Tropsch Mechanism are: (1) the pathway for CO dissociation (whether it is unassisted – prior to hydrogenation. or assisted – after some hydrogenation), (2) the structure of the initiator species, and (3) the structure of the propagator species. See Table 1 for a presentation of the four mechanisms listed above.

Table 4.1 Role of hydrogen in CO dissociation, initiator, and propagator for four proposed FTS mechanisms. Information from Reference 16.

Mechanism	Alkyl	Alkenyl	Enol	CO Insertion
CO Dissociation	Unassisted	Unassisted	Assisted	Assisted
Initiator	RCH_2	RCHCH	RCOH or RCHOH	RCH_2
Propagator	CH_2	CH_2	CHOH	CO

For non-oxygenate mechanisms, the formation of oxygenates is often explained as being due to a different termination step, usually CO insertion [4,16,17]. In preliminary work, we observed a significant selectivity to diesel-length aldehydes on an iron-zinc catalyst promoted with copper and potassium. The remainder of this study was undertaken to determine the role of these products in the reaction pathway.

4.3 Experimental

4.3.1 Catalyst Synthesis

Three batches of catalyst were made and used in this study (all compositions are molar):

A 1.0 Fe : 0.10 Zn : 0.02 K : 0.01 Cu

B 1.0 Fe : 0.10 Zn : 0.02 K : 0.01 Cu

C 1.0 Fe : 0.01 Cu : 0.02 K

The batches were synthesized by a procedure similar to one published by Enrique Iglesia's group [18]. The materials for this procedure are as follows (all listed here and elsewhere used as received):

Water - DIUF Water (Fisher W2-4)

Ethanol - Absolute Ethyl Alcohol (Pharmco-Aaper E200)

INH - ACS Reagent Grade Iron (III) Nitrate Nonahydrate (Sigma-Aldrich 216828-500G)

ZNH - Reagent Grade Zinc Nitrate Hexahydrate (Sigma-Aldrich 228737-100G)

AC - ACS Reagent Grade Ammonium Carbonate (Sigma-Aldrich 207861-500G)

CNH - ACS Reagent Grade Copper (II) Nitrate Hydrate (Sigma Aldrich 223395-100G)

PC - ACS Reagent Grade Potassium Carbonate (Sigma Aldrich209619-100G)

For each batch, a stock iron solution (1M INH and 0.1M ZNH in Water for Batch A and Batch B, 1M INH for Batch C) and a stock reducing solution (AC in Water – saturated at room temperature) were made.

At a controlled rate (2mL / minute for Batches A and Batch C, 6 mL / minute for Batch B), the iron solution was added to Water (50mL for Batch A and Batch C, 150 mL for Batch B) maintained at 80^{o}C using an Eldex Laboratories Syringe Pump (B-100-S). The reducing solution was added manually to maintain the pH at 7.0 (as measured by a Denver Instrument UB-10 pH meter) with vigorous stirring (via magnetic stir bar). At the end of the co-precipitation (15 minutes for Batch A, 45 minutes for Batch B, 90 minutes for Batch C), reagent addition was stopped and the solution allowed to cool with continued stirring. The slurry was then vacuum filtered. The filter cake was re-slurried in Water and then re-filtered 4 times. The filter cake was then re-slurried in Ethanol and then vacuum filtered twice. The filter cake was then dried overnight at 80^{o}C.

The dried catalyst was then calcined at atmospheric pressure in flowing air, the temperature ramped at 5^{o}C per minute and held at 400^{o}C for 240 minutes. When the catalyst had cooled, the pore volume was determined by the addition of water (measured by mass). The catalyst was then dried again at 80^{o}C.

The potassium (PC) and copper (CNH) promotion were done by incipient wetness impregnation, with the catalyst dried overnight at 80^{o}C and calcined in flowing air with the temperature ramped at 5^{o}C per minute to 400^{o}C and held for 4 hours after each impregnation. For Batch A and Batch B, the potassium impregnation was done prior to copper impregnation. For Batch C, the copper impregnation was done first.

For every experiment, the calcined catalyst was activated (reduced) in situ using syngas (50 SCCM / gram) at 270^{o}C.

4.3.2 Apparatus

Two reactor systems were used in this study: a fixed bed reactor for GP-FTS and SC-FTS and a stirred Parr Reactor for SP-FTS.

A schematic of the fixed bed reactor system is shown in Figure 4.1 below.

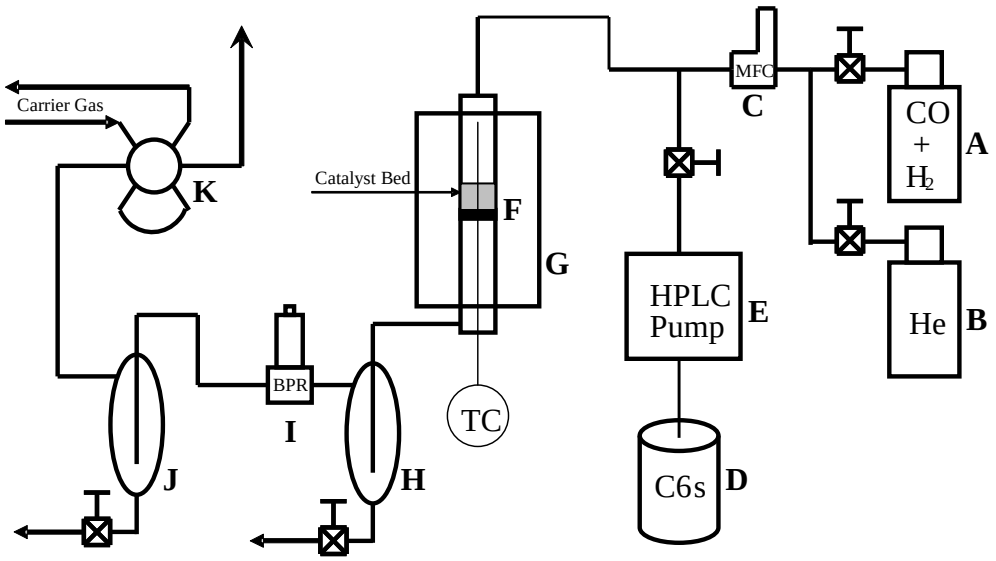

Figure 4.1 Schematic of the fixed bed reactor system (used for GP-FTS and SC-FTS). (A) syngas cylinder, (B) helium cylinder, (C) mass flow controller, (D) hexanes bottle, (E) HPLC pump, (F) reactor, (G) furnace, (H) hot trap, (I) BPR, (J) cold trap, (K) 6-way valve.

In this system, syngas (A) and helium (B, when appropriate) are fed through a mass flow controller (C) and mixed with hexanes (D, for SC-FTS) fed through a positive displacement HPLC pump (E). The mixture passes through heated lines to the reactor (F, downflow) in a split tube furnace (G). From the reactor, the effluent passes through heated tubing to the hot trap (H, maintained at 200^{o}C to condense heavy wax, ideally without significant partitioning below C20). The hot trap condensate is allowed to accumulate and can be periodically collected and analyzed. The vapor from the hot trap passes through heated tubing to the BPR (I, back pressure regulator, used to maintain the reactor pressure), and through heated tubing to the cold trap (J, maintained at slightly sub-ambient temperature). Liquids are allowed to accumulate in the cold trap and are periodically collected and analyzed via manual injection to the FID GC. The gasses from the

cold trap pass to a six-way injection valve (K) used to automatically inject them to the TCD GC. From there the gasses are vented to the fume hood.

The reactor in this system is an HIP microreactor with a length of 10 inches and an ID of 0.5 inches. The upper half has been reamed out to an ID of 0.625 inches. A stainless steel filter disk rests on the rim between the larger and smaller ID sections, with the catalyst resting upon the disk, further immobilized by glass wool. The thermocouple is a 6-point profile thermocouple (Omega Engineering PP6-36-K-G-18) with the third junction in the catalyst bed and used to control the furnace.

A schematic of the Parr Reactor is shown in Figure 4.2 below.

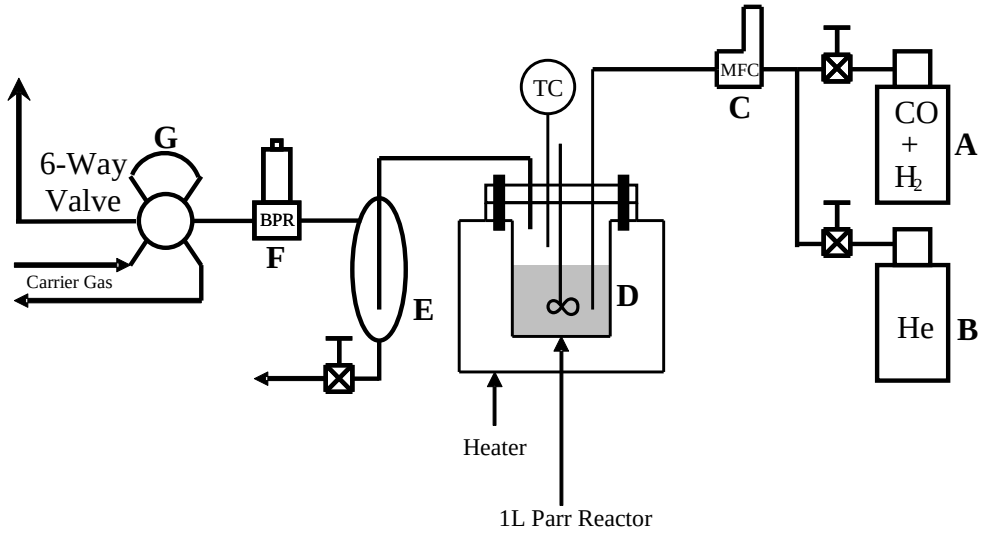

Figure 4.2 Schematic of the Parr Reactor (used in the SP- FTS). (A) syngas cylinder, (B) helium cylinder, (C) mass flow controller, (D) reactor, (E) Cold Trap, (F) BPR, (G) 6-way valve.

In this system, syngas (A) and helium (B, when appropriate) are fed through a mass flow controller (C), then through a heated line into the reactor (D) where they are bubbled through the agitated (600 RPM) slurry. Vapor is pulled off of the top of the reactor and passes through a heated line to the cold trap (E, maintained at sub-ambient temperature). The condensate in the

cold trap is allowed to accumulate to be periodically collected and analyzed by manual injection to the FID-GC. The vapor from the cold trap passes through a BPR (F, used to maintain the reactor at the desired pressure), then the 6-way valve (G, used to automatically inject to the TCD-GC), and finally is vented to the fume hood. Positioning the BPR after the cold trap creates some analytical problems (loss of light products during liquid collection), but improves the reliability of the system. The reactor was pre-filled with 500mL of wax which was slurried with 4g of iron catalyst.

The syngas was purchased pre-mixed from Airgas (Certified Standard) with 1.5% N_2 (internal standard) and $H_2/CO = 1.65$. The helium is UHP grade and is used for pressure testing, startup, and shut-down. The hexanes (the media used during SC-FTS) was purchased in bulk from Fisher Scientific. The paraffin wax (the media used during SP-FTS) was purchased from Fisher Scientific (CAS 8042-47-5). It is a complex mixture of unknown components that elutes from the FID-GC between the C22 and C35 n-paraffins.

Analysis of the cold trap vapor stream was done by online injection (Valco 6-way valve) to a Varian 3800 GC with a TCD detector and a Hayesep column (Grace Davison 2836PC). Standards were used to determine the response factors of the various components and the N_2 internal standard was used to determine the rate of the cold trap vapor stream. Analysis of the cold trap liquids and Parr reactor residual liquids was done by manual injection to a Varian 3300 GC with an FID detector and a DB-5 column (Agilent 125-5032). The mass response factors were assumed to be identical for all pure hydrocarbon components (olefins, paraffins, and isomers) and determined by standard injection for oxygenates (alcohols and aldehydes).

The GC/MS analysis was done at the Auburn University Mass Spec Center in cooperation with Dr. Yonnie Wu, the director of the center. The analysis utilized a Waters

6890N GC with a DB5-MS column (Cat# 1225532, J&W Scientific) coupled to a Time of Flight Mass Analyzer (GCT Premier, Waters). Component identification was done by comparing the electron impact fragmentation pattern (70eV) with those in the compound library (NIST 2003). Compounds with Match and Reverse Match scores above 800 and probabilities above 90% were selected as matches. The identification was confirmed by elemental composition analysis using accurate mass measurement with an internal calibrant (lockmass 218.9856 m/z, heptacosafluorotributylamine, Sigma) with an acceptable error of less than 5 ppm and by isotope modeling comparing the experimental and theoretical isotope distribution. The component identifications from the GC/MS were also confirmed by retention time of standard compounds on the FID-GC. Quantitative analysis was done on the FID-GC with response factors determined though the analysis of corresponding standards.

4.3.3 Procedure

First Study (GP-FTS and SC-FTS Study): The first study used 2g of the Batch A catalyst in the fixed bed reactor system. After a brief (ca. 10 hours) period under GP-FTS conditions the system was converted to SC-FTS operation. After a series of system upsets due to mechanical issues, the reactor was stabilized and a brief study was conducted at various syngas rates (150 SCCM syngas, 100 SCCM, 50 SCCM, 300 SCCM, 150 SCCM, sequentially), with the media (hexanes) to syngas ratio kept at 1 mL/min per 50 SCCM (approx 3.5 mol media per mol syngas). During GP-FTS operation, the pressure was maintained at 17.5 bar. During SC-FTS operation, the pressure was maintained at 75 bar (maintaining the syngas partial pressure at 17.5 bar). With the exception of the catalyst activation (done at 270^{o}C and 1 bar), the reaction temperature was maintained at 240^{o}C.

Second Study (GP-FTS and SP-FTS comparison): The second study used the Batch B catalyst, testing it both for GP-FTS and SP-FTS. In the GP-FTS study 2g of catalyst were loaded into the fixed bed reactor. Once conversion had stabilized, the syngas rate was varied (100 SCCM, 200 SCCM, 100 SCCM, 50 SCCM, sequentially) to determine the reactor performance over a broad range of conversion levels over the 150 hours time on stream. The experiment was done at 240^{o}C. For the SP-FTS portion of the second study, the reactor was loaded with 500mL of paraffin wax and 4g of catalyst. After the reduction, the reactor was briefly run at double rate (syngas rate = 400 SCCM) and 270^{o}C, then regular rate (200 SCCM) and 270^{o}C before going to the regular rate (200 SCCM) and temperature (240^{o}C). For both the GP-FTS and SP-FTS the pressure was held at 17.5 bar.

Third Study (SC-FTS): The third study used the Batch C catalyst, diluting 1g of catalyst in 10g of acid washed and calcined silica sand (Acros Organics 370940010) under SC-FTS conditions. After allowing the system performance to stabilize, the syngas rate was varied: 100 SCCM, 50 SCCM, 100 SCCM, 200 SCCM, then 100 SCCM to test selectivity at moderate, high, and low conversion levels (the hexanes rate was maintained at 1 mL per minute per 50 SCCM). After the study of the selectivity at different conversion levels, the incorporation of aldehydes, alcohols, and olefins were studied.

In the incorporation portion of this study, the system was first run under normal SC-FTS conditions to give a baseline. The media was then doped with octyl aldehyde (Acros Organics 129481000). After returning to baseline, fresh media was doped with octyl alcohol (Aldrich 47232-8). Following another return to baseline, the fresh media was doped with 1-octene (Acros Organics 301250025), and the study concluded with a return to baseline. Each portion of the incorporation half of this study lasted approximately 12 hours with each dopant fed at a

concentration of 0.20 mol per mol CO. The effects of the attempted incorporation were determined by comparing the conversion and amounts of various products seen during attempted incorporation with that seen during the baseline preceding and following it.

4.4 Results

4.4.1 Overall Product Distribution

The overall product distribution for the first study (SC-FTS – Figure 4.3), the second study (GP-FTS – Figure 4.4 and SP-FTS – Figure 4.5), and the third study (SC-FTS – Figure 4.6) are as follows. The slurry-phase ASF plot has the three separate product fractions (cold trap gasses, cold trap liquids, and reactor residual liquids).

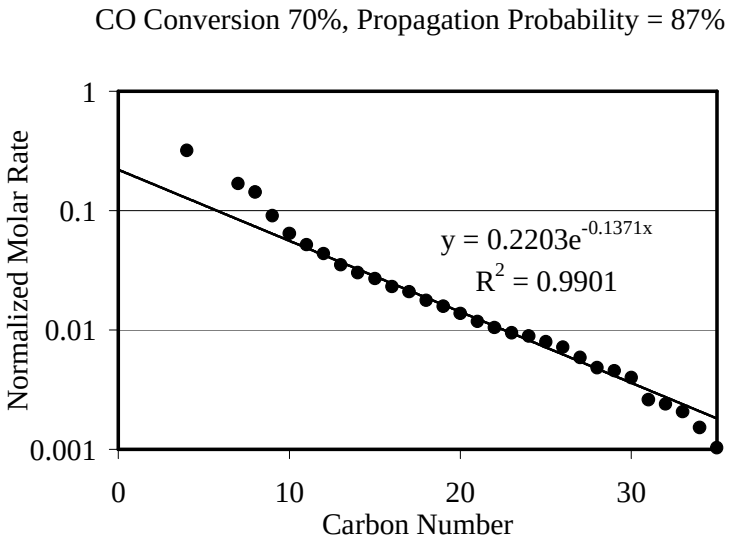

Figure 4.3 First Study (SC-FTS) - ASF Plot (2g catalyst, 150 SCCM syngas, 3mL/min hexanes, P = 75 bar, T = 240^{o}C, XCO = 70%)

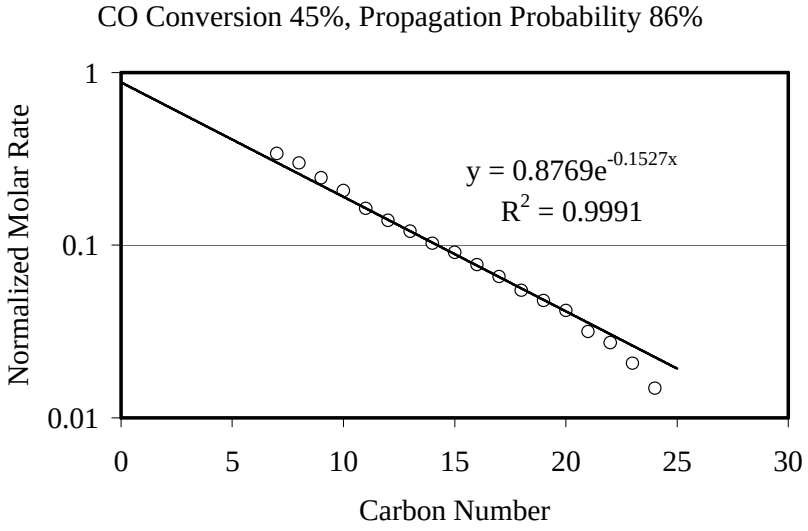

Figure 4.4 Second Study (GP-FTS) - ASF plot (2g catalyst, 100 SCCM syngas, P = 17.5 bar, T = 240°C, X_{CO} = 45%)

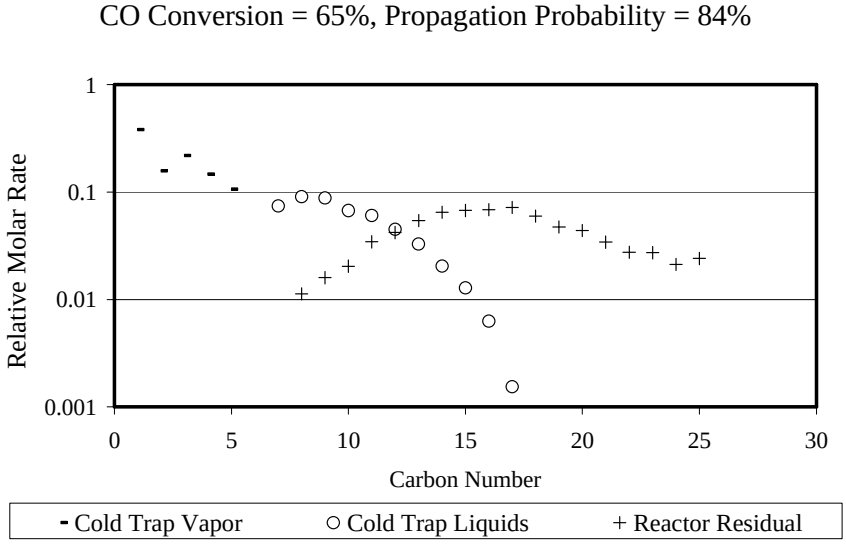

Figure 4.5 Second Study (SP-FTS) - ASF plots (not normalized) (4g catalyst, 200 SCCM, P = 17.5 bar, T = 240°C, X_{CO} = 65% for Cold Trap Vapor and Cold Trap Liquid. Products from whole run for Reactor Residual).

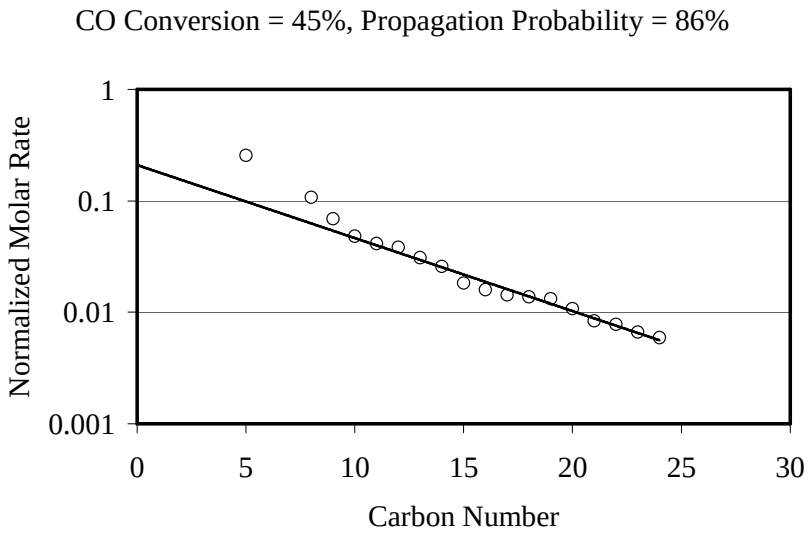

Figure 4.6 Third Study (SC-FTS) – ASF plot (1g catalyst, 200 SCCM syngas, 4mL/min hexanes, P = 75 bar, T = 240^{o}C, X_{CO} = 45%)

With the possible exception of GP-FTS, each of the ASF plots shows a 2-alpha distribution with the two regions meeting in the low teens. For this work, the most important observation is that the high-carbon number alpha values are consistent among the different catalyst batches and reaction media. Additionally, the ASF plots for different conversion levels under GP-FTS and SC-FTS are not shown, but there is little influence of conversion level on the ASF plots.

4.4.2 Gas Product Analysis

The crossplot of CO_2, CH_4, and C3 olefin selectivity versus CO conversion for the first study is presented in Figure 4.7 below. The CO_2 selectivity is calculated on a CO basis [CO_2 generated / CO consumed], the methane selectivity on a CO_2-free basis [CH_4 generated / (CO consumed – CO_2 generated)], and the C3 olefin selectivity on a C3 hydrocarbon basis [propene / (propene + propane)]. Operation under SC-FTS conditions suppressed the methane and CO_2 selectivity significantly and the C3 olefin selectivity slightly relative to GP-FTS. The methane and CO_2 selectivity both decreased markedly with decreasing CO conversion, appearing to

extrapolate to zero as the CO conversion approaches zero and the product distribution becomes the primary product distribution. Additionally, the C3 olefin selectivity appeared to drop as the CO conversion decreased, though not appearing to extrapolate to zero as CO conversion approached zero, indicating that propene is likely both a primary and secondary product.

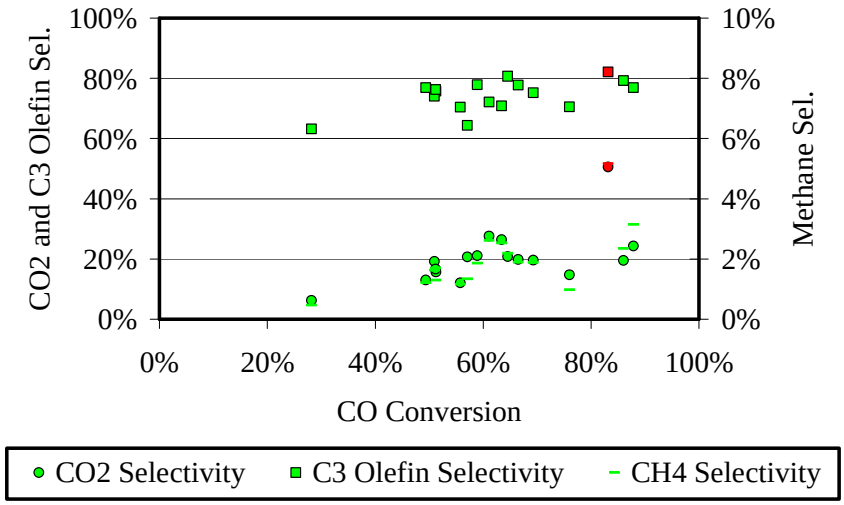

Figure 4.7 First Study (SC-FTS (green) and GP-FTS (red)) – CO_2, C3 Olefin, and CH_4 vs. CO Conversion

The crossplot of CO_2, CH_4, and C3 olefin selectivity versus CO conversion for the second study is presented in Figure 4.8 below.

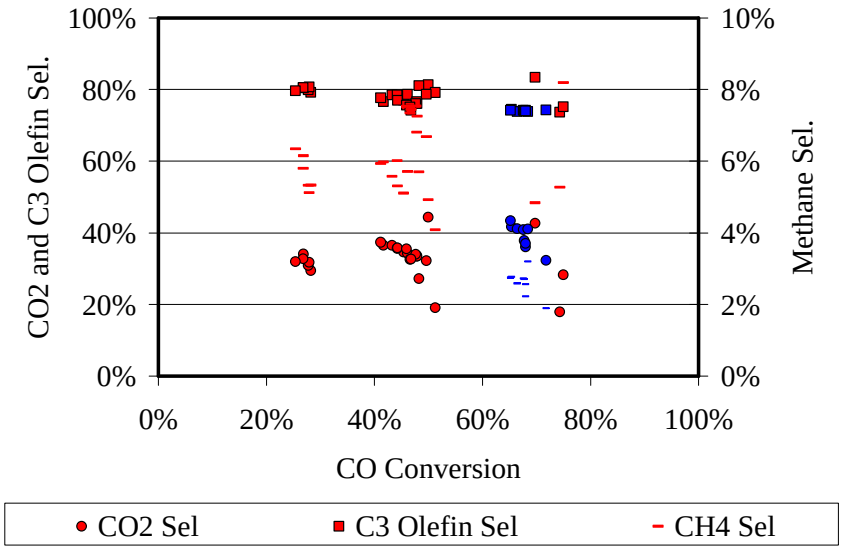

Figure 4.8 Second Study (GP-FTS (red) and SP-FTS (blue)) – CO_2, C3 Olefin, and CH_4 vs. CO Conversion

Under GP-FTS operation, there was no trend in CO_2, CH_4, or C3 olefin selectivity versus CO conversion. Going from GP-FTS to SP-FTS gave a mild suppression in C3 olefin selectivity, a mild increase in CO_2 selectivity, and a large decrease in CH_4 selectivity. The decrease in methane selectivity in going from GP-FTS to SP-FTS is comparable to that seen in going from GP-FTS to SC-FTS.

The crossplot of CO_2, CH_4, and C3 olefin selectivity versus CO conversion for the third study is presented in Figure 4.9 below.

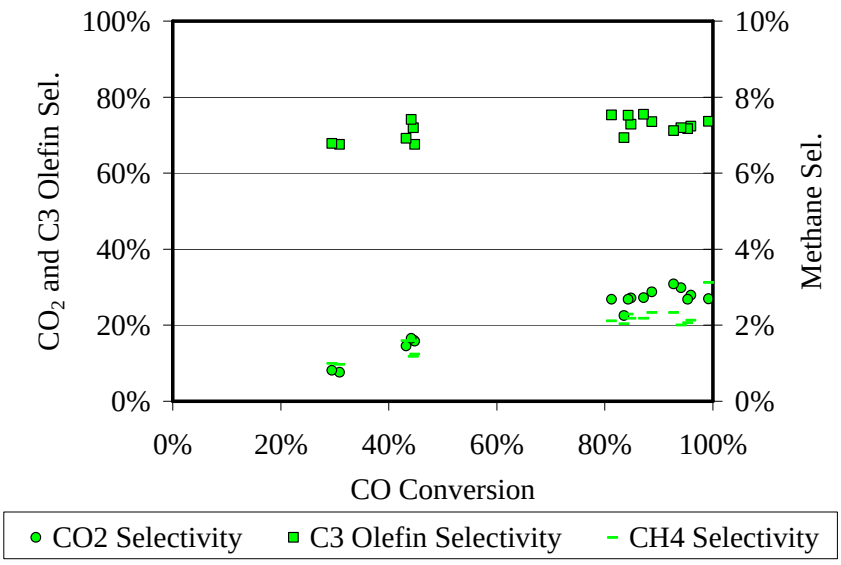

Figure 4.9 Third Study (SC-FTS) – CO_2, C3 Olefin, and CH_4 vs. CO Conversion

The SC-FTS results seen in this study (with a zinc-free catalyst) match those seen in SC-FTS operation in the first study. Methane and CO_2 again appear to be secondary products while propene appears to be both a primary and secondary product.

4.4.3 Liquid Product Breakdown by Type

The breakdown of the liquid product by type versus carbon number for the first study during SC-FTS operation is shown in Figure 4.10 (the same liquid sample used to generate the ASF plot shown in Figure 4.3).

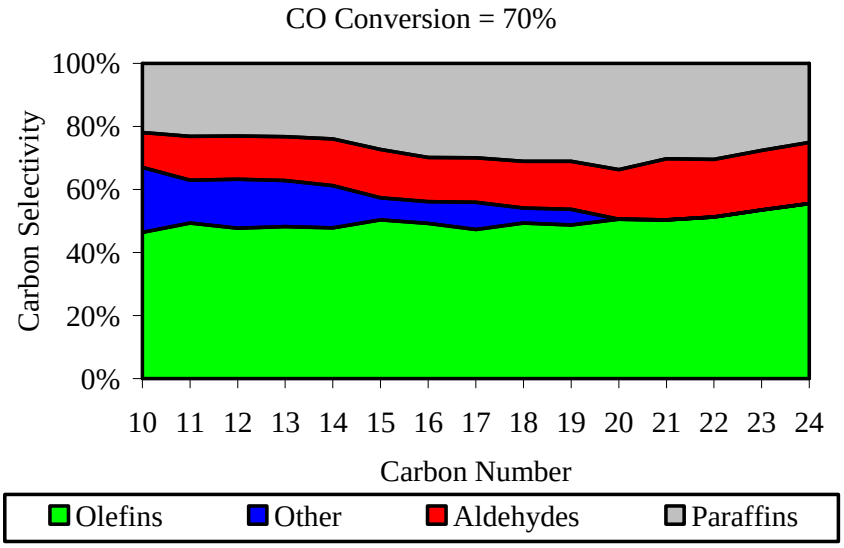

Figure 4.10 First Study (SC-FTS) – Breakdown of liquid product by type –v– carbon number (2g catalyst, 150 SCCM syngas, 3mL/min hexanes, P = 75 bar, T = 240^{o}C, X_{CO} = 70%, Propagation Probability = 87%)

With the exception of the "Other" products gradually disappearing, there is little influence of carbon number on the relative amounts of olefins, paraffins, and aldehydes (the aldehyde identification was confirmed by GC retention time and GC-MS analysis). The analytical procedure used in this study lumped the alcohols into the "Other" category. Branching has been shown to decrease with increasing carbon number [4].

The breakdown of the liquid product by type versus carbon number for the second study is shown in Figure 4.11 (GP-FTS operation – the same sample used for the ASF plot in Figure 4) and Figure 4.12 (SP-FTS operation cold trap liquids – the same liquid sample used for the ASF plot in Figure 4.5).

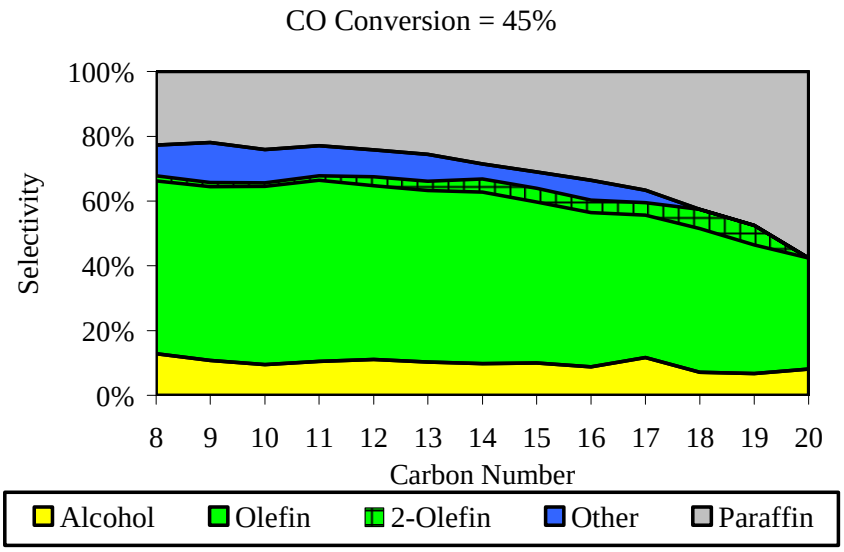

Figure 4.11 Second Study (GP-FTS) – Breakdown of liquid product by type –v– carbon number (2g catalyst, 100 SCCM syngas, P = 17.5 bar, T = 240^{o}C, X_{CO} = 45%, Propagation Probability = 86%)

The GP-FTS breakdown showed different behavior than that seen in Figure 4.10 with SC-FTS. First, the liquid aldehydes were not present in GP-FTS in detectable quantities while internal olefins were observed. Second, with increasing carbon number the GP-FTS liquid product became much less olefinic and more paraffinic, indicating the hydrogenation of olefins to their corresponding paraffins.

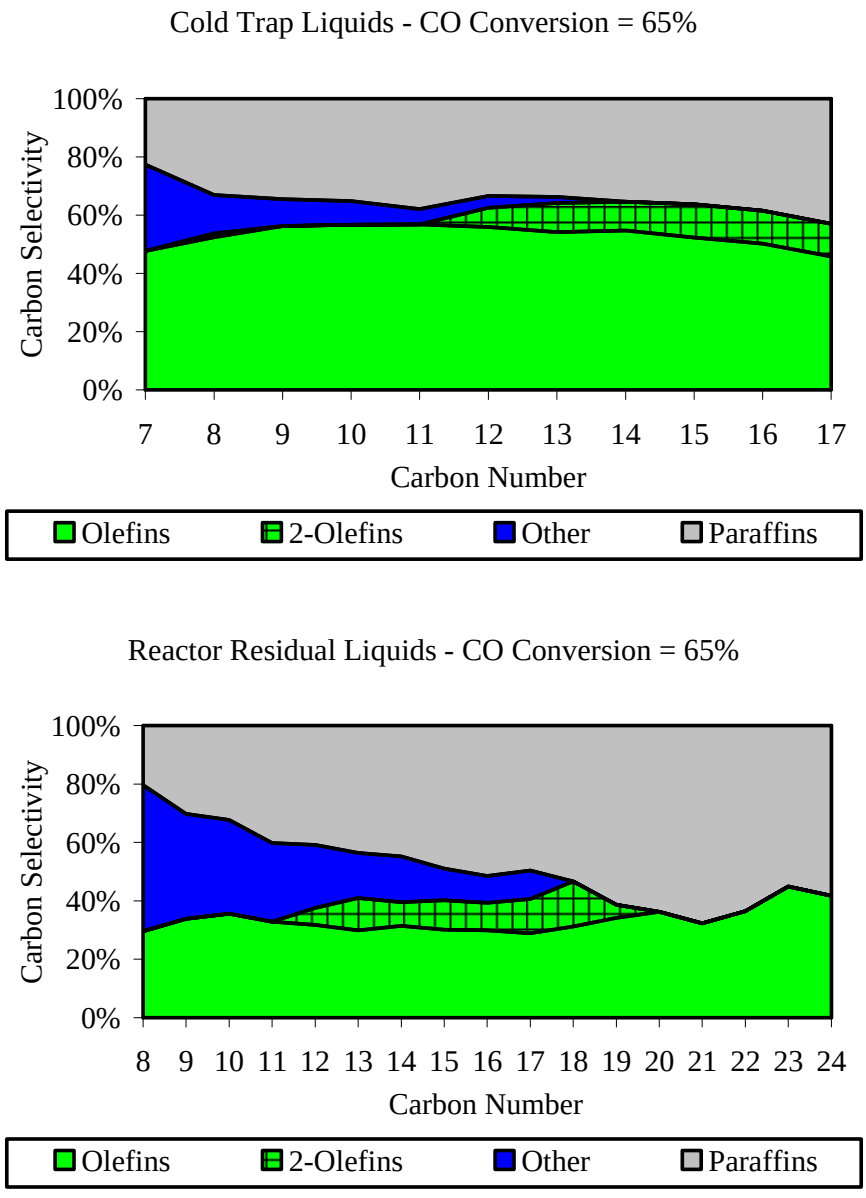

Figure 4.12 Second Study (SP-FTS) – Breakdown of liquid product by type –v– carbon number (4g catalyst, 200 SCCM syngas, P = 17.5 bar, T = 240^{o}C, X_{CO} = 65%, Propagation Probability = 84%)

The SP-FTS product breakdown by type, like that in the first study, did not isolate alcohols from the "Other" category. As with GP-FTS, no liquid aldehydes were seen in this SP-FTS study while significant quantities of internal olefins were detected. Like SC-FTS, the

product distributions in the cold trap liquids and reactor residual liquids were independent of carbon number, apart from the gradual disappearance of the "Other" products. The cold trap liquids in SP-FTS were far more olefinic than the reactor residual liquids, which is consistent with the reactor residual liquids having a far higher contact time. A greater fraction of the reactor residual liquids are present as "Other" products than in the cold trap liquids. Assuming that these products are predominately branched products, the higher selectivity in the reactor residual liquids supports branched compounds as secondary products, likely formed from olefins. The apparent disappearance of internal olefins at the end of the diesel range is due to analytical limitations at the corresponding high retention times for these compounds.

The breakdown of liquid product by type versus carbon number for SC-FTS on a zinc-free iron catalyst from the third study is shown in Figure 4.13 below.

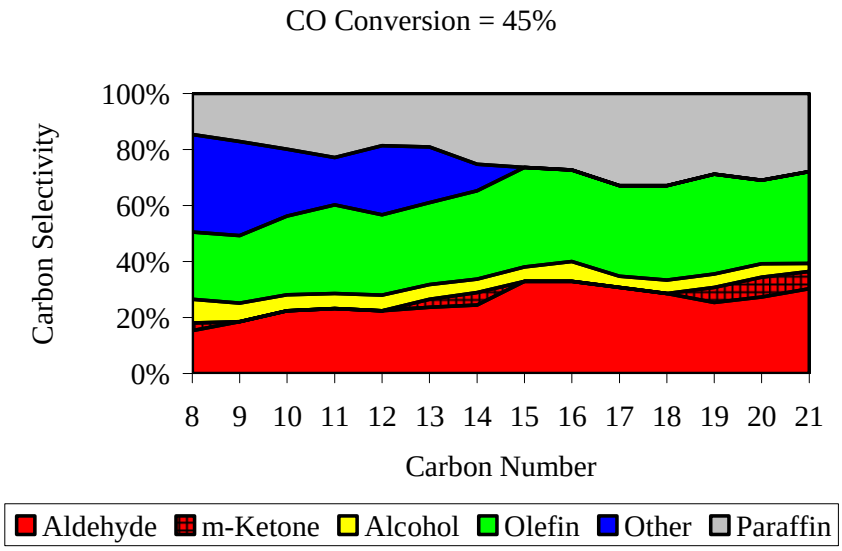

Figure 4.13 Third Study (SC-FTS) – Breakdown of liquid product by type –v– carbon number (1g catalyst, 200 SCCM syngas, 4mL/min hexanes, P = 75 bar, T = 240^{o}C, X_{CO} = 45%, Propagation Probability = 86%)

This SC-FTS study gave very similar results to those obtained from the first SC-FTS study (Figure 4.10), with little change versus carbon number apart from the gradual

disappearance of “Other” products. It is important to note that the analytical procedures employed during the third study were improved to allow for the detection of alcohols and methyl-ketones (the methyl ketone identification was confirmed by GC retention time and GC-MS analysis). As in the first study, significant quantities of liquid aldehydes were detected in this SC-FTS investigation. A significant quantity of methyl ketones was also found.

In Figure 4.13, it appears that methyl ketones are only present at C8, from C13-C14, and >C18. However, this sporadic appearance is due to analytical limitations. The methyl ketones retention time is similar to that of the paraffin of two greater carbon number. At a low carbon number (C8), the methyl ketone elutes prior to the olefin. At higher carbon numbers (C9-C12) the methyl ketone is indistinguishable from the olefin. The methyl ketone can again be observed from C13-C14 between the paraffin and the olefin. The methyl ketone peak then merges with the paraffin peak from C15 to C18. Above C19 the methyl ketone elutes after the paraffin and is observed until it disappears into signal noise. It is prohibitively likely that the methyl ketones are present at the carbon numbers where the peak cannot be resolved with selectivities similar to the carbon numbers where they are resolvable.

The breakdown of the liquid products by type versus conversion level for the first study under SC-FTS conditions is shown in Figure 4.14 with the analysis limited to the C11-C17 range.

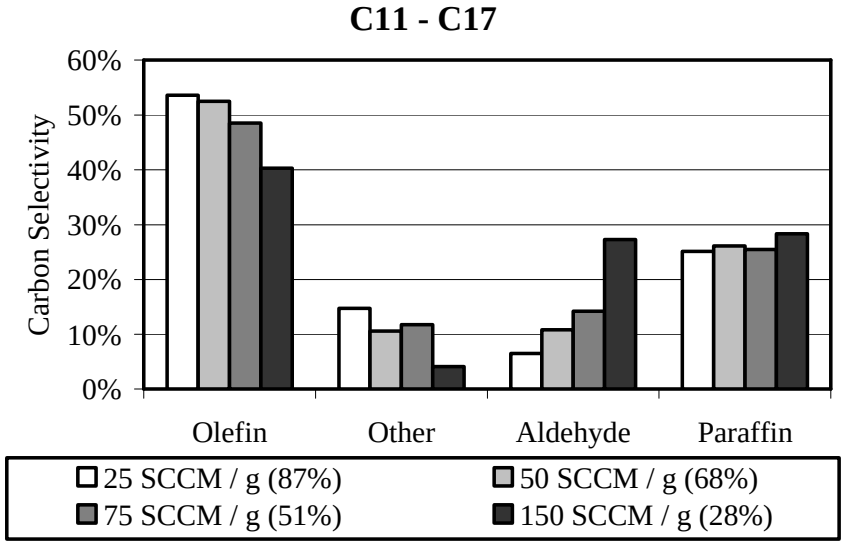

Figure 4.14 First Study (SC-FTS) – Breakdown of liquid product by type –v– conversion level (P = 75 bar, T = 240^{o}C, CO conversion in parenthesis).

As CO conversion decreased and the product spectrum approached the primary product spectrum (left to right), the aldehyde selectivity increased markedly while the "Other" and olefin selectivity decreased. The paraffin selectivity was largely unaffected by conversion level. This indicates that aldehydes are primary products. The "Other" products appear to be secondary products. The olefins appear to be secondary products as well, but it is doubtful that the olefin selectivity would go to zero if the CO conversion was extrapolated to zero, indicating that olefins are both primary and secondary products. Paraffins appear to be primary products, and the hydrogenation of olefins to paraffins appears to be effectively suppressed under supercritical conditions, as evidenced by the lack of an increase in paraffinicity with increasing carbon number (Figure 4.10) or increasing CO conversion (Figure 4.14).

The breakdown of the liquid products by type versus conversion level for the second study under GP-FTS conditions is shown in Figure 4.15 for the C10-C17 range.

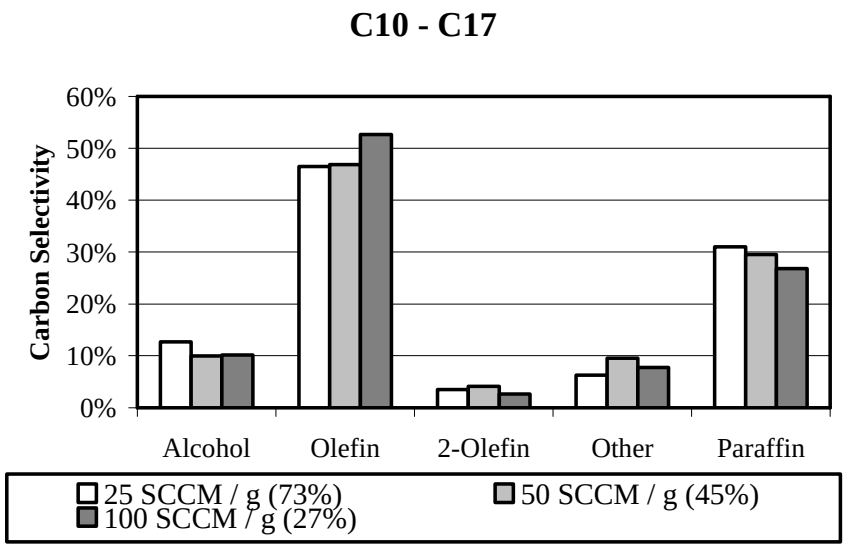

Figure 4.15 Second Study (GP-FTS) – Breakdown of liquid product by type –v– conversion level (P = 17.5 bar, T = 240^{o}C, CO conversion in parenthesis)

With decreasing CO conversion, here the product becomes less paraffinic and more olefinic. This supports olefins as primary products that are converted by secondary reactions to paraffins, contrary to what was seen in SC-FTS operation. We believe this to be due to the failure the GP-FTS media to inhibit the consumption of the aldehyde or aldehyde-like reaction intermediate. Consequently, because the consumption of aldehydes is nearly complete even at low conversion levels in GP-FTS, with increasing CO conversion the secondary reaction that is observed is the hydrogenation of the olefins giving a false view of the primary product spectrum.

The breakdown of the liquid products by type versus conversion level for the third study under SC-FTS conditions is shown in Figure 4.16 for the C11-C17 range.

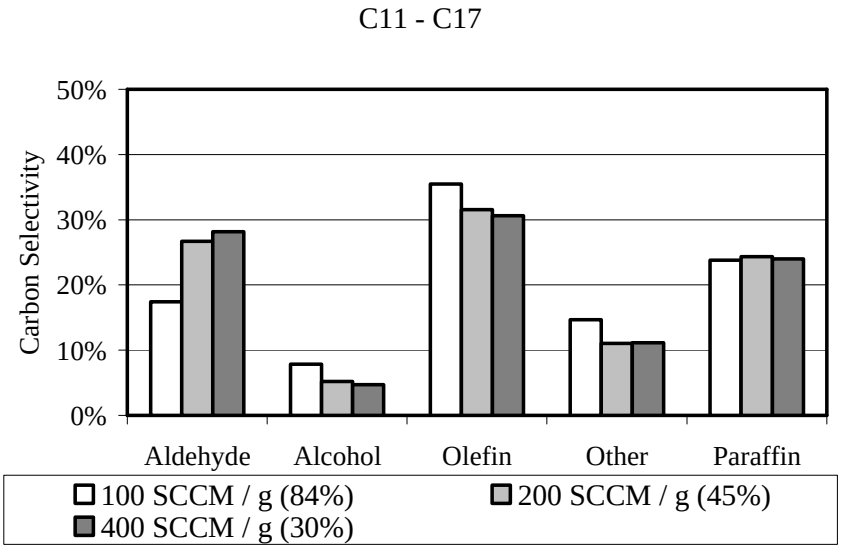

Figure 4.16 Third Study (SC-FTS) – Breakdown of liquid product by type –v– conversion level (P = 75 bar, T = 240^{o}C, CO conversion in parenthesis)

This data confirms much of what was seen in the first study in SC-FTS (Figure 4.14) while adding additional information, with aldehydes appearing to be primary products that are converted via secondary reactions to alcohols and olefins. It appears that olefins would have a significant selectivity even with a CO conversion approaching 0%, making it likely that they are both primary and secondary products. Paraffins appear to be primary products and their formation through secondary reactions appears to be suppressed.

The breakdown of the liquid products by type versus conversion level for the third study under SC-FTS conditions is shown in Figure 4.17 for the C20-C24 range.

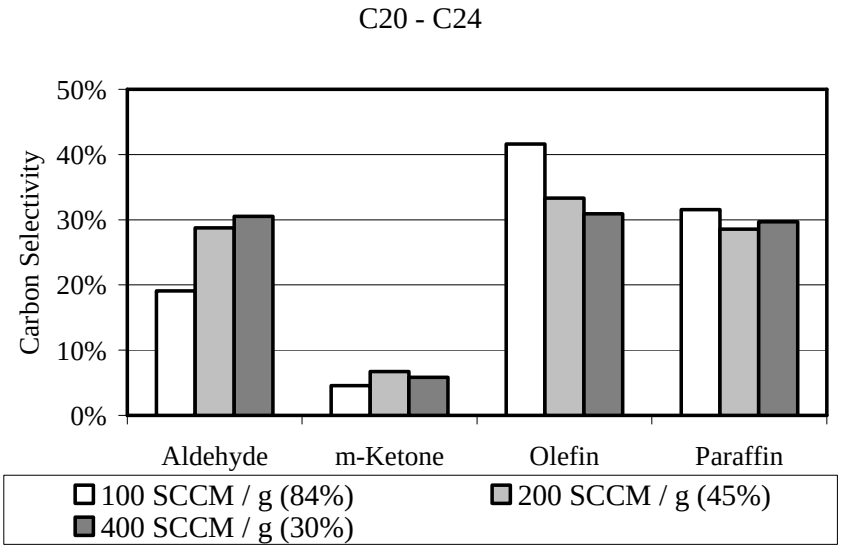

Figure 4.17 Third Study (SC-FTS) – Breakdown of liquid product by type –v– conversion level (P = 75 bar, T = 240^{o}C, CO conversion in parenthesis)

While "Other" products are no longer distinguishable from the chromatogram noise and the alcohol peak can no longer be distinguished from the olefin peak, the olefin, paraffin, methyl-ketone, and aldehyde peaks are still distinguishable. This data again confirms aldehydes as primary products that are partially converted to olefins, olefins as both primary and secondary products, methyl-ketones as likely secondary products, and paraffins as primary products. The primary products in the diesel range appear to be approximately 30% aldehyde, 30% olefin, 30% paraffin, 5% alcohol, and 5% methyl-ketone.

The observations reported here for SC-FTS have been replicated in our laboratory multiple times, but, for simplicity, only selected experiments are reported here. The same results (i.e., significant selectivity to liquid aldehydes, minimal influence of carbon number on the product type breakdown, an increase in aldehyde selectivity with decreasing CO conversion, a decrease in olefin selectivity with decreasing CO conversion, and no influence of CO conversion on the paraffin selectivity) were obtained in another SC-FTS study using a 1 Fe : 0.1 Zn : 0.01

Cu : 0.02 K by mol catalyst and another study using the Batch C catalyst without a hot trap in the reactor system.

4.4.4 Aldehyde, Alcohol, and Olefin Incorporation

After the completion of the third study presented above, an additional investigation was undertaken to explore the incorporation of added C8 aldehyde, C8 alcohol, and 1-octene in the Fischer Tropsch reaction. The incorporant was added to the hexanes media such that it was present at the reactor inlet at a rate 20% of that of the CO in the syngas. The analysis was performed by comparing the performance during the attempted incorporation (conversion of CO and H_2 and the production rate of the different products) with that observed during a period of SC-FTS operation without an incorporant immediately preceding and following the attempted incorporation. C8 aldehyde incorporation was studied first, followed by C8 alcohol incorporation, and finally 1-octene incorporation.

The addition of the C8 aldehyde resulted in some incorporation into heavier products with a selectivity comparable to that seen in the baselines (i.e. no incorporant added). There was no distinguishable effect of the C8 aldehyde on conversion, methane selectivity, or CO_2 selectivity. The formation of C2 and C3 products appear to have been suppressed. In addition to incorporation, the C8 aldehyde was converted to the C7 paraffin, C8 olefin, C8 alcohol, C9 methyl-ketone, C9 alcohol, and an unknown C15 oxygenate (likely the symmetric ketone).

The addition of the C8 alcohol resulted in some incorporation into heavier products with a selectivity comparable to that seen in the baselines. There was no distinguishable effect of the C8 alcohol on conversion, methane selectivity, CO_2 selectivity, C2 selectivity, or C3 selectivity. In addition to the incorporation, the C8 alcohol appears to have been converted to the C8 aldehyde, C9 alcohol, and C9 aldehyde.

The addition of 1-octene resulted in no discernible incorporation into heavier products. There was no change in CO conversion, though a drop in usage ratio was observed. The methane, CO_2, C2 and C3 selectivities were unchanged. The 1-octene was converted to C8 internal olefins, the C8 paraffin, and a product that is likely the C10 olefin.

4.5 Discussion

Low Temperature Fischer Tropsch produces two classes of products: hydrocarbons and oxygenates. The predominant hydrocarbon products are n-paraffins, n-olefins (mostly terminal), and branched paraffins and olefins. Minor hydrocarbon products include aromatics and dienes. The predominant oxygenates are aldehydes (mostly linear), alcohols (mostly terminal and linear), ketones (with the carbonyl group mainly on the β-carbon), carboxylic acids (mostly linear), and esters (mostly linear). Minor oxygenate products include acetals, ethers, furans, and phenols. [19]

Paraffins are shown to be primary products by varying the residence time (conversion level) under SC-FTS conditions. There are several possible pathways for their formation. Burt Davis' group observed the conversion of added alcohols to the one carbon shorter paraffin in a process that also formed CO_2 [20] in a slurry phase reactor. However, under SC-FTS conditions, we did not observe the formation of the one shorter paraffin from an added alcohol, but did observe this phenomenon with the added aldehyde. The conversion of the aldehydic intermediate to a 1-carbon shorter paraffin is a possible pathway to the primary formation of paraffins. However, the apparent absence of CO_2 as a primary product, the absence of methane as a primary product, and the absence of heavier paraffins as secondary products made us consider this unlikely at the time, though in Chapter 6 (Future Work) we will discuss why we are

reconsidering that view. As such, we prefer the alpha-hydrogenation of a surface alkyl group as a more plausible mechanism for the primary production of paraffins.

The selectivity to diesel-length olefins decreased with decreasing conversion under SC-FTS conditions, contrary to what was seen on the same catalyst under GP-FTS conditions and to what we have observed previously in SC-FTS on a cobalt catalyst. The conversion of octyl aldehyde to 1-octene was observed in the incorporation study, confirming the conversion of aldehydes to olefins as evidenced by the changes is selectivity with variations in conversion. However, the olefin selectivity does not appear to approach zero as CO conversion extrapolates to zero, suggesting that olefins are also primary products. Beta hydrogen elimination from a surface alkyl group is a plausible mechanism for the primary production of olefins. No discernable internal olefins were detected under SC-FTS operation, though internal olefins were seen in GP-FTS and SP-FTS, supporting internal olefins as only secondary products. Additionally, 1-octene, when added to SC-FTS, did form some internal octenes, supporting this conclusion.

Branched compounds have been shown to be formed from the incorporation of non-terminal alcohols [20]. The high selectivity to 'Other' products (presumed to be predominantly branched compounds) in the reactor residual liquids in SP-FTS also suggests their formation from olefins. While the incorporation of 1-octene was not seen in this work, it has been generally observed, albeit at a lower rate than that for alcohols [20]. A terminal olefin should allow for initiation at the 1 carbon (giving an n-paraffin) or 2 carbon (giving a methyl-branched product). A 2-olefin should allow for initiation at the 2 carbon (giving a methyl-branched product) or the 3 carbon (giving an ethyl-branched compound). The formation of methyl-ketones from aldehydes offers a pathway beside isomerization to get from a terminal species to a

methyl-branched one. However, under supercritical conditions methyl ketones are present at carbon numbers into the wax product range while branched products die out in the diesel range.

Aldehydes are demonstrated to be primary products by varying the residence time in SC-FTS. The incorporation study demonstrated their capacity to incorporate into heavier products. Burt Davis' group has shown that incorporated alcohols act as chain initiators [20]; we believe that this is likely to also be the means of incorporation for aldehydes. Aldehydes have been previously shown to give incorporation behavior comparable to that of alcohols [21]. Aldehydes and alcohols appeared to interconvert in the incorporation study, suggesting that either could be the primary and either the secondary product. To study this uncertainty, a simulation was done in AspenPlus using the Peng Robinson equation of state. In this simulation, a stream of hexane, hydrogen, water, octyl aldehyde, 1-octyl alcohol, and 1-octene were fed to an equilibrium reactor at typical SC-FTS conditions (P = 75 bar, T = 240^{o}C) where the aldehyde, alcohol, and olefin were free to be interconverted to minimize the Gibbs Free Energy of the system. The results of this simulation are shown in Table 4.2 below.

Table 4.2 Simulation of the thermodynamics of aldehyde, alcohol, and olefin inter-conversion at SC-FTS conditions

	Feed (mol / hr)	**Product (mol / hr)**
Hexane	3.5	3.5
Hydrogen	0.25	0.24
Water	0.25	0.27
Octyl Aldehyde	0.01	$4.5 * 10^{-7}$
1-Octyl Alcohol	0.01	$6.1 * 10^{-5}$
1-Octene	0.01	0.030

The simulation indicates that the conversion of aldehydes to alcohols and alcohols to olefins should be, under typical SC-FTS conditions, near total. Consequently, given the high ratio of aldehydes to alcohols observed, we conclude that aldehydes are primary over alcohols. The fact that added 1-octene did not react to give an aldehyde further establishes that the

aldehydes are not secondary products of olefins, but that the reverse is true. Additionally, in 1962 Irving Wender [22] demonstrated that the synthesis of an aldehyde from an olefin of one fewer carbon number with cobalt hydrocarbonyls readily occurs.

Alcohols are likely secondary products from the hydrogenation of aldehydes given the two products' capacity for interconversion, the drop in alcohol selectivity with decreasing CO conversion, and their capacity to be converted to heavier products.

Methyl-ketones appear to be secondary products formed from aldehydes, though they have been asserted to be formed via carboxylic acid decomposition [19]. The pseudo-dimerization product of the added C8 aldehyde to a C15 oxygenate is likely a symmetrical ketone [23].

Our analytical system does not allow for the detection of carboxylic acids or esters. The inability to measure carboxylic acids is particularly unfortunate since formate-type species have been proposed as being the chain initiator on iron [20].

The high selectivity to aldehydes suggests an oxygenate mechanism (likely CO Insertion [4,16,17]) as, if nothing more, a termination mechanism for the reaction. However, the capacity for an aldehyde to be converted to possibly all of the reaction product types suggests a broader role for CO insertion. The fact that the aldehyde can also initiate chain growth suggests the oxygenate process as the growth mechanism for the reaction as well.

The broad spectrum of apparent primary products suggests that there are multiple types of surface species. However, the consistency of the product type with carbon number suggests sequential termination pathways as opposed to parallel mechanisms. As such, we believe the initiator to be fundamentally different from the intermediate (the product of the initiator reacting with the propagator). The specific identity of these two species is still a matter of inquiry. We

believe a CO Insertion mechanism to be more likely given the product spectrum than an enol mechanism. Several variations on CO insertion have been proposed [24].

The mechanism for CO dissociation in Fischer Tropsch Synthesis is still a matter of dispute. However, we believe that the case for hydrogen assisted dissociation has been compellingly made [25-27]. Additionally, if hydrogen assisted dissociation is accepted, an oxygenate mechanism in general and CO insertion specifically becomes highly plausible (see Figure 4.18).

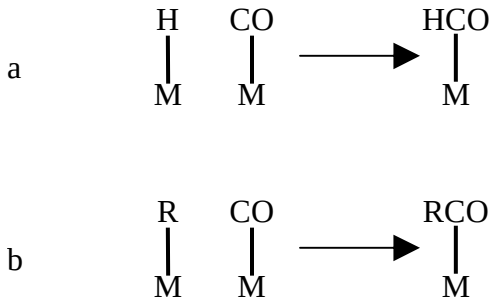

Figure 4.18 Presentation of (a) the hydrogenation of CO prior to dissociation (Hydrogen Assisted Dissociation) and (b) CO Insertion. No claim as to the nature of the bond between the CO and the catalyst is intended.

A C14 labeling incorporation study would be very useful to bring clarity here. Enrique Iglesia's group [17] has made a very strong case that the behavior of an added incorporant does not necessarily match that of the same component produced in situ. Our group has carried out a number of investigations [9,10,12,28] of SC-FTS on a cobalt catalyst and we have not observed diesel length aldehydes. There are two possibilities here. The first is that cobalt-based FTS has a different mechanism that would not produce aldehydes as primary products. The second is that, even if cobalt based FTS utilizes the same mechanism as iron, cobalt is a much stronger hydrogenation catalyst than iron [29], so the aldehydes would be too rapidly converted to olefins and paraffins to be observed at higher carbon numbers. As such, while we feel based on the data

presented here that an oxygenate mechanism in some form is the chain growth mechanism for FTS on an iron catalyst, we cannot make any claims for cobalt.

4.6 Conclusions

We have used an iron based FT catalyst (1 Fe: 0.1 Zn: 0.02 K: 0.01 Cu by mol) for Fischer Tropsch Synthesis in a supercritical (SC-FTS), gas phase (GP-FTS), and slurry phase (SP-FTS) environment. In SC-FTS, a significant selectivity in the diesel range to aldehydes and methyl-ketones was observed (both products confirmed by GC-MS). These products were not detected under GP-FTS or SP-FTS operation. Additionally, another iron-based FT catalyst (1 Fe: 0.01 Cu: 0.02 K by mol) was studied under SC-FTS conditions and similar products were observed. We attribute this to the supercritical media having a high capacity to extract and stabilize products, inhibiting secondary reactions. Decreasing the residence time of the reaction (decreasing conversion to make the product spectrum more primary) gave increased aldehyde and decreased olefin selectivity. From this, we conclude that the aldehydes are primary products and are converted by secondary reactions to olefins. Doping the supercritical media with octyl aldehyde resulted in the aldehyde being incorporated into heavier products, indicating that the process that forms the aldehyde is part of the propagation mechanism. From this, we have concluded that an oxygenate mechanism is the active pathway for the FTS reaction on iron based catalysts. At the time of this study, we concluded in favor of conventional CO Insertion. As will be discussed in Chapter 6 (Future Work), we have modified that view.

4.7 References

[1] Mark E. Dry, Catal. Today 71 (2002) 227-241.

[2] Fernando Morales, Bert M. Weckhuysen, Catalysis 19 (2006) 1-40.

[3] Andrei Y Khodakov, Wei Chu, Pascal Fongarland, Chemical Reviews 107 (2007) 1692-1744.

[4] Mark E. Dry, Appl. Catal., A 138 (1996) 319-344.

[5] R.L. Espinoza, A.P. Steynberg, B. Jager, A.C. Vosloo, Appl. Catal., A 186 (1999) 13-26.

[6] Kohshiroh Yokota, Kaoru Fujimoto, Fuel 68 (1989) 255-256.

[7] Shirun Yan, Li Fan, Zhixin Zhang, Jinglai Zhou, Kaoru Fujimoto, Appl. Catal., A 171 (1998) 247-254.

[8] Gary Jacobs, Karuna Chaudhari, Dennis Sparks, Yongqing Zhang, Buchang Shi, Robert Spicer, Tapan K. Das, Jinlin Li, Burtron H. Davis, Fuel 82 (2003) 1251-1260.

[9] Xiwen Huang, Christopher B. Roberts, Fuel Process. Technol. 83 (2003) 81-99.

[10] Nimir O. Elbashir, P. Dutta, A. Manivannan, M. S. Seehra, Christopher B. Roberts, Appl. Catal., A 285 (2005) 169-180.

[11] TANG Haodong, LIU Huazhang, YANG Xiazhen, LI Ying: J. Chem. Eng. Chin. 22 (2008) 259.

[12] Ed Durham, Sihe Zhang, Christopher B. Roberts, AIChE Annual Meeting (2008): Presentation 678d.

[13] Kohshiroh Yokota, Yoshio Hanakata, Kaoru Fujimoto, Fuel 70 (1991) 989-994.

[14] Xiaosu Lang, Aydin Akgerman, Dragomir B. Bukur, Ind. Eng. Chem. Res. 34 (1995) 72-77.

[15] Dragomir B. Bukur, Xiaosu Lang, Aydin Akgerman, Zhentao Feng, Ind. Eng. Chem. Res. 36 (1997) 2580-2587.

[16] M. Claeys, E. van Steen, in Andre Steynberg, Mark Dry (Eds.), Studies in Surface Science and Catalysis 152 – Fischer Tropsch Technology, Elsevier Science p 601-680.

[17] Enrique Iglesia, Catal., A 161 (1997) 59-78.

[18] Senzi Li, Sundaram Krishnamoorthy, Anwu Li, George D. Meitzner, Enrique Iglesia, J. Catal. 206 (2002) 202-217.

[19] Arno de Klerk, Fischer Tropsch Refining. PhD Thesis, University of Pretoria, Pretoria, South Africa, 2008.

[20] Burtron H. Davis, Catal. Today 141 (2009) 25-33.

[21] W. Keith Hall, R. J. Kokes, P. H. Emmett, J. Am. Chem. Soc. 82 (1960) 1027– 1037.

[22] Irving Wender, Heinz W. Sternberg, Robert A. Friedel, Sol J. Metlin, Raymond E. Markby, Technical Report (1962) OSTI ID: 7193411.

[23] Yuguo Wang and Burtron H. Davis, Appl. Catal., A 180 (1999) 277-285.

[24] Mingkum Zhuo, Kong Fei Tan, Armando Borgna, Mark Saeys: J. Phys. Chem. C 113 (2009) 8357-8365.

[25] G. Blyholder, M. Lawless, Langmuir 7 (1991) 140-141.

[26] Oliver R. Inderwildi, Stephen J. Jenkins, David A. King, J. Phys. Chem. C 112 (2008), 1305-1307.

[27] Xiaoping Dai, Changchun Yu, J. Nat. Gas Chem. 17 (2008) 365-368.

[28] Nimir O. Elbashir, Christopher B. Roberts, Ind. Eng. Chem. Res. 44 (2005) 505-521.

[29] Mark E Dry, Appl. Catal., A 138 (1996) 319-344.

4.8 Supplementary Materials

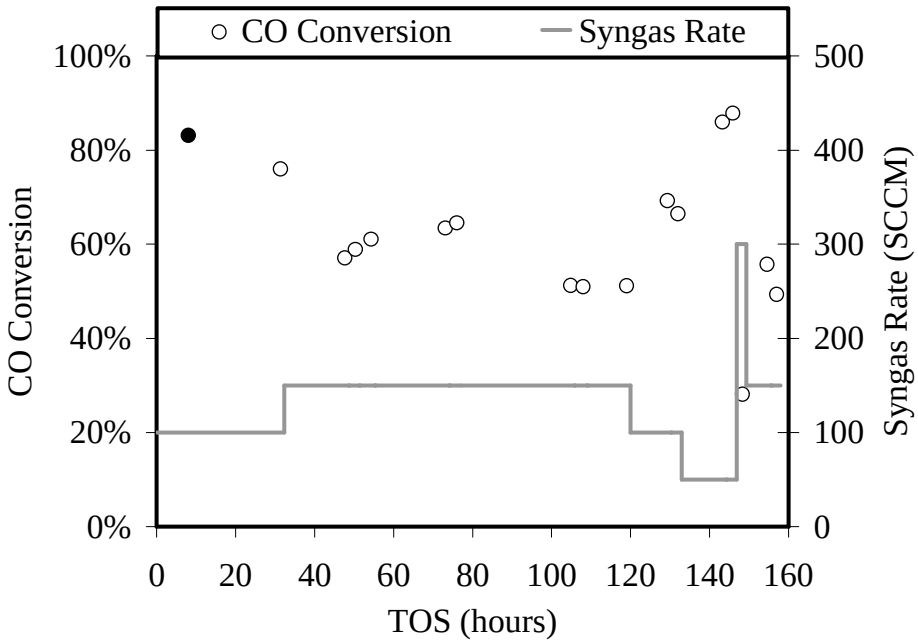

Figure 4.19 First Study - Conversion for GP-FTS (solid circles) and SC-FTS (empty circles) versus Time-on-Stream while varying syngas rate at constant syngas/media ratio (2g catalyst, P_{syngas} = 17.5 bar, T = 240^{o}C). System upsets occurred around hours 40 and 90. For the period after the second system upset, the catalyst activity is highly stable.

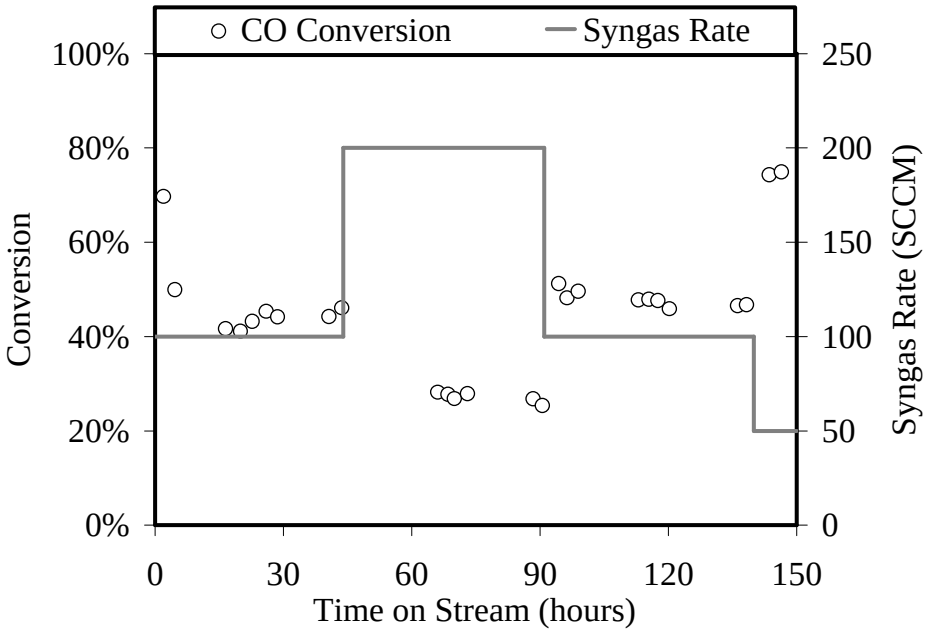

Figure 4.20 Second Study (GP-FTS) - CO conversion versus Time-on-Stream at various syngas rates (2g catalyst, P = 17.5 bar, T = 240^{o}C). There is a rapid initial decline in catalyst activity followed by a gradual decline in activity with time-on-stream.

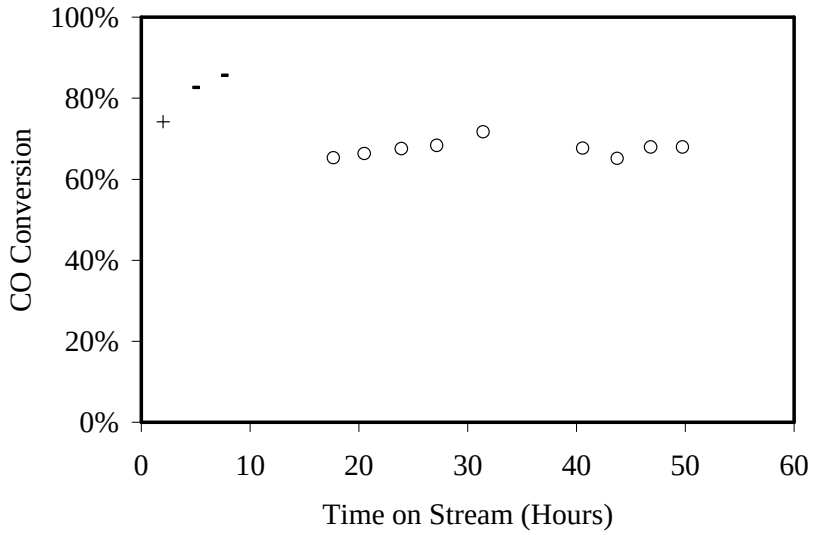

Figure 4.21 Second Study (SP-FTS) - CO conversion versus Time-on-Stream (4g catalyst, P = 17.5 bar) - (+) 400 SCCM, 270^{o}C : (-) 200 SCCM, 270^{o}C : (o) 200 SCCM, 240^{o}C. Using the same catalyst (formulation, batch, and powder size), this catalyst is more active than that used in GP-FTS (Figure 4.20).

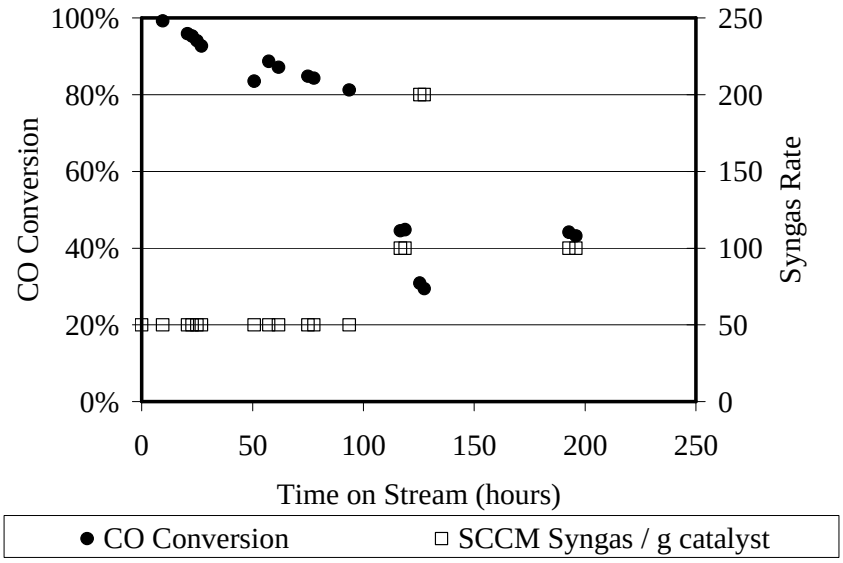

Figure 4.22 Third Study (SC-FTS) – CO conversion versus Time-on-Stream while varying syngas rate at a constant syngas/media ratio (2g catalyst, P = 75 bar, T = 240^{o}C). After a gradual induction period, the catalyst showed stable activity (compare 120 hours to 200 hours.

Chapter 5

Supercritical Adiabatic Reactor for Fischer Tropsch Synthesis

5.1 Introduction

Fischer Tropsch Synthesis (FTS) is a catalytic reaction for the conversion of syngas (CO + H_2) to hydrocarbon fuels and chemicals. The process is operated in two modes: High Temperature (HTFT) for the production of gasoline and light olefins and Low Temperature (LTFT) for the production of diesel fuel and wax. This chapter focuses on LTFT exclusively [1]. The reaction is highly exothermic:

$$CO + 2H_2 \rightarrow (CH_2) + H_2O + 146\ kJ$$

Removal of this heat is an important factor in LTFT reactor design [1]. The initial Sasol LTFT reactor (ARGE) managed the heat release by having a high velocity in a large number of narrow packed tubes, resulting in a reactor with 2050 12m long, 5cm ID tubes having a capacity of 900 BPD [2]. This design has a number of problems, including middling thermal uniformity, high pressure drop, difficult catalyst replacement, and poor economies of scale [2].

To overcome these limitations Sasol developed their slurry reactor (in which the catalyst particles are suspended in a liquid, through which the syngas is bubbled), which gives lower capital cost, lower pressure drop, better thermal uniformity, and online catalyst replacement [2]. However, the slurry reactor requires separation of the wax media from the solid catalyst [2] and involves greater development cost and time [3].

In order to attempt to realize the advantages of traditional fixed-bed LTFT (Gas Phase FTS: GP-FTS) and slurry phase FTS (SP-FTS), Kaoru Fujimoto's group pioneered the use of a supercritical fluid as the media for LTFT (SC-FTS) [4]. This type of operation involves the addition of a solvent (typically C3-C7 hydrocarbons) to the syngas and a corresponding increase in the reactor operating pressure. Operating in this way has been shown (relative to GP-FTS) to give suppressed methane selectivity, enhanced olefin selectivity, suppressed CO_2 selectivity, enhanced activity and activity maintenance, enhanced diesel and wax selectivity, and other advantages [4-26]. SC-FTS operation offers excellent opportunities to study the reaction, preserving primary products against some secondary reactions [27]. For a thorough review of SC-FTS, please consult the recent review by Elbashir et al [28].

One aspect of SC-FTS that has been little remarked upon is its effect on the adiabatic temperature rise of the reaction. A GP-FTS reactor operating at 50% conversion would have an adiabatic temperature rise on the order of 800^{o}C. For mechanical, catalyst selectivity, and activity stability reasons this is not acceptable. As such, LTFT reactors have usually been designed to remove heat as it is generated. This high adiabatic temperature rise also involves the danger of a runaway reaction [29], damaging both the reactor and the catalyst. The dilution effects of SC-FTS (at 3.5 moles hexane per mole syngas, the contents of the reactor are 96.4% media by mass) decrease the adiabatic temperature rise to approximately 30^{o}C, making adiabatic operation possible. Two primary obstacles stand in the way of industrial utilization of SC-FTS: capital cost (due to more robust design required due to the higher operating pressure) and operating cost (due to the compression and recompression of the syngas and media).

The design principle utilized here is to use the low adiabatic temperature rise of SC-FTS to run the reaction in stages of an adiabatic reaction followed by cooling. The number of stages

is determined by the allowable temperature rise. It is our belief that this design will allow for SC-FTS to be carried out with a reactor cost competitive with traditional fixed bed FTS. It is also hoped that the properties of the supercritical fluid media combined with separation of the reaction and heat removal processes will allow for decreased pressure drop, decreasing the operating cost of SC-FTS.

While adiabatic operation has been used in FTS, both by recycling gas (operating at a very low one-pass conversion) or by recycling produced liquid and operating a trickle-bed reactor, it is our belief that the use of a supercritical fluid media to allow for adiabatic operation is a new concept for FTS.

5.2 Experimental

All of the simulations used in this study were done using AspenPlus with the Peng-Robinson EOS. The reaction was modeled on the simplifying assumption of the only products being 1-decene and water. The reactor design was done to match the capacity, operating conditions, and dimensions of the Sasol ARGE reactor, but with an allowable temperature range of 5^{o}C. For the sake of comparison, the reactor was also modeled using 1 reactor to achieve the full 50% conversion (30^{o}C temperature rise).

The reactor and heat exchanger designs were done using the Blasius Equation (equation 5.1) and the Dittus-Boelter equation (equation 5.2).

$$f = 0.079 * Re^{-0.25} \qquad \text{Equation 5.1}$$

$$Nu = .023 * Re^{0.8} * Pr^{0.3} \qquad \text{Equation 5.2}$$

The properties used in this study are as follows in Table 5.1.

Table 5.1 SC-FTS bulk property estimates

Property	Value	Units
Density	300	kg / m^3
Viscosity	$1.2*10^{-4}$	Pa-sec
Thermal Conductivity	0.075	W / m-K

The reactor is assumed to operate between 240^{o}C and 245^{o}C, with heat removal carried out in the heat exchangers by boiling water at 230^{o}C, giving a ΔT_{lm} of 12.3^{o}C. Pricing of the Sasol ARGE reactor was done based on publicly available information, and is consequently a rough estimate.

5.3 Sizing

Table 5.2 Reactor geometry: Sasol ARGE reactor [2] and the same geometry applied to Supercritical Adiabatic Reactor design.

Reactor		
	ARGE	**Supercritical Adiabatic Reactor (SCAR)**
Number of Reactors in Series	1	6
# of Tubes	2050	1
Tube Diameter	0.05 m	2.3 m
Tube Length	12 m	2 m

Table 5.3 Heat Exchanger Design for SCAR System

Heat Exchanger for 6-Reactor SCAR System	
Duty (W)	2,023,000
ΔT_{lm} (K)	12.3
Tube D (m)	.025
Number of Tubes	94
U (W / m^2-K)	750
Heat Exchanger Area (m^2)	219
Tube Length (m)	30
Pressure Drop (bar)	.12

5.4 Price Estimates

Table 5.4 Reactor and Heat Exchanger Price estimates for Sasol ARGE reactor, Sasol Arge reactor upgraded for SC-FTS operation, single-stage SCAR system, and multi-stage SCAR system.

System Type	ARGE	ARGE Upgraded for SC-FTS	SCAR (1 Reactor)	SCAR (6 Reactors)
# of Reactors	1	1	1	6
Adiabatic Temperature Rise (K)	X	X	5	30
Reactor P (bar)	45	200	200	200
Reactor Volume (m^3)	48	48	48	8
Tube Surface Area (m^2)	3864	3864	85.4	14.2
Reactor Cost	$1,000,000	$2,000,000	$240,000	$45,000
# of Heat Exchangers	X	X	1	6
Heat Exchanger Surface Area (m^2)	X	X	1316	219
Heat Exchanger Cost	X	X	$600,000	$100,000
Total Cost	$1,000,000	$2,000,000	$840,000	$870,000

5.5 Discussion

The sizing and cost values are rough estimates, and the SCAR system has not been optimized. Despite this, while upgrading the traditional GP-FTS reactor for SC-FTS operation would result in a large increase in the reactor capital cost, the SCAR reactor should allow for SC-FTS operation with a lower reactor system capital cost than the Sasol ARGE reactor.

Additionally, because the SCAR system separates the reaction step from the heat removal step, interesting opportunities to optimize the catalyst and system design exist. Because the reactor(s) itself is the small part of the capital cost, a catalyst design that offers lower pressure drop to the detriment of activity could be a viable alternative. Additionally, enhanced mass transfer in SC-FTS operation may allow for the use of a catalyst with decreased pressure drop, improving the operating cost of the process. Another benefit of this system is that it will allow for far easier catalyst replacement than the ARGE design, a not inconsequential consideration. Finally, it is unlikely that the optimized system would include a reactor diameter as high or a reactor aspect ratio as low as this one. The optimized system would likely have a small number of reactors in parallel.

A possible modification to this design would be to include a knockout pot after each stage to remove heavy wax if the bulk media is not single stage, as can be the case in high-alpha operation [30]. Additionally, this design allows for the different reactor stages to be controlled independently. Among other benefits, this will allow the inlet and outlet temperature of each section to be adjusted independently to compensate for catalyst deactivation. It is possible that partially or totally distributing the syngas flow between the stages instead of directing all of the system feeds to the first stage would be part of the optimal design.

5.6 Conclusions

Based on the reduced adiabatic temperature rise seen in SC-FTS relative to GP-FTS, an alternate LTFT reactor system has been roughly designed and priced. This system allows for the benefits of SC-FTS (suppressed methane formation, enhanced olefin selectivity, decreased chance of a runaway reaction, etc.) at a lower reactor system capital cost than the Sasol ARGE

reactor. Additionally, this reactor increases operational flexibility and greatly eases catalyst replacement. We believe this to be a potentially viable industrial LTFT reactor design.

5.7 References

[1] Mark E. Dry, Appl. Catal., A 138 (1996) 319-344.

[2] B. Jager, R. Espinoza, Catal. Today 23 (1995) 17-28.

[3] Kenneth Agee, Rafael Espinoza: *Future Role and Characteristics of the Fischer-Tropsch Technology*. **Presentation - AIChE Spring Meeting** (2010): Coal, Biomass, and Natural Gas to Liquids I, 10a.

[4] Kohshiroh Yokota, Kaoru Fujimoto: *Supercritical Phase Fischer-Tropsch Synthesis Reaction.* **Fuel**. (1989): V 68, p 255-256.

[5] Kohshiroh Yokota, Kaoru Fujimoto: *Supercritical-Phase Fischer-Tropsch Synthesis Reaction. 2. The Effective Diffusion of Reactant and Products in the Supercritical-Phase Reaction*. **Industrial and Engineering Chemistry Research** (1991): V 30, I 1, p 95.

[6] Kohshiroh Yokota, Yoshio Hanakata, Kaoru Fujimoto: *Supercritical-Phase Fischer-Tropsch Synthesis Reaction. 3: Extraction Capability of Supercritical Fluids*. **Fuel** (1991): V 70, I 8, p 989.

[7] Xiaosu Lang, Aydin Akgerman, Dragomir B. Bukur: *Steady State Fischer-Tropsch Synthesis in Supercritical Propane*. **Industrial and Engineering Chemistry Research** (1995): V 34, I 1, p 72.

[8] Dragomir B. Bukur, Xiaosu Lang, Aydin Akgerman, Zhentao Feng: *Effect of Process Conditions on Olefin Selectivity during Conventional and Supercritical Fischer-Tropsch Synthesis*. **Industrial and Engineering Chemistry Research** (1997): V 36, N 7, p 2580.

[9] Shirun Yan, Li Fan, Zhixin Zhang, Jinglai Zhou, Kaoru Fujimoto: *Supercritical-Phase Process for Selective Synthesis of Heavy Hydrocarbons from Syngas on Cobalt Catalysts*. **Applied Catalysis A: General** (1998): V 171, p 247.

[10] Li Fan, Kaoru Fujimoto: *Fischer-Tropsch Synthesis in Supercritical Fluid: Characteristics and Application*. **Applied Catalysis A: General** (1999): V 186, p 343.

[11] Noritatsu Tsubaki, Kiyotaka Yoshii, Kaoru Fujimoto: *Anti-ASF Distribution of Fischer-Tropsch Hydrocarbons in Supercritical-Phase Reactions*. **Journal of Catalysis** (2002): V 207, p 371.

[12] Gary Jacobs, Karuna Chaudhari, Dennis Sparks, Yongqing Zhang, Buchang Shi, Robert Spicer, Tapan K. Das, Jinlin Li, Burtron H. Davis: *Fischer–Tropsch Synthesis: Supercritical Conversion Using a Co/Al_2O_3 Catalyst in a Fixed Bed Reactor*. **Fuel** (2003): V 82, I 10, p 1251.

[13] Xiwen Huang, Christopher B. Roberts: *Selective Fischer-Tropsch Synthesis Over an Al_2O_3 Supported Cobalt Catalyst in Supercritical Hexane*. **Fuel Processing Technology** (2003): V 83, p 81.

[14] Wensheng Linghu, Xiaohong Li, Kenji Asami, Kaoru Fujimoto: *Supercritical Phase Fischer-Tropsch Synthesis over Cobalt Catalyst*. **Fuel Processing Technology** (2004): V 85, p 1121.

[15] Xiwen Huang, Nimir O. Elbashir, Christopher B. Roberts: *Supercritical Solvent Effects on Hydrocarbon Product Distributions from Fischer Tropsch Synthesis Over an Alumina-Supported Cobalt Catalyst*. **Industrial and Engineering Chemistry Research** (2004): V 43, p 6369.

[16] Nimir O. Elbashir, P. Dutta, A. Manivannan, M. S. Seehra, Christopher B. Roberts: *Impact of Cobalt-Based Catalyst Characteristics on the Performance of Conventional Gas-Phase and Supercritical-Phase Fischer Tropsch Synthesis*. **Applied Catalysis A: General** (2005): V 285, p 169.

[17] Nimir O. Elbashir, Christopher B. Roberts: *Enhanced Incorporation of α-Olefins in the Fischer-Tropsch Synthesis Chain-Growth Process Over an Alumina-Supported Cobalt Catalyst in Near-Critical and Supercritical Hexane Media*. **Industrial and Engineering Chemistry Research** (2005): V 44, p 505.

[18] Dragomir Bukur, Xiaosu Lang, Lech Nowicki: *Comparative Study of an Iron Fischer Tropsch Catalyst Performance in Stirred Tank Slurry and Fixed-Bed Reactors*. **Industrial and Engineering Chemistry Research** (2005): V 44, p 6038.

[19] Buchang Shi, Gary Jacobs, Dennis Sparks, Burtron H. Davis: *Fischer-Tropsch Synthesis: 14C Labeled 1-Alkene Conversion Using Supercritical Conditions with Co / Al_2O_3*. **Fuel** (2005): V 84, p 1093.

[20] Wen-Sheng Linghu, Xiao-Hong Li, Kenji Asami, Kaoru Fujimoto: *Process Design and Solvent Recycle for the Supercritical Fischer-Tropsch Synthesis*. **Energy and Fuels** (2006): V 20, p 7.

[21] Xiaohao Liu, Wen-Sheng Linghu, Xiao-Hong Li, Kenji Asami, Kaoru Fujimoto: *Effect of Solvent on Fischer Tropsch Synthesis*. **Applied Catalysis A: General** (2006): V 303, p 251.

[22] Wen-Sheng Linghu, Xiao-Hong Li, Kaoru Fujimoto: *Supercritical and Near-Critical Fischer-Tropsch Synthesis: Effects of Solvents*. **Journal of Fuel Chemistry and Technology** (2007): V 35, I 1, p 51.

[23] Abdullah Irankhah, All Haghtalab, Ebrahim Vasheghani Farahani, Kambiz Sadaghianizadeh: *Fischer-Tropsch Reaction Kinetics of Cobalt Catalyst in Supercritical Phase*. **Journal of Natural Gas Chemistry** (2007): V 16, I 2, p 115.

[24] Abdullah Irankhah, All Haghtalab: *Fischer-Tropsch Synthesis Over Co-Ru / γ-Al_2O_3 Catalyst in Supercritical Media*. **Chemical Engineering Technology** (2008): V 31, N 4, p 525.

[25] TANG Haodong, LIU Huazhang, YANG Xiazhen, LI Ying: *Supercritical Phase Fischer-Tropsch Synthesis Reaction over Highly Active Fused Iron Catalyst at Low Temperature*. **Journal of Chemical Engineering of Chinese Universities** (2008): V 22, N 2, p 259.

[26] Ed Durham, Sihe Zhang, Christopher B. Roberts*: Supercritical Reactivation of Fischer Tropsch Catalysts*. **AIChE Annual Meeting** (2008): Presentation 678d.

[27] Ed Durham, Sihe Zhang, Christopher Roberts: *Diesel-Length Aldehydes and Ketones via Supercritical Fischer Tropsch Synthesis on an Iron Catalyst*. **Applied Catalysis A: General** (2010): V 386, p 65-73.

[28] Nimir O. Elbashir, Dragomir B. Bukur, Ed Durham, Christopher B. Roberts: *Advancement of Fischer-Tropsch Synthesis via Utilization of Supercritical Fluid Reaction Media*. **AIChE Journal** (2010): V 56, p 997.

[29] Xiaowei Zhu, Diane Hildebrandt, David Glasser: *A Study of Radial Heat Transfer in a Tubular Fischer-Tropsch Synthesis Reactor*. **AIChE Spring Meeting** (2010): Presentation 10b.

[30] M. Claeys, E. van Steen: *Basic Studies*. **Studies in Surface Science and Catalysis 152** (ISBN 978-0-444-51354-0): Ch 8.

Chapter 6

Future Work

6.1 Gas-Phase, Supercritical, Slurry Phase Fischer Tropsch Comparison Using both Iron and Cobalt Catalysts (Chapter 2 Continuation)

Because it uses the same reactor design, supercritical FTS (SC-FTS) has been frequently compared with gas-phase FTS (GP-FTS), but only infrequently compared with slurry-phase FTS (SP-FTS). The first purpose of this study is to compare the catalytic activity, selectivity, and stability of both a cobalt and an iron FTS catalyst in all three reaction mediums.

The Fischer Tropsch reaction is a combination of primary and secondary reactions [1]. Two important secondary reactions are the hydrogenation and incorporation of olefins, especially on cobalt [1]. That olefin selectivity decreases with increasing conversion on cobalt is a known, as is that olefin selectivity usually decreases with increasing carbon number [2]. This suggests that secondary reactions consume olefins and are chain-length dependant. Enrique Iglesia's group has demonstrated [3] by olefin co-feeding and residence time studies that, while added olefins are predominately hydrogenated, in situ generated olefins are predominately incorporated. This is important because hydrogenation of olefins has no effect on the inter-carbon number product distribution, while incorporation can shift the inter-carbon number product distribution to heavier products. This is how Iglesia [3] explains his observation that increasing conversion enhances chain growth (this observation is not universal [2]).

Additionally, deviations from the ASF product distribution have also been attributed to secondary reactions [4]. Burt Davis [5] studied accumulation and attributed many of the phenomena observed by Iglesia and others to reactor holdup.

By operating each catalyst (iron and cobalt) in each reaction media (gas-phase, supercritical, and slurry) at three CO conversion levels (≈25%, ≈50%, ≈75%) the generation and consumption of each reaction product with increasing conversion can be modeled.

6.2 Activity Restoration (Chapter 3 Continuation)

The experiment conducted in Chapter 3 was not conducted at industrially realistic conditions. To continue this work, a study composed of six experiments should be conducted: three for an iron-based catalyst and three for a cobalt-based catalyst. For each catalyst, one experiment should be an extended GP-FTS run, the second should be GP-FTS portions separated by supercritical hexanes (inert) washings, the third should be GP-FTS portions separated by SC-FTS (reactive) washings. Each experiment should be conducted at a CO conversion of approximately 50%.

6.3 Aldehyde Formation (Chapter 4 Continuation)

In the work presented in Chapter 4, an unprecedented selectivity of the Fischer Tropsch reaction to heavy aldehydes and methyl-ketones was demonstrated. To continue this work, the effect of media ratio (0 to 3.5: transitioning from GP-FTS to SC-FTS), media choice (pentane, hexane, and heptane), temperature, pressure, and catalyst composition (alkali choice, alkali level, etc.) should be studied in iron-based SC-FTS. This work is of interest first because of the theoretical benefit of studying a number of parameters in SC-FTS due to its capacity to stabilize

primary products creating opportunities to study the fundamentals of the FTS reaction. This is of practical interest due to the potential market value of aldehydes and chemicals that can be derived from them.

6.4 FTS Mechanism (Chapter 4 Continuation)

In the work presented in Chapter 4, we concluded that the FTS mechanism on an iron-based catalyst is the conventional CO Insertion mechanism. Reconsideration of our observations from that study, previous observations by other research groups, and subsequent observations by other research groups has led us to a different conclusion.

Observation #1: Aldehydes appear to be primary products of the FTS reaction on iron, can generate all classes of products, and can incorporate in the reaction [6].

Observation #2: Alcohols (and likely aldehydes [6,7]) incorporate into the FTS reaction on iron as initiators [8]. Terminal alcohols produce straight-chain hydrocarbons, while internal alcohols produce branched products [8].

Observation #3: On an iron-based FTS catalyst, CO_2 can initiate the reaction without first being converted to CO, while acting as a propagator requires it being first converted to CO [8].

Observation #4: Incorporation of C_2D_5OH on an iron-based catalyst gave some D_1, D_2, D_3, and D_4 heavier products, but no D_5 heavier products [9].

Observation #5: Incorporation of an aldehyde gave, in addition to general incorporation, the n+1 methyl ketone [6].

Observation #6: Incorporation of an aldehyde gave a 2n-1 oxygenate [6], likely the symmetrical ketone [10].

Observation #7: Incoporation of an aldehyde [6] or alcohol [8] produced the n-1 paraffin.

The first observation strongly suggests an oxygenate mechanism. The third observation suggests that the initiator and the monomer are fundamentally different. This supports the conventional CO Insertion mechanism. The second observation can be interpreted as supporting an oxygenate initiator (if the C-O bond is not broken prior to initiation), but is inconclusive. The fifth observation strongly argues that the propagation mechanism is by the addition of a C1 unit to an oxygenate. The seventh observation shows that an alkyl unit can be generated from an aldehyde, with the sixth observation indicating that the alkyl unit can react with an aldehyde. Finally, the fourth observation suggests that incorporation of an alcohol requires the removal of one bond from the substituted carbon, supporting CHRO as the reaction initiator. This would leave a non-oxygenate species, likely CH_2, as the propagator.

The questions with this proposed mechanism are the specific identity of the propagator and the pathway for the propagation reaction. One possible pathway for the reaction is to pass through an epoxide. This would not be unlike the mechanism of catalytic epoxidation of ethylene [11].

There are three experiments that can be conducted to study this mechanism. The first is to incorporate an O^{18} substituted aldehyde and determining O^{18} content of different products. The second is to carry out molecular simulations of the proposed pathway. The third is to attempt to incorporated an aldehyde in a cobalt-based system. Alcohols have been observed to inert in cobalt-based FTS, but observation 4 suggests that an important step in the incorporation

of alcohols on an iron catalyst is the cleaving of a C-H bond. Because an aldehyde would not require this step, it may be that aldehydes will incorporate over cobalt where alcohols will not. Hydrogenation of CO_2 on cobalt produces methane [12], a result similar to the third observation, suggesting that the mechanism may be the same on the two catalysts. Taken together, the results of the these three investigations could lead a viable, new mechanism

6.5 SC-FTS Diffusion Resistance (Chapter 5 Continuation)

There are two primary barriers to the industrial utilization of SC-FTS: capital cost and operating cost. In the work presented in Chapter 5, I believe we have addressed a large part of the capital cost problem. While the higher pressure will necessarily require more front-end compression costs, an optimized catalyst for the system may lower pressure drop, decreasing recompression and the operating cost penalty for SC-FTS.

Kaoru Fujimoto's group [13] has demonstrated that the supercritical environment leads to a more uniform intra-pellet syngas ratio than does GP-FTS operation, indicating that larger catalyst particles may be feasible. To this end, it is recommended to study a broad range of catalyst sizes for both cobalt and iron in both GP-FTS and SC-FTS conditions.

6.6 Co-Precipitated Cobalt LTFT Catalysts

An important area of inquiry in cobalt-based FTS is particle size effects. Enrique Iglesia's group [3] studied cobalt catalysts on oxide supports and found that the TOF and selectivity were minimally dependent upon dispersion (the fraction of cobalt atoms on the surface of the cobalt crystals, a number that correlates strongly with cobalt crystal size). Bezemer et al [14] impregnated cobalt nanoparticles on carbon nanofibers and found no effect of

dispersion/cobalt crystal size on TOF or selectivity at particle sizes above approximately 5nm. Below that crystal size, the catalyst activity declined and the methane selectivity increased.

Non-oxide supports are of interest for this kind of study due to the strong interactions between cobalt and oxide supports. However, there is another option: the use of co-precipitated cobalt to study particle size effects for FTS in a low-conversion slurry bed reactor.

By varying the precipitation conditions between batches, we believe that it is possible to control the catalyst characteristics. Early work precipitating cobalt nitrate with ammonium carbonate (forming cobalt carbonate that, when calcined, had a particle size of 13 nm and a surface area of 40.5 m^2/g) and with sodium hypochlorite (forming cobalt oxide directly that, when calcined, had a particle size of 7nm and a surface area of 30.6 m^2/g). Sodium hypochlorite presents a number of problems: incompatibility with metallic equipment, loss of surface area in the preliminary samples, and contamination with sodium in the preliminary sample. As such, ammonium carbonate appears to be the more promising precipitating agent.

As Dr. Roberts' research group has expertise both in nanoparticle synthesis and FTS operation, this study is a natural way to use the group's unique expertise to address the issue of particle size effects in cobalt-based FTS.

6.7 Three-Bed Reactor for Integrated FTS and Syncrude Upgrading

6.7.1 Background

Sihe Zhang has been and will continue to work on this project, though I have made contributions in catalyst choice and reactor design.

Fischer Tropsch Synthesis is unselective to particular fuel fractions [15]. Consequently, increasing the selectivity of the overall process to a particular fraction requires upgrading reactions. Additionally, raw FT fuels are not ideal, with the diesel having poor cold flow properties and the gasoline having a low octane rating [16]. Upgrading reactions are necessary for this as well.

Product distributions from Chapter 2 are shown in Figure 6.1 below.

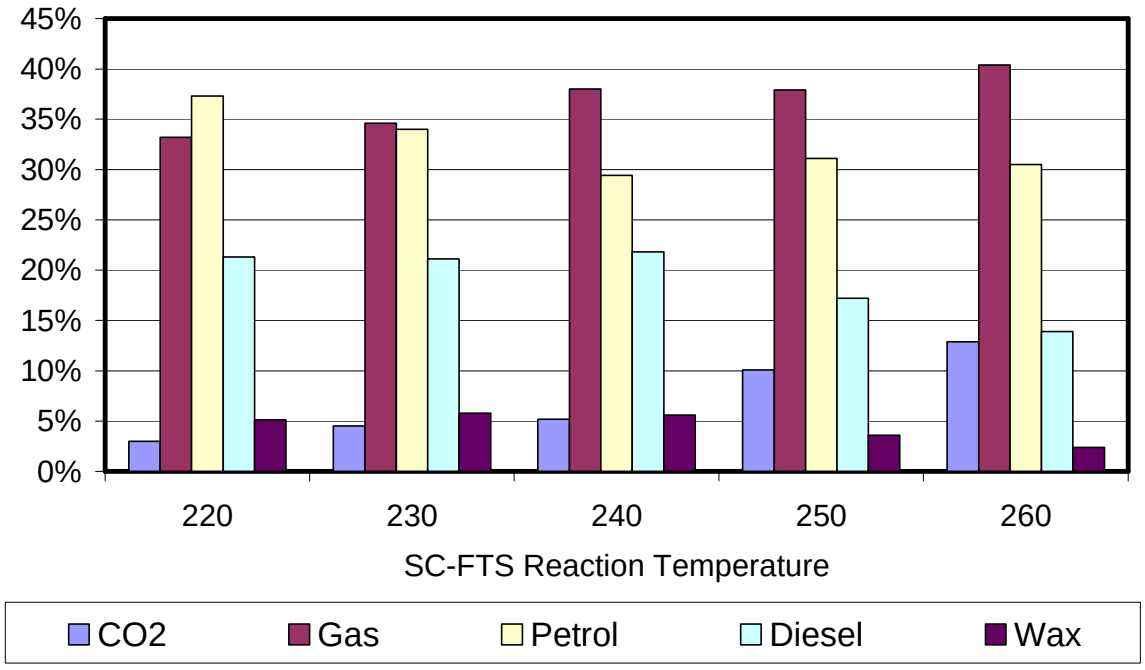

Figure 6.1 Product fraction selectivities for SC-FTS on cobalt at various temperatures

There are a number of processes that can be used to enhance the selectivity of FT to fuels and to improve their quality (alkylation, aromatization, cracking, hydrocracking, isomerization, and oligomerization) [16]. Our current work focuses on oligomerization of olefins and hydrocracking operated sequentially. Because the hydrocaracking process also saturates olefins, the reactions will need to be carried out as: FTS → Oligomerization → Hydrocaracking.

The primary purpose of oligomerization is to shift gaseous olefins into the gasoline-diesel range. A secondary benefit is the synthesis of branched compounds, which enhance diesel cold flow and gasoline octane rating. ZSM-5 and Solid Phosphoric Acid (SPA) have been used industrially for oligomerization of Fischer Tropsch olefins [17], while Amorphous Silica-Alumina (ASA)[18] and thermal oligomerization (no catalyst) [19] have also been studied. The industry standard for oligomerization in petro-refining is the UOP process based upon SPA [20]. ZSM-5 is the basis of Mobil's Olefins to Gasoline and Distillates (MOGD) and Sasol's Conversion of Olefins to Distillates (COD) process [20].

The shape selectivity of ZSM-5 leads to a product with less branching than SPA [21]. Further, ZSM-5 gives a significantly higher cetane value (but worse octane rating and lower density) than both SPA and ASA [17]. As was noted previously, thermal, non-catalytic oligomerization is also possible and has been studied by Sasol [19]. The slow reaction rate makes it difficult to pursue currently. For the time being, we intend to pursue ASA as our primary oligomerization catalyst. This is for two reasons. First, ASA is more like a traditional support, allowing for easier use. Second, it gives oligomerization products clearly different from raw FT products, giving an easier contrast between FT and oligomerization products.

Arno de Klerk [18] points out that two of the difficulties encountered in oligomerization are deactivation due to the accumulation of heavy oligomers (leading to that study requiring high

pressure) and dissipation of heat (the oligomerization reaction being, like Fischer Tropsch itself, highly exothermic). To us, this gives the appearance of an excellent opportunity to utilize supercritical fluids as a reaction media.

The primary purpose of hydrocracking is to shift heavy wax into the fuel range, with a secondary benefit being isomerization. It is a common process in both petro-refining and FT syncrude refining. However, FT-crude is different from petro-crude in a number of ways, including the presence of oxygenates, the absence of sulfur, higher olefin content, and lower aromatic content in syncrude [22].

Because of the clean nature of FT-syncrude, noble metal / acid catalysts can be used for hydrocracking, leading to higher isomerization activity [16]. These catalysts are bifunctional, including a metal site for hydrogenation / dehydrogenation and acidic sites for isomerization / cracking [23]. Large molecules are preferentially cracked over small ones [24], with the cracking location determined by random beta scission [16].

There are two basic approaches to combining FTS with hydrocracking. The first is to combine the two reactions into one catalyst bed (whether fixed or slurry). If the two catalysts are physically mixed in a slurry bed, the need for separating the wax and catalyst can be eliminated. If the catalysts are combined into one multi-functional catalyst, the plugging of catalyst pores with wax can be mediated. This has two problems. First, it can damage the FT performance. Botes and Bohringer [25] showed that contact between the iron and the zeolite let to migration of the alkali promoter to the zeolite, hurting activity and selectivity. Fujimoto's group [26] supported cobalt on a number of conventional and acidic supports for slurry-phase and supercritical FTS. Montmorillonite behaved like silica and alumina while the zeolites had lower conversion, higher methane selectivity, higher isomer selectivity, and suppressed wax selectivity

than conventional supports. The second problem with combining the two reactions is that cracking is done at a significantly higher temperature than LTFT [27]. Fujimoto's group [28] concluded that the two-stage process is preferable to combining the reactions in a single stage.

Using sequential reactors, Fujimoto's group concluded that palladium was superior to platinum and that zeolites impregnated by ion exchange gave higher isomer selectivity than those loaded by impregnation [29]. Botes and Bohringer [25] concluded that low acidity ZSM-5 (a high silica to alumina ratio of 280) gave better activity maintenance than a high acidity ZSM-5 (Si/Al = 30). Fujimoto's group [30], working with β-zeolite, concluded that the optimal Si/Al ratio was 25.6. Calemma et al [16] presented work in which 0.3% Pt / ASA (35-70 bar, 330^{o}C-355^{o}C) processed a light feed (61% in the distillate range) to a diesel with excellent cold properties.

Dardas et al [31] studied the cracking of n-heptane on a Y-Type commercial zeolite under sub-critical and supercritical conditions and found that, among other things, supercritical conditions imparted much better activity maintenance, indicating potential for supercritical fluids in FT syncrude cracking.

For our initial work in cracking we have chosen to use Pd supported on ASA. We will use ASA for the same reasons given in the oligomization discussion.

6.7.2 Proposed Work

The reactor to be used in this study has been shown to be effective for FTS using both iron and cobalt catalysts. Additionally, the cracking catalyst has been successfully tested on a representative mixture of C20 in C6. The oligomerization catalyst has been demonstrated to be effective as well.

With all of the individual components proven effective, the following set of experiments can be done:

1 FTS (1st bed)

2 FTS (1st bed) + Oligomerization (2nd bed)

3 FTS (1st bed) + Hydrocracking (3rd bed)

4 FTS (1st bed) + Oligomerization (2nd bed) + Hydrocracking (3rd bed)

Having completed these gas phase runs, the next logical step will be to repeat them using a supercritical fluid media to look for differences in activity, selectivity, and stability.

6.7.3 Experimental

A schematic of the reactor to be used in this experiment is as shown in Figure 6.2 below.

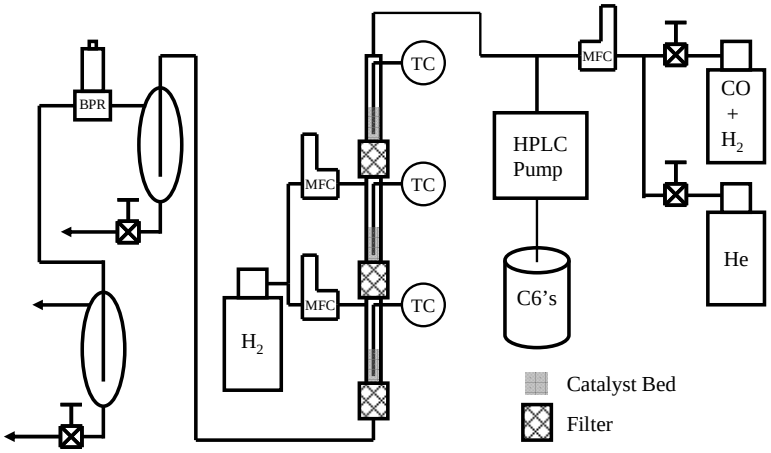

Figure 6.2 Schematic of the reactor system (3BR) used in this study. The first catalyst bed is for FTS, the second for oligomerization, the third for hydrocracking.

Syngas and helium (when appropriate) will be fed through a mass flow controller and mixed with hexanes (when appropriate) fed through a positive displacement HPLC pump. This mixture will pass though a heated line to the 1st part the reactor. After passing through the 1st catalyst bed (held in place by a filter (3B: S82-2P2P-10), the 1st bed effluent is mixed with

external feed to the 2nd bed (if appropriate). This mixture enters the 2nd bed of the reactor. After passing through the 2nd catalyst bed, the effluent is mixed with the external feed for the 3rd bed. After passing through the third catalyst bed, the system effluent passes through heated tubing to the hot trap (used to precipitate wax). The hot trap liquids are allowed to accumulate for intermittent collection and analysis. The hot trap vapor stream passes though the BPR (Back Pressure Regulator: used to control the system pressure), and through heated lines to the cold trap (maintained at a sub-ambient temperature). The cold trap liquids are allowed to accumulate for intermittent collection and analysis while the cold trap vapor stream passes through a six way valve (for automatic injection of the gasses to the TCD GC), through a flow meter, and is then vented to the fume hoods.

Each reactor is made from ½" SS tubing. The each catalyst bed is held in place by glass wool backed by an in-line filter (3B Filters S82-2P2P-10).

6.7.4 Objectives

The primary objective of this work is to demonstrate the capacity of the 3-Bed Reactor system to enhance the selectivity to gasoline and diesel fuel while adjusting the chemical characteristics (degree of branching, aromaticity) and utilization characteristics (octane and cetane ratings) of these fuels.

The secondary objective is to determine if the use of a supercritical solvent as the reaction media for these three reactions will enhance their performance.

6.8 FTS Upgrading Process Engineering Study

Once the proof of concept work has been completed on the 3-bed reactor, a study in which the both oligomerization and hydrocracking are examined (each paired individually with

FTS) by varying the different parameters (catalyst type, catalyst formulation, temperature, pressure, conversion level, etc.) in order to optimize the three-bed reactor system should be undertaken.

6.9 References

[1] M. Claeys, E. van Steen: *Basic Studies*. **Studies in Surface Science and Catalysis 152** (ISBN 978-0-444-51354-0): Ch 8.

[2] Gerard P. Van Der Laan, A. A. C. M. Beenackers: *Kinetics and Selectivity of the Fischer-Tropsch Synthesis: A Literature Review*. **Catalysis Reviews** (1999): V 41, I 3&4, p 255.

[3] Enrique Iglesia: Design, Synthesis, and Use of Cobalt-Based Fischer-Tropsch Synthesis Catalysts. **Applied Catalysis A: General** (1997): V 161, p59.

[4] E. W. Kuipers, C. Scheper, J. H. Wilson, I. H. Vinkenburg, H. Oosterbeek: *Non-ASF Product Distributions Due to Secondary Reactions during Fischer–Tropsch Synthesis*. Journal of Catalysis (1996): V 158, I 1, p 288.

[5] Buchang Shi, Burtron H. Davis: *Fischer–Tropsch Synthesis: Accounting for Chain-Length Related Phenomena*. **Applied Catalysis A: General** (2004): V 277, I 1-2, p 61.

[6] Ed Durham, Sihe Zhang, Christopher Roberts: *Diesel-Length Aldehydes and Ketones via Supercritical Fischer Tropsch Synthesis on an Iron Catalyst*. **Applied Catalysis A: General** (2010): V 386, p 65-73.

[7] W. Keith Hall, R. J. Kokes, P. H. Emmett, J. Am. Chem. Soc. 82 (1960) 1027–1037.

[8] Burtron H. Davis: *Fischer–Tropsch Synthesis: Reaction Mechanisms for Iron Catalysts*. **Catalysis Today** (2009): V 141, I 1-2, p 25-33.

[9] Muthu K. Gnanamani, Robert A. Keogh, Wilson D. Shafer, Buchang Shi, Burtron H. Davis: *Fischer–Tropsch Synthesis: Deuterium Labeled Ethanol Tracer Studies on Iron Catalysts*. **Applied Catalysis A: General** (2010): V 385, p 46-51.

[10] Yuguo Wang and Burtron H. Davis, Appl. Catal., A 180 (1999) 277-285.

[11] Suljo Linic, Mark A. Barteau: *Control of Ethylene Epoxidation Selectivity by Surface Oxymetallacycles*. **Journal of the American Chemical Society** (2003): V 125, p 4034.

[12] Thomas Riedel, Michael Claeys, Hans Schulz, Georg Schaub, Sang-Sung Nam, Ki-Won Jun, Myoung-Jae Choi, Gurram Kishan, Kyu-Wan Lee: *Comparative Study of Fischer–Tropsch Synthesis with H_2/CO and H_2/CO_2 Syngas using Fe- and Co-Based Catalysts*. **Applied Catalysis A: General** (1999): V 186, I 1-2, p201.

[13] Shirun Yan, Li Fan, Zhixin Zhang, Jinglai Zhou, Kaoru Fujimoto: *Supercritical-Phase Process for Selective Synthesis of Heavy Hydrocarbons from Syngas on Cobalt Catalysts*. **Applied Catalysis A: General** (1998): V 171, p 247.

[14] G. L. Bezemer; J. H. Bitter; H. P. C. E. Kuipers; H. Oosterbeek; J. E. Holewijn,; X. Xu; F. Kapteijn; A. J. van Dillen; K. P. de Jong: *Cobalt Particle Size Effects in the Fischer-Tropsch Reaction Studied with Carbon Nanofiber Supported Catalysts***. Journal of the American Chemical Society** (2006): V 128, p 3956.

[15] M. E. Dry: *The Fischer-Tropsch Synthesis*. **Catalysis Science and Technology Volume 1** (ISBN 3-540-10353-8): Chapter 4.

[16] L. P. Dancuart, R. de Haan, A de Klerk: *Processing of Primary Fischer Tropsch Products*. **Studies in Surface Science and Catalysis 152** (ISBN 978-0-444-51354-0): Ch 6.

[17] Arno de Klerk: *Effect of Oxygenates on the Oligomerization of Fischer−Tropsch Olefins over Amorphous Silica−Alumina*. **Energy and Fuels** (2007): V 21, I 2, p 625.

[18] Arno de Klerk: *Oligomerization of Fischer-Tropsch Olefins to Distillates Over Amorphous Silica-Alumina*. **Energy and Fuels** (2006): V 20, I 5, p 1799.

[19] Arno de Klerk: *Thermal Upgrading of Fischer-Tropsch Olefins*. **Energy and Fuels** (2005): V 19, I 4, p 1462.

[20] Arno de Klerk, Dan J. Engelbrecht, Herman Boikanyo: *Oligomerization of Fischer−Tropsch Olefins: Effect of Feed and Operating Conditions on Hydrogenated Motor-Gasoline Quality*. **Industrial and Engineering Chemistry Research** (2004): V 43, I 23, p 7449.

[21] Arno de Klerk: *Properties of Synthetic Fuels from H-ZSM-5 Oligomerization of Fischer–Tropsch Type Feed Materials*. **Energy and Fuels** (2007): V 21, I 6, p 3084.

[22] Arno de Klerk: *Hydroprocessing Peculiarities of Fischer-Tropsch Syncrude*. **Catalysis Today** (2008): V 130, p 439.

[23] L. Pellegrini, S. Locatelli, S. Rasella, S. Bonomi, V. Calemma: *Modeling of Fischer–Tropsch Products Hydrocracking*. **Chemical Engineering Science** (2004): V 59, I 22-23, p 4781.

[24] John Abbot, Paul R. Dunstan: *Catalytic Cracking of Linear Paraffins: Effects of Chain Length*. **Industrial and Engineering Chemistry Research** (1997): V 36, p 76.

[25] F. G. Botes, W. Bohringer: *The Addition of HZSM-5 to the Fischer Tropsch Process for Improved Gasoline Production*. **Applied Catalysis A: General** (2004): V 267, p 217.

[26] Chawalit Ngamcharussrivichai, Xiaohao Liu, Xiaohong Li, Tharapong Vitidsant, Kaoru Fujimoto: *An active and selective production of gasoline-range hydrocarbons over bifunctional Co-based catalysts*. **Fuel** (2007): V 86, p 50.

[27] Guillermo Calleja, Antonio de Lucas, Rafael van Grieken: *Co/HZSM-5 Catalyst for Syngas Conversion: Influence of Process Variables*. **Fuel** (1995): V 74, N 3, p 445.

[28] Xiaohong Li, Xiaohao Liu, Zhong-Wen Liu, b, Kenji Asami, Kaoru Fujimoto*: Supercritical Phase Process for Direct Synthesis of Middle Iso-Paraffins from Modified Fischer–Tropsch Reaction*. **Catalysis Today** (2005): V 106, p 154.

[29] Zhong-Wen Liu, Xiaohong Li, Kenji Asami, Kaoru Fujimoto: *Syngas to Iso-Parffins over Co/SiO_2 Combined with Metal/Zeolite Catalysts*. **Fuel Processing Technology** (2007): V 88, p 165.

[30] Zhong-Wen Liu, Xiaohong Li, Kenji Asami, Kaoru Fujimoto*: High Performance Pd/beta Catalyst for the Production of Gasoline-Range Iso-Paraffins via a Modified Fischer–Tropsch Reaction*. **Applied Catalysis A: General** (2006): V 300, p 162.

[31] Zissis Dardas, Murat G. Süer, Yi. H. Ma, William R. Moser: *A Kinetic Study of n-Heptane Catalytic Cracking over a Commercial Y-Type Zeolite under Supercritical and Subcritical Conditions*. **Journal of Catalysis** (1996): V 162, p 327.